Westinghouse Non-Proprietary Class 3

WCAP-17788-NP
Volume 4, Revision 0

July 2015

Comprehensive Analysis and Test Program for GSI-191 Closure (PA-SEE-1090) – Thermal-Hydraulic Analysis of Large Hot leg Break with Simulation of Core Inlet Blockage

Westinghouse

WCAP-17788-NP
Volume 4, Revision 0

Comprehensive Analysis and Test Program for GSI-191 Closure (PA-SEE-1090) – Thermal-Hydraulic Analysis of Large Hot leg Break with Simulation of Core Inlet Blockage

James P. Spring*
LOCA Integrated Services II

Gordon J. Wissinger
AREVA NP

July 2015

Reviewer: Brett. E. Kellerman*
LOCA Integrated Services II

Approved: Matthew B. Cerrone*, Manager
LOCA Integrated Services II

This work was performed under PWR Owners Group Project Authorization PA-SEE-1090.

*Electronically approved records are authenticated in the electronic document management system.

Westinghouse Electric Company LLC
1000 Westinghouse Drive
Cranberry Township, PA 16066, USA

LEGAL NOTICE

This report was prepared as an account of work performed by Westinghouse Electric Company LLC. Neither Westinghouse Electric Company LLC, nor any person acting on its behalf:

A. Makes any warranty or representation, express or implied including the warranties of fitness for a particular purpose or merchantability, with respect to the accuracy, completeness, or usefulness of the information contained in this report, or that the use of any information, apparatus, method, or process disclosed in this report may not infringe privately owned rights; or

B. Assumes any liabilities with respect to the use of, or for damages resulting from the use of, any information, apparatus, method, or process disclosed in this report.

COPYRIGHT NOTICE

DISTRIBUTION NOTICE

This report was prepared for the PWR Owners Group. This Distribution Notice is intended to establish guidance for access to this information. This report (including proprietary and non-proprietary versions) is not to be provided to any individual or organization outside of the PWR Owners Group program participants without prior written approval of the PWR Owners Group Program Management Office. However, prior written approval is not required for program participants to provide copies of Class 3 Non-Proprietary reports to third parties that are supporting implementation at their plant, and for submittals to the NRC.

PWR Owners Group United States Member Participation* for PA-SEE-1090			
Utility Member	**Plant Site(s)**	**Participant**	
		Yes	**No**
Ameren Missouri	Callaway (W)	X	
American Electric Power	D.C. Cook 1 & 2 (W)	X	
Arizona Public Service	Palo Verde Unit 1, 2, & 3 (CE)	X	
Dominion Connecticut	Millstone 2 (CE)	X	
	Millstone 3 (W)	X	
Dominion VA	North Anna 1 & 2 (W)	X	
	Surry 1 & 2 (W)	X	
Duke Energy Carolinas	Catawba 1 & 2 (W)	X	
	McGuire 1 & 2 (W)	X	
	Oconee 1, 2, & 3 (B&W)	X	
Duke Energy Progress	Robinson 2 (W)	X	
	Shearon Harris (W)	X	
Entergy Palisades	Palisades (CE)	X	
Entergy Nuclear Northeast	Indian Point 2 & 3 (W)	X	
Entergy Operations South	Arkansas 1 (B&W)	X	
	Arkansas 2 (CE)	X	
	Waterford 3 (CE)	X	
Exelon Generation Co. LLC	Braidwood 1 & 2 (W)	X	
	Byron 1 & 2 (W)	X	
	TMI 1 (B&W)	X	
	Calvert Cliffs 1 & 2 (CE)	X	
	Ginna (W)	X	
FirstEnergy Nuclear Operating Co.	Beaver Valley 1 & 2 (W)	X	
	Davis-Besse (B&W)	X	
Florida Power & Light \ NextEra	St. Lucie 1 & 2 (CE)	X	
	Turkey Point 3 & 4 (W)	X	
	Seabrook (W)	X	
	Pt. Beach 1 & 2 (W)	X	
Luminant Power	Comanche Peak 1 & 2 (W)	X	

PWR Owners Group United States Member Participation* for PA-SEE-1090			
Utility Member	**Plant Site(s)**	**Participant**	
		Yes	**No**
Omaha Public Power District	Fort Calhoun (CE)	X	
Pacific Gas & Electric	Diablo Canyon 1 & 2 (W)	X	
PSEG – Nuclear	Salem 1 & 2 (W)	X	
South Carolina Electric & Gas	V.C. Summer (W)	X	
So. Texas Project Nuclear Operating Co.	South Texas Project 1 & 2 (W)	X	
Southern Nuclear Operating Co.	Farley 1 & 2 (W)	X	
	Vogtle 1 & 2 (W)	X	
Tennessee Valley Authority	Sequoyah 1 & 2 (W)	X	
	Watts Bar 1 & 2 (W)	X	
Wolf Creek Nuclear Operating Co.	Wolf Creek (W)	X	
Xcel Energy	Prairie Island 1 & 2 (W)	X	
* **Project participants as of the date the final deliverable was completed. On occasion, additional members will join a project. Please contact the PWR Owners Group Program Management Office to verify participation before sending this document to participants not listed above.**			

PWR Owners Group International Member Participation* for PA-SEE-1090			
Utility Member	**Plant Site(s)**	**Participant**	
		Yes	**No**
Asociación Nuclear Ascó-Vandellòs	Asco 1 & 2 (W)	X	
	Vandellos 2 (W)	X	
Axpo AG	Beznau 1 & 2 (W)	X	
Centrales Nucleares Almaraz-Trillo	Almaraz 1 & 2 (W)	X	
EDF Energy	Sizewell B (W)	X	
Electrabel	Doel 1, 2 & 4 (W)	X	
	Tihange 1 & 3 (W)	X	
Electricite de France	58 Units	X	
Eletronuclear-Eletrobras	Angra 1 (W)	X	
Eskom	Koeberg 1 & 2 (W)	X	
Hokkaido	Tomari 1, 2 & 3 (MHI)	X	
Japan Atomic Power Company	Tsuruga 2 (MHI)	X	
Kansai Electric Co., LTD	Mihama 1, 2 & 3 (W)	X	
	Ohi 1, 2, 3 & 4 (W & MHI)	X	
	Takahama 1, 2, 3 & 4 (W & MHI)	X	
Korea Hydro & Nuclear Power Corp.	Kori 1, 2, 3 & 4 (W)	X	
	Hanbit 1 & 2 (W)	X	
	Hanbit 3, 4, 5 & 6 (CE)	X	
	Hanul 3, 4 , 5 & 6 (CE)	X	
Kyushu	Genkai 1, 2, 3 & 4 (MHI)	X	
	Sendai 1 & 2 (MHI)	X	
Nuklearna Electrarna KRSKO	Krsko (W)	X	
Ringhals AB	Ringhals 2, 3 & 4 (W)	X	
Shikoku	Ikata 1, 2 & 3 (MHI)	X	
Taiwan Power Co.	Maanshan 1 & 2 (W)	X	

*** Project participants as of the date the final deliverable was completed. On occasion, additional members will join a project. Please contact the PWR Owners Group Program Management Office to verify participation before sending this document to participants not listed above.**

TABLE OF CONTENTS

LIST OF TABLES

LIST OF FIGURES

LIST OF ACRONYMS AND ABBREVIATIONS

AFP	Alternate Flow Path
ANS	American Nuclear Society
B&W	Babcock and Wilcox
BAP	Boric Acid Precipitation
BAPC	Boric Acid Precipitation Control
BB	Barrel/Baffle
BE	Best Estimate
BWR	Boiling Water Reactor
BWST	Borated Water Storage Tank(s)
CE	Combustion Engineering
CFR	Code of Federal Regulations
CLB	Cold Leg Break
CSS	Containment Spray System
CQD	Code Qualification Document
DEG	Double-Ended Guillotine
DHHE	Decay Heat Heat Exchanger
DHR	Decay Heat Removal
ECCS	Emergency Core Cooling System
EM	Evaluation Model
FA	Fuel Assembly
GSI	Generic Safety Issue
GL	Generic Letter
HLB	Hot Leg Break
HPI	High Pressure Injection
HPSI	High Pressure Safety Injection
INEL	Idaho National Engineering Laboratory
LBLOCA	Large Break Loss-of-Coolant Accident
LOCA	Loss-of-Coolant Accident
LP	Lower Plenum
LPI	Low Pressure Injection
LPSI	Low Pressure Safety Injection
LTCC	Long-Term Core Cooling
LWR	Light Water Reactor
MHI	Mitsubishi Heavy Industries
MW	Megawatt
NRC	Nuclear Regulatory Commission
NSSS	Nuclear Steam Supply System

LIST OF ACRONYMS AND ABBREVIATIONS

PA	Project Authorization
PCT	Peak Cladding Temperature
PIRT	Phenomena Identification and Ranking Table(s)
PWR	Pressurized Water Reactor(s)
PWROG	Pressurized Water Reactor Owners Group
RCP	Reactor Coolant Pump(s)
RCS	Reactor Coolant System
RHR	Residual Heat Removal
RV	Reactor Vessel
RWST	Refueling Water Storage Tank
RWT	Refueling Water Tank
SBLOCA	Small Break Loss-of-Coolant Accident
SEE	Systems & Equipment Engineering
SG	Steam Generator(s)
TH	Thermal-Hydraulic(s)
UHSN	Upper Head Spray Nozzle(s)
UP	Upper Plenum
UPI	Upper Plenum Injection
U.S.	United States
WCAP	Westinghouse Technical Report Number Preface (formerly Westinghouse Commercial Atomic Power)

1 EXECUTIVE SUMMARY

The Pressurized Water Reactor Owners Group (PWROG) has undertaken a comprehensive test and analysis program to increase the in-vessel fibrous debris limit per fuel assembly (FA). An important aspect of this effort is associated with assessing the reactor coolant system (RCS) response to core inlet blockage due to the collection of debris following a postulated large hot leg break (HLB) loss-of-coolant accident (LOCA).

In order to assess the RCS response to post-LOCA debris, a comprehensive thermal-hydraulic (TH) analysis was completed for the United States (U.S.) pressurized water reactor (PWR) operating fleet. The TH analysis simulated the RCS following a large HLB and modeled debris resistance at the core inlet using a dimensionless form-loss coefficient. The use of existing codes and plant models previously developed for analysis of short-term peak cladding temperature (PCT) and cladding oxidation allowed the assessment to be completed with simple modifications to the codes and plant models utilized.

Given the differences associated with the three PWR vendors' nuclear steam supply system (NSSS) designs currently operating in the U.S., four unique TH analyses were completed; two for Westinghouse plants, one for Combustion Engineering (CE) plants, and one for Babcock and Wilcox (B&W) plants. The entire U.S. operating fleet was reviewed and binned into these four analysis categories. Westinghouse upper plenum injection (UPI) plants are an exception, and were not considered as part of this analysis given their unique emergency core cooling system (ECCS) configurations. A discussion of the Westinghouse UPI plant is provided in Volume 1, Section 8.

Section 2 of this volume provides the relevant background for completing the TH analysis and provides a description of the simulated transient. In addition, the detailed objectives of the analysis are provided in Section 2 along with the acceptance criteria used to judge successful long-term core cooling (LTCC) after debris build-up at the core inlet. Section 3 provides a description of the unique features associated with each of the four independent analyses and provides a summary of the U.S. PWR operating fleet considered in the analysis. Section 4 introduces the major assumptions and critical inputs defined for the analyses. Sections 5 and 6 provide a description of the computer codes and plant models used as the starting point, respectively. These sections also provide a description of the modifications made to the codes and models. Sections 7 through 11 summarize and discuss the results of the simulations.

The outcome of the simulations confirms that LTCC can be maintained for all plant types considered when post-LOCA debris is modeled. When a debris bed of uniform resistance is modeled at the core inlet, the simulations predict that, while flow through the core inlet decreases, removal of decay heat continues since sufficient flow is able to bypass the core inlet and reach the core region. Even if the collection of debris at the core inlet results in complete core inlet blockage, this bypass flow is sufficient to remove decay heat and keep PCT at acceptably low levels, provided complete core inlet blockage occurs after the times predicted by the TH simulations presented in this report. Due to the large amount of liquid carryover out the break before and after complete core inlet blockage, boric acid precipitation (BAP) is controlled and boron concentrations in the reactor vessel (RV) will remain well below the solubility limit for the duration of the transient.

The results from this TH analysis are used as acceptance criteria in subsequent debris testing performed as part of the PWROG program, as described in Volumes 5 and 6. Debris testing provides the link between

what was modeled in the analysis and a physical debris limit. In addition, simulation results are used as inputs to the overall methodology that allows PWR licensees to calculate a plant specific in-vessel fibrous debris limit. Section 12 summarizes the output from the TH analysis that is used in subsequent work, and the overall methodology is described in detail in Volume 1.

2 INTRODUCTION

2.1 BACKGROUND

The Nuclear Regulatory Commission (NRC) issued Generic Letter (GL) 2004-02 (Reference 2-1) requesting that licensees of PWRs perform an evaluation of the ECCS and containment spray system (CSS) based on the identified potential susceptibility of PWR recirculation sump screens to debris blockage during design basis accidents requiring recirculation operation of ECCS or CSS and on the potential for additional adverse effects due to debris blockage of flow paths necessary for ECCS and CSS recirculation. In addition, GL 2004-02 (Reference 2-1) states, "Debris blockage at flow restrictions within the ECCS recirculation flow path downstream of the sump screen is a potential concern for PWRs. Debris that is capable of passing through the recirculation sump screen may have the potential to become lodged at a downstream flow restriction, such as a high pressure injection throttle valve or fuel assembly inlet debris screen. Debris blockage at such flow restrictions in the ECCS flow path could impede or prevent the recirculation of coolant to the reactor core, thereby leading to inadequate core cooling." The overall objective of the evaluation by the licensees is to assure LTCC, thus, satisfying the requirements of 10 Code of Federal Regulations (CFR) 50.46 (Reference 2-2).

To support this objective, fuel assembly (FA) testing was performed under the initial Pressurized Water Reactor Owners Group (PWROG) program, to quantify the amount of post-LOCA debris that can be tolerated in the RV and core. The work completed under that program is summarized in WCAP-16793-NP-A, Rev. 2 (Reference 2-3). The FA testing showed that fibrous debris could accumulate and form debris beds at the core inlet and upstream edges of spacer grids near the core inlet that are within the region of the core containing single-phase liquid. When chemical precipitates were introduced during testing, the precipitates collected in the fibrous debris beds and, for certain debris loadings, stopped flow through the debris bed entirely. This result implied that flow to the core through the normal flow path may be impeded under certain post-LOCA scenarios. Consequently, additional work has been completed to examine the effectiveness of alternate flow paths (AFPs) to remove decay heat from the core when the core inlet is blocked by debris.

All U.S. PWRs have design flow paths in the RV that allow fluid to bypass the heated core during normal operations. Examples include the barrel/baffle (BB) channel (for upflow BB plants) and the upper head spray nozzles (UHSNs). Both the BB channel and the UHSNs provide a path for coolant to reach the core in the event that the core inlet becomes blocked with debris. In this context, these are termed AFPs as they provide an alternate path for coolant to bypass the core inlet and reach the core.

For many PWR designs, the BB channel connects the RV lower plenum (LP) to the RV upper plenum (UP). These designs are commonly referred to as "upflow" plants. CE, B&W, and some Westinghouse designs are upflow plants. In addition, all B&W plants and some Westinghouse upflow plants have communication between the BB region and the core peripheral FAs via pressure relief holes (also referred to as LOCA holes) in the baffle plates. In another Westinghouse design, referred to as a "downflow" plant, the top of the BB channel is connected to the downcomer and there is no appreciable flow path to allow communication between the BB region and the UP. For this design, the AFP credited in this analysis is the UHSNs, which connect the upper downcomer to the RV upper head and thus the UP and core. It is noted that Westinghouse upflow plants also have UHSNs that are modeled as part of this analysis.

The smallest holes in the BB and UHSN AFPs are much larger than debris that reaches the RCS, and testing described in Volume 6 confirms that these flow paths will not block with debris. However, additional analytical work is needed to demonstrate that these AFPs can provide sufficient flow to remove decay heat and maintain PCTs at acceptably low levels. Specifically, computer simulations were completed to assess the effectiveness of these AFPs in removing decay heat following a postulated large HLB LOCA with simulated core inlet blockage for the currently operating U.S. PWR fleet. The results of these simulations are used as acceptance criteria in subsequent debris testing as described in Volumes 5 and 6. Debris testing provides the link between what was modeled in the analysis and a physical debris limit. In addition, simulation results are used as inputs to the overall methodology that allows PWR licensees to calculate a plant specific in-vessel fibrous debris limit, as described in Volume 1.

2.2 TRANSIENT DESCRIPTION

PWR containment buildings are designed to contain radioactive material releases and facilitate core cooling in the event of a postulated LOCA. The cooling process requires clean coolant discharged from the refueling water storage tank (RWST[1]) and accumulators to initially reflood and cool the core. The RCS fluid and excess ECCS fluid that exits the break, along with the containment spray liquid and condensate, are collected in the containment sump for recirculation by the ECCS and CSS after the RWST empties. Typically, the containment sump contains one or more screens in series that filter(s) debris generated as a consequence of the LOCA that is dispersed within the sump liquid. Filtering of the ECCS flow removes some of the debris and protects the downstream RCS components, limiting the potential impact during the sump recirculation phase. Fibrous debris could form a mat on the sump screen that would collect particulates, keeping them from being ingested into the suction piping for ECCS and CSS pumps. However, while the fiber mat is forming, or for very large screens with significant open area, some particulates and fibrous material may pass through the sump screens and flow through the ECCS into the RCS.

During operation of the ECCS to recirculate coolant from the containment sump, debris in the recirculating fluid that passes through the sump screen(s) may collect on the bottom surface of the FAs or on spacer grids in the core region. It is postulated that the collection of sufficient debris at the core inlet forms a debris bed and impedes flow into the FAs and thus into the core.

The limiting scenario for debris blockage at the core inlet is a double-ended guillotine (DEG) break in a hot leg as discussed in Volume 1, Section 3.6. This scenario provides the largest fraction of ECCS flow to the core inlet and thus the largest amount of debris available for capture at the core inlet. Consequently, it has the highest propensity to form a highly-resistive bed at the core inlet. Therefore, assessment of the AFPs to provide sufficient coolant to the core to maintain LTCC after complete core inlet blockage will consider the large HLB scenario.

Observations from previous Generic Safety Issue - 191 (GSI-191) testing (Reference 2-3) indicate that complete core inlet blockage does not occur until chemical precipitates arrive in the RCS. The evolution

[1] The term RWST is specific to the Westinghouse plant design. In the B&W plant design, the like component is the borated water storage tank (BWST). In the CE plant design, the like component is the refueling water tank (RWT). In order to limit the complexity of the discussion, the Westinghouse plant components will be referenced throughout this report. Where the differences in design are important, they will be specifically discussed. Volume 1, Section 3.1 identifies and discusses the differences in plant components.

of debris bed formation begins upon entering sump recirculation. At that time, fiber and particulate debris contained in the sump fluid enter the RCS. The debris constituents are transported to the core inlet, where they have the potential to collect and develop resistive beds that reduce flow to the core but do not stop it completely. After some delay, chemical precipitates may begin to form in the sump liquid or ECCS and are transported to the RCS, where they have the potential to collect on any debris beds that may have formed at the core inlet. These chemical precipitates have the potential to fill any voids in the debris bed and completely block the core inlet. As a result, assessment of the AFPs is broken into two distinct phases of the post-LOCA transient. The first phase simulates the arrival and collection of fiber and particulate debris constituents at the core inlet and the second phase simulates arrival and collection of chemical precipitates at the core inlet that leads to complete core inlet blockage.

2.3 OBJECTIVES

The overall goal of this analysis is to evaluate the adequacy of RV AFPs at maintaining LTCC following switchover to sump recirculation and the postulated formation of a highly-resistive debris bed at the core inlet for a large HLB LOCA scenario. Achieving the overall goal requires the definition of specific objectives that will guide the evaluation process:

- Determine an appropriate and manageable number of plant models that will be used for the analysis. It is not practical or necessary to model every plant in the PWR fleet. Plants will be divided into categories with similar AFP designs. The categories analyzed and the basis for the selection is provided in Section 3.

- Define an appropriate analysis methodology and qualify the analysis models to meet traditional safety analysis requirements, including the critical model inputs and major assumptions. Determine and qualify values for those critical inputs that represent the specific category of plant type under consideration. The analysis methodology is described in Section 4 and a description of the computer codes and plant models used are provided in Sections 5 and 6, respectively.

- Document analytical results and provide output parameters that are used in the overall methodology described in Volume 1. It is expected that the output parameters will be different for each of the plant categories being analyzed. A summary of the analysis results for each plant category is provided in Sections 8 through 11. The output parameters are defined in Section 2.4.

2.4 OUTPUT PARAMETERS

Four output parameters from the simulations are used in the overall methodology contained in Volume 1. The simulations modeled the evolution of debris collection at the core inlet over a broad range of conditions to determine the following four parameters:

1. The minimum time that complete core inlet blockage can occur and meet the acceptance criteria defined in Section 2.5. This time is defined as t_{block} and represents the earliest possible time for which chemical precipitates can be tolerated on a completely-formed fiber and particulate debris bed at the core inlet, which is assumed to lead to complete core inlet blockage. This value is compared to results from chemical effects testing contained in Volume 5.

2. The maximum resistance at the core inlet that can occur prior to reaching complete core inlet blockage and meet the acceptance criteria defined in Section 2.5. This parameter is defined as K_{max} and represents the resistance of a bed comprised of only fibrous and particulate debris that can be tolerated from the time of sump switchover to the time that chemical precipitates arrive at the core inlet. This value is compared to the results from subscale head loss testing contained in Volume 6 to establish an upper bound on the amount of fibrous debris that can be tolerated at the core inlet.

3. The resistance at the core inlet that begins to divert flow into the AFP. This parameter is defined as K_{split} and is a function of ECCS flow rate. The subscale head loss testing defined a correlation between the amount of fiber and an equivalent form-loss coefficient, as discussed in Volume 1. K_{split} can then be used to define how much fiber accumulates at the core inlet before flow is diverted to the AFP.

4. The flow split between the core inlet and the AFP after K_{split}. This parameter is defined as m_{split}. Combined with K_{split} and the subscale head loss test results, m_{split} will be used to track the fraction of debris that bypasses the core inlet through the AFPs.

The use of these parameters in defining the final HLB debris limit is discussed in detail in Volume 1, Section 6.

2.5 ACCEPTANCE CRITERIA

The analysis acceptance criteria are developed to ensure LTCC after a postulated large HLB LOCA event. The two aspects of LTCC considered in this work that pertain to 10 CFR 50.46 (Reference 2-2) are:

1. Decay Heat Removal (DHR) - DHR requires that sufficient coolant be supplied to the core such that the core temperature is maintained at an acceptably low level. For previous GSI-191 evaluations, the maximum allowable post-quench PCT is 800°F (Reference 2-3). This conservative limit will be retained.

2. Boric Acid Precipitation Control (BAPC) - BAPC requires that boron concentrations in the RV remain below the solubility limit. For the large HLB scenario with core inlet blockage, BAPC requires demonstration of adequate break quality to flush boron from the RV and demonstration of adequate mixing within the RV to ensure effectiveness of the flushing flow.

2.6 REFERENCES

2-1 GL 2004-02, "Potential Impact of Debris Blockage on Emergency Recirculation During Design Basis Accidents at Pressurized-Water Reactors," ADAMS Accession Number ML042360586, September 2004.

2-2 10 CFR Part 50 §50.46, "Acceptance Criteria for Emergency Core Cooling Systems for Light Water Nuclear Reactors," 72 Federal Register 49494, August 28, 2007.

2-3 WCAP-16793-NP-A, Rev. 2, "Evaluation of Long-Term Cooling Considering Particulate, Fibrous and Chemical Debris in the Recirculation Fluid," July 2013.

3 PLANT CATEGORIES

For this evaluation, the PWR fleet can be broken into several categories. By doing so, the entire operating fleet can be represented by several manageable analyses.

The PWR fleet is first organized by NSSS vendor (Westinghouse, CE, and B&W) and then by BB design (design-upflow, converted-upflow, or downflow). The B&W, CE, and a portion of the Westinghouse fleet have upflow BB designs that provide a direct flow path between the lower support region and the UP (Figure 3-1 through Figure 3-3). Westinghouse design-upflow and B&W plants also have pressure relief holes (LOCA holes) that allow direct communication between the BB and core periphery.

Conversely, in Westinghouse downflow plants, the top of the BB channel is connected to the downcomer and there is no appreciable flow path to allow communication between the BB region and the UP (Figure 3-4). For this design, the AFPs credited are the UHSNs that connect the upper downcomer to the RV upper head and thus the UP and core (Figure 3-5). It is noted that Westinghouse upflow plants also have UHSNs that are modeled as part of this analysis. The flow area through the spray nozzles are categorized by the upper head temperature during normal operation. Two categories will be considered; T-cold and T-hot plant types. The T-cold design has a fairly large available flow area and low flow resistance between the downcomer and upper head, such that increased bypass flow can be expected and the upper head temperature is consistent with the cold side (i.e., cold leg) temperature. The T-hot design has smaller nozzle openings and will not provide as much bypass flow as the T-cold design, such that the upper head temperature is consistent with the hot side (i.e., hot leg) temperature.

Table 3-1 summarizes the PWR fleet BB and UHSN designs.

Table 3-1 Summary of PWR Fleet Alternate Flow Paths Considered in Analysis

NSSS Design	No. of Units[1]	Barrel/Baffle Design			Upper Head Spray Nozzle Design	
		Upflow	Converted Upflow	Downflow	T-Cold	T-Hot
Westinghouse 4-Loop	30	16	5	9	23	7
Westinghouse 3-Loop	13	2	5	6	2	11
CE	12	12	-	-	-	-
B&W	6	6	-	-	-	-
Total	61	36	10	15	25	18

Note: 1. The number of units includes Watts Bar Unit 2.

Since all B&W plants have low-resistance upflow BBs, one B&W design plant will be modeled. Since Westinghouse plants can have design-upflow, converted-upflow, and downflow BB designs, more than one analysis is required. At a minimum, an analysis that bounds all upflow (design or converted) and an analysis that bounds all downflow plants are necessary. CE plants will be assessed in a separate analysis.

Given these insights, four sets of analyses are needed to evaluate the AFPs:

1. Westinghouse design with upflow BB
2. Westinghouse design with downflow BB
3. CE design
4. B&W design

The first two sets of analyses were performed by Westinghouse and the third and fourth sets of analyses were performed by AREVA.

In order to bin all Westinghouse upflow plants into a single category, pressure relief holes are not modeled. The presence of pressure relief holes results in a less resistive flow path from the core support region, through the BB and into the core region. As a result, neglecting the pressure relief holes is conservative since the driving head necessary to flow coolant through the BB region and into the core is higher. The effect of pressure relief holes can be seen by comparing the results from the Westinghouse upflow plant category to the B&W plant category that models pressure relief holes.

The Westinghouse upflow plant category also models the presence of UHSNs. In order to limit the contribution to core inlet bypass flow through this AFP, the upflow plant model applies a T-hot upper head design which has a higher-resistance UHSN flow path. As a result, the quantity of bypass flow through the UHSNs in the Westinghouse upflow plant category after core inlet blockage is only a small fraction compared to the bypass flow through the BB channel. The analysis results for the Westinghouse upflow plant category demonstrate that the BB bypass flow is sufficient to meet the LTCC acceptance criteria defined in Section 2.5 and the bypass flow through the UHSNs is not credited.

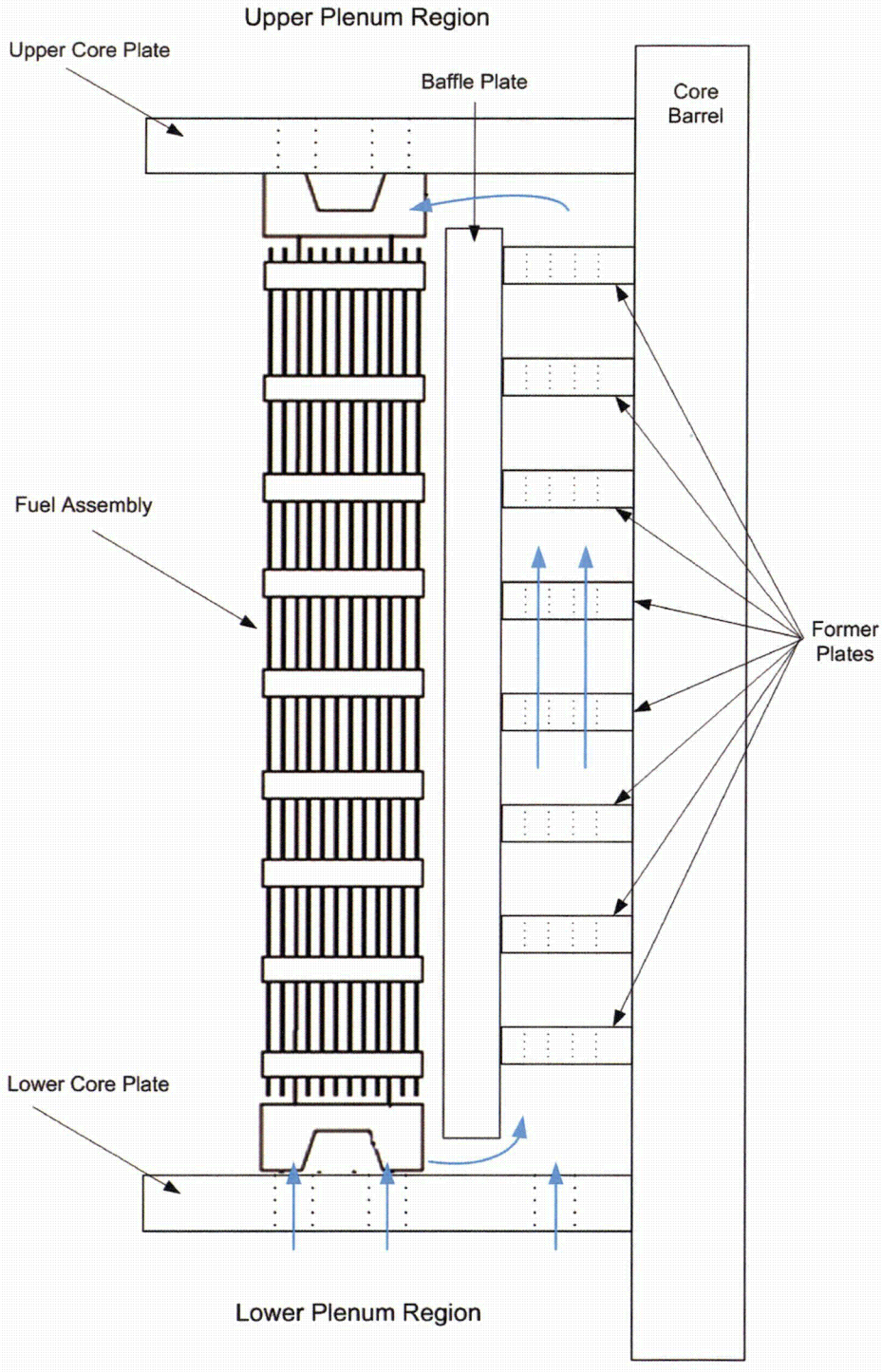

Figure 3-1 Westinghouse Upflow Barrel/Baffle Design (No Pressure Relief Holes)

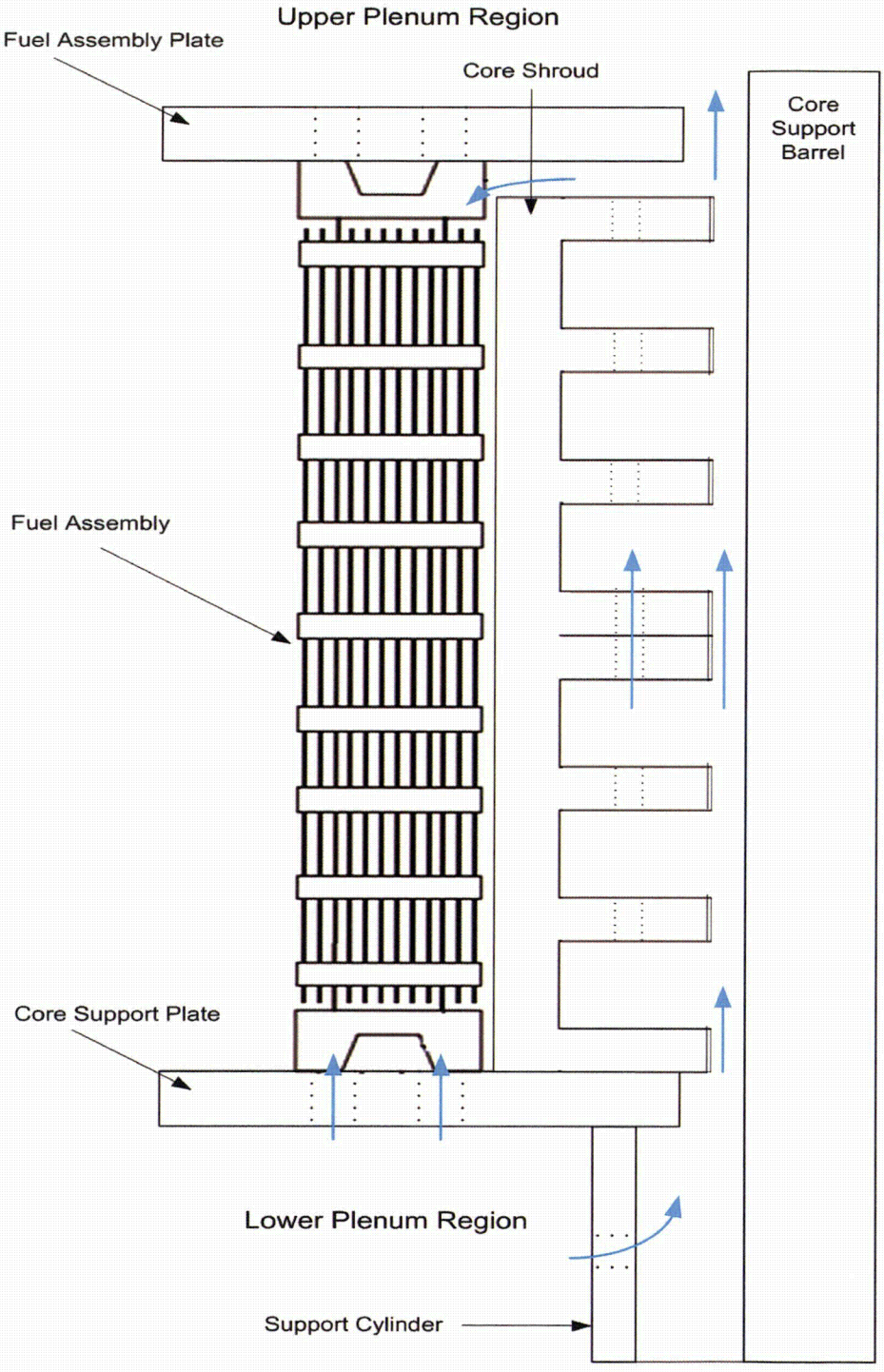

Figure 3-2 CE Barrel/Baffle Design

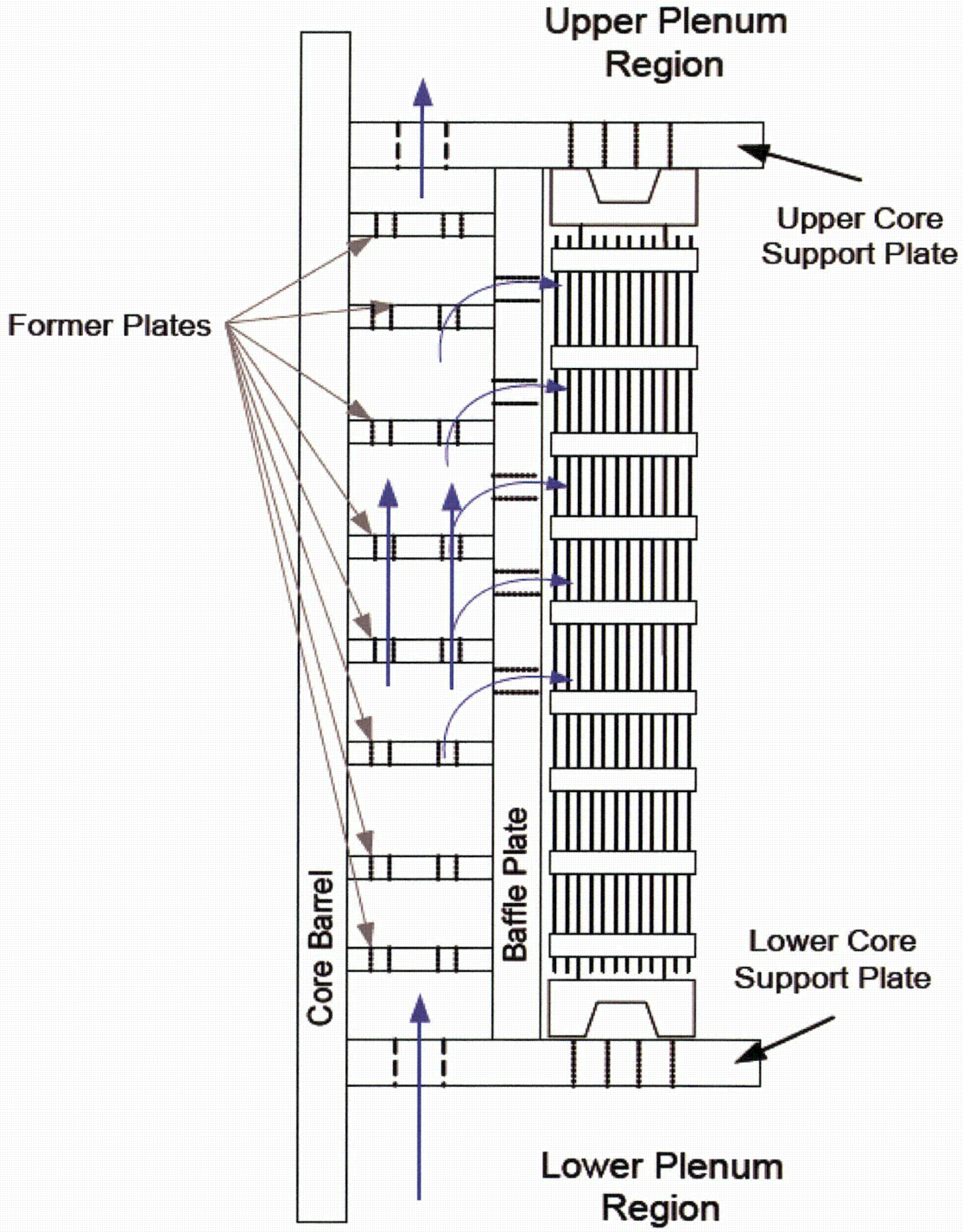

Figure 3-3 B&W Barrel/Baffle Design

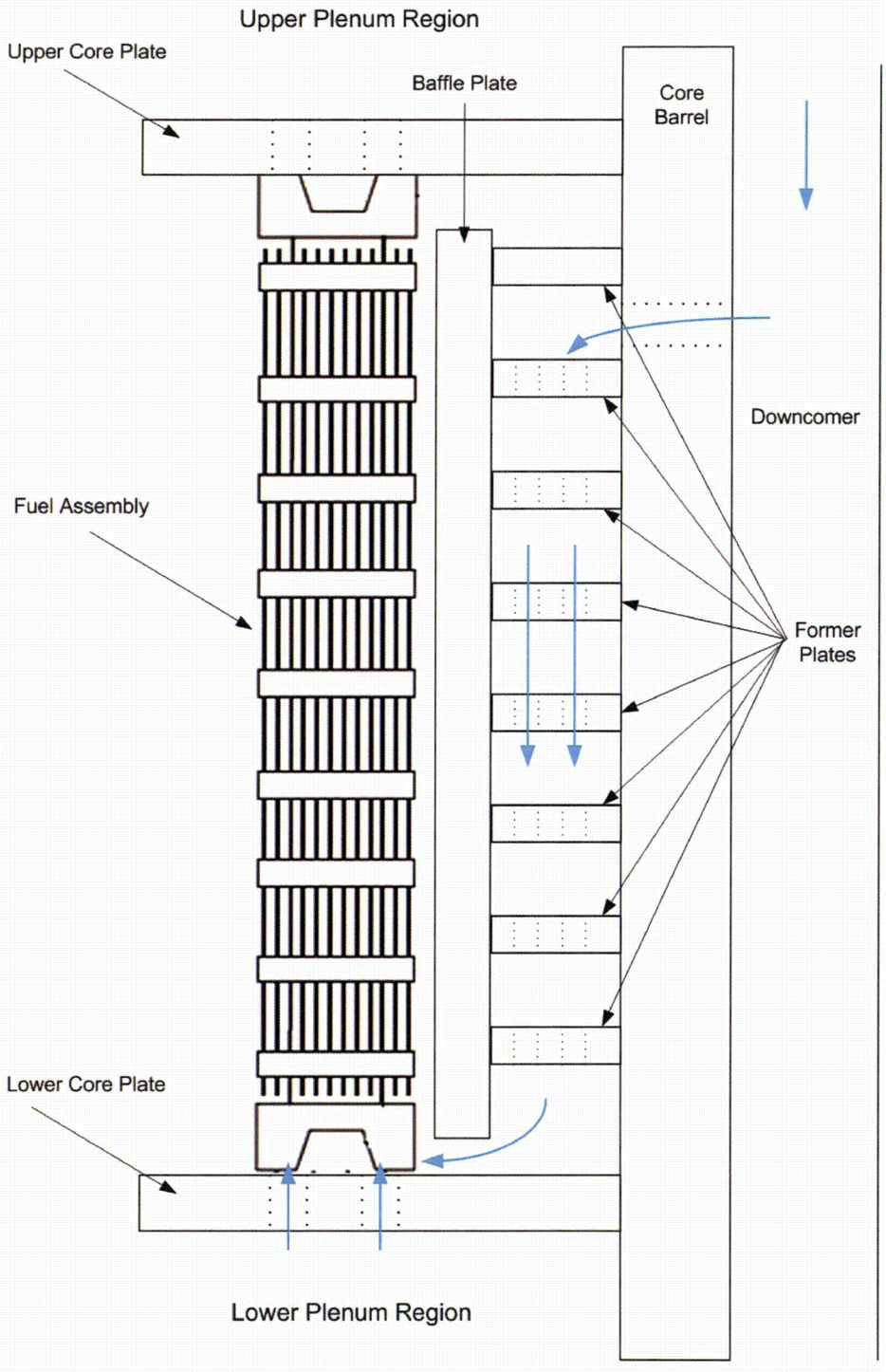

Figure 3-4 Westinghouse Downflow Barrel/Baffle Design

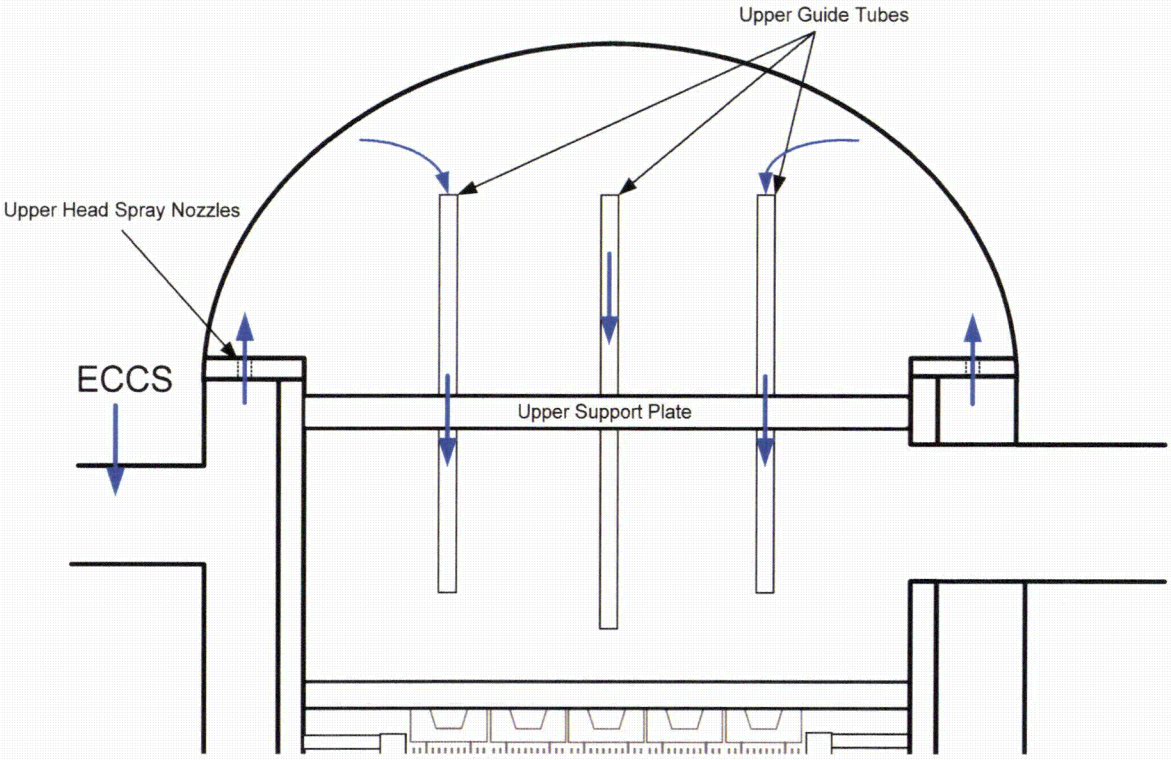

Figure 3-5 Westinghouse Upper Head Spray Nozzle Design

4 METHODOLOGY

In this section, the methodology for evaluating AFPs during the sump recirculation phase of the post-LOCA transient following a postulated large HLB is presented. This is a generic methodology that applies to all plant categories.

The generic methodology is summarized below:

- Identification of Important Phenomena and Critical Inputs

The first step in the methodology is to identify important physical phenomena expected during the phase of the post-LOCA transient under consideration and to derive a list of critical inputs. Completing this step provides the basis for selection of the computer codes and plant models used by the analysis. For this scope of work, the most important phase of the transient is during sump recirculation, when the plant is injecting coolant from the ECCS into the cold legs because this is the phase of the transient when the majority of debris enters the RV. A phenomena identification and ranking table (PIRT) was completed as part of this program (Volume 2) and was used to identify the most important physical phenomena affecting the RCS response to core inlet blockage during this phase of the post-LOCA transient.

A list of critical inputs is provided in Section 4.2. The list was defined by considering the most important parameters for this evaluation. Values for these inputs were then carefully considered during the model development phase to ensure overall conservatism in the resulting model predictions.

- Selection of Computer Codes and Methods

In this step, the computational tools and methods used as a starting point for the analysis were selected. The GSI-191 PIRT contained in Volume 2 and the list of critical inputs was used to establish criteria to assess the capabilities of the available computer codes and methods. Other considerations were given to vendor code availability, experience, existing code models and pedigree. It was determined that NRC-approved LOCA evaluation models (EMs) and code packages provide an appropriate starting point for all plant categories. A description of the computer codes and methods used for these analyses is presented in Section 5. It was determined that all computer codes and methods utilized have the ability to accurately predict the RCS response to simulated core inlet blockage during the sump recirculation phase of the post-LOCA transient.

- Selection of Base Plant Models

In this step, a base plant model was selected. For all plant categories, a plant model originally developed for licensing basis analysis of the short-term LOCA transient (PCT and clad oxidation) was selected. Review of these models indicates a high level of noding detail to ensure accurate simulation of the post-LOCA transient into the LTCC phase. Further, these models were developed and are maintained under 10 CFR 50 Appendix B (Reference 4-1) guidelines.

When reviewing the models, emphasis was placed on modeling of the AFPs being considered in this scope of work. The age of the plant model was also considered. Since both vendors frequently update

their LOCA guidelines, selection of a newer model ensured that the highest fidelity models were utilized. Further details on the category-specific base plant models are available in Section 6.

- Selection of Plant Operating Conditions

Since the entire PWR operating fleet is binned into four distinct plant categories, a review of the PWR fleet operating conditions is required to define appropriate conditions to be applied to each analysis. The parameters considered are based on the critical input list developed as part of the methodology. A set of these parameters is chosen as initial conditions for each plant category model. For parameters that vary across the PWR fleet, (e.g. ECCS flow) a range of values has been defined for each plant category model. For other parameters (e.g. resistance at the core inlet due to the collection of debris), sensitivity analyses were performed using a range of values. Based on these parametric variations and sensitivity analyses, the most limiting input conditions are combined into the model and will represent the limiting state for each plant category.

4.1 MAJOR ASSUMPTIONS

The following major assumptions are applied to the analysis discussed herein. Additional assumptions, specific to each plant category, may also be discussed in the model descriptions contained in Section 6.

1. The code simulations assume that sump debris will collect across the core inlet in a uniform manner and blockage is only considered at the core inlet. This is a simplifying, conservative assumption. In reality, it is expected that the collection of debris at the core inlet will follow the flow distribution at the core inlet. Some regions of the core with higher-power will have a higher flow at the core inlet, while other regions of the core with lower-power will have lower flow (or even downflow) at the core inlet. (See Volume 1, Section 3.3.1 for additional discussion.) From a DHR standpoint, applying a uniform build-up at the core inlet is more challenging as was demonstrated in the TH analysis contained in WCAP-16793-NP-A, Rev. 2 (Reference 4-2).

2. Fluid properties of pure water will be assumed. During the LTCC phase of the post-LOCA transient, the build-up of solute concentrations in the inner regions of the RV changes the fluid properties. If the concentrations reach high enough levels, the effect on fluid properties may need to be considered. Since these analyses will simulate a large HLB scenario, it is expected that the liquid carryover out the break will be sufficient to limit the concentration build-up of solutes in the RV and thus limit the influence on fluid properties. This assumption is justified by the simulation results discussed in Sections 8 through 11.

3. In some cases an "instantaneous" ramp of core inlet resistance will be considered. The instantaneous ramp will occur over a one-minute period to aid in code stability. The modeling of debris build-up over one minute is a non-realistic condition since debris transport from the sump to the core inlet occurs over a longer period of time. This modeling approach creates a worst case scenario and bounds any realistic debris build-up rate that a specific plant might encounter. In other cases, a longer ramp period will be considered; i.e., it will be assumed that the resistance due to the build-up of debris occurs over a more realistic time period.

4. A top-skewed power shape is assumed to be most limiting for core uncovery and cladding heatup. The uncovery process is governed by boil-off and subsequent dry out that begins at the top of the core and propagates downward. Using a top-skewed power shape will maximize cladding heatup and provide the most challenge for meeting the 800°F acceptance criterion.

5. It is assumed that the guide thimble tubes in the FAs are blocked, and thus no bypass flow through the tubes will be credited. This assumption removes an additional potential path for fluid to bypass the core inlet and reach the core region after core inlet blockage.

6. The ECCS temperature during sump recirculation will be set at or near saturation temperature at containment pressure. Ice condenser plants will likely have some subcooling in the containment sump at the time of sump switchover, while other plants with residual heat removal (RHR) heat exchangers in operation could have subcooled ECCS entering the cold legs during the recirculation phase. Neglecting the presence of subcooling is conservative because it maximizes the steaming rate in the core and minimizes the cooldown rate of the RV and steam generators (SGs).

7. The code simulations assume that the secondary side is isolated and not depressurized, consistent with the short-term LOCA analysis approach. This creates a high secondary side temperature that helps to inhibit flooding the SG on the primary side such that SG spillover, if predicted, is limited in magnitude and delayed in time.

4.2 CRITICAL INPUTS

The following critical inputs are considered in the analyses discussed herein. Additional inputs specific to each plant category may also be discussed in the model descriptions contained in Section 6.

1. Barrel/Baffle Flow Resistance – For all plant categories with an upflow BB configuration, both the maximum and minimum BB flow resistance that bound all plants in the category are examined.

    a. To determine K_{max} and t_{block}, selecting the maximum resistance will require the largest driving head to force flow through the BB and into the core region. If it can be shown that a highly-resistive BB channel provides adequate bypass flow to achieve LTCC, then lower resistance BBs will do the same due to the consequent higher flow through the BB channel.

    b. To determine K_{split} and m_{split}, selecting the minimum resistance will minimize the resistance due to debris (and hence the amount of debris at the core inlet) that will begin to divert flow to the AFP. Minimizing the debris at the core inlet required to divert flow to the AFP will maximize the amount of debris predicted to bypass the core inlet and transport to the core region through the AFP.

2. Upper Head Spray Nozzle Resistance – For the Westinghouse downflow plant category, the UHSN flow resistance will be adjusted similar to the BB flow resistance. The UHSNs will be modeled using a maximum flow resistance for cases that are used to determine K_{max} and t_{block} and

a minimum flow resistance will be applied for cases that are used to determine K_{split} and m_{split}. The maximum flow resistance cases will effectively model a T-hot upper head plant, while the minimum flow resistance cases will model a T-cold upper head plant.

The UHSN resistance is also considered for the Westinghouse upflow plant category. Since the primary AFP considered for this plant category is the BB channel, the UHSN resistance is set to a large value such that any bypass flow through the UHSNs is minimized. This approach is conservative, since limiting bypass flow through the UHSNs requires more bypass flow through the BB channel for DHR.

3. Core Power – The 10 CFR 50 Appendix K Decay Heat Model (1.2 times the 1971 ANS Infinite Standard [Reference 4-3]) will be used (or bounded). Appendix K decay heat will generate the highest steaming rate which maximizes the flow requirements for DHR. As discussed in the major assumptions, a top-skewed power shape is applied.

4. Switchover Time to Sump Recirculation – A minimum switchover time will be used such that the decay heat will be maximized at the time core inlet blockage occurs. This input maximizes the core flow requirement to remove decay heat.

5. Break Flow – To maximize break flow during the recirculation phase, the pressure boundary condition at the break will be set to 14.7 psia, or some other low pressure justified by a containment analysis, during the recirculation phase of the event.

6. Cold leg ECCS Flow – For each category of plants, a range of ECCS flows is selected that represents all plants in the category. In all cases, the ECCS fluid temperature is set at or near the saturation temperature at containment pressure. Doing so will maximize the steaming rate in the core as well as the cooldown rate of the RV and SGs.

7. Core Inlet Blockage – All core channels will be blocked uniformly at the same time and blockage will begin as early as possible after the sump switchover time. The added resistance will be ramped up such that it takes a finite period of time to reach "complete" core inlet blockage. The ramp rates will be varied as part of the analysis.

4.3 REFERENCES

4-1 10 CFR Part 50, Appendix B to Part 50, "Quality Assurance Criteria for Nuclear Power Plants and Fuel Reprocessing Plants," 72 Federal Register 49505, August 28, 2007.

4-2 WCAP-16793-NP-A, Rev. 2, "Evaluation of Long-Term Cooling Considering Particulate, Fibrous and Chemical Debris in the Recirculation Fluid," July 2013.

4-3 10 CFR Part 50, Appendix K to Part 50, "ECCS Evaluation Models," 65 Federal Register 34921, June 1, 2000.

5 DESCRIPTION OF COMPUTER CODES AND METHODS

In this section, the computer codes and methods used for the analysis starting point are identified and described. All codes and methods used as the starting point for these analyses are NRC-approved for licensing basis analysis of the short-term LOCA transient (PCT and clad oxidation). The section is broken into four subsections. The first three subsections describe the different computer codes and methods used to analyze the different plant categories. The fourth subsection describes a set of analyses completed for the same plant and transient condition but with different codes and methods.

5.1 WESTINGHOUSE PLANT CATEGORIES

The WCOBRA/TRAC computer code was used to analyze the Westinghouse upflow and downflow plant categories. The COBRA/TRAC code was originally developed at Pacific Northwest Laboratory (Reference 5-1) by combining the COBRA-TF code (Reference 5-2) and the TRAC-PD2 codes (Reference 5-3). The COBRA-TF code, which has the capability to model three-dimensional flow behavior in a RV, was incorporated into TRAC-PD2 to replace its vessel model. TRAC-PD2 is a systems transient code designed to model all major components in the primary system. Westinghouse continued to make modifications and improvements to COBRA/TRAC and renamed the revised code WCOBRA/TRAC. Development of WCOBRA/TRAC continued to extend its application to three- and four-loop Westinghouse PWRs with cold leg injection with version MOD7A. This computer code is described in WCAP-14747, referred to as the Code Qualification Document (CQD) (Reference 5-4) as well as WCAP-16009-NP-A, which describes the ASTRUM methodology (Reference 5-5). Both the CQD and ASTRUM methodologies are approved by the NRC for short-term LOCA analysis. Version MOD7A is the baseline computer code utilized for this scope of work.

In order to simulate transient resistance at the core inlet due to the build-up of debris, it was necessary to modify the baseline WCOBRA/TRAC version. The code modification allows for the dimensionless form-loss coefficient, C_D, to be ramped in time at the first node of specified core channels. The single-application code version ramps the value of the loss coefficient by a specified amount for a specified channel over a specified amount of time. This was the only modification made to WCOBRA/TRAC for this analysis.

WCOBRA/TRAC combines two-fluid, three-field and multi-dimensional fluid equations used in the vessel with one-dimensional drift-flux equations used in the loops to allow a complete and detailed simulation of a PWR. This computer code contains the following features:

1. Ability to model transient three-dimensional flows in different geometries inside the vessel
2. Ability to model thermal and mechanical non-equilibrium between phases
3. Ability to mechanistically represent interfacial heat, mass, and momentum transfer in different flow regimes
4. Ability to represent important reactor components such as fuel rods, SGs, reactor coolant pumps (RCPs), etc.

The two-fluid formulation uses a separate set of conservation equations and constitutive relations for each phase. The effects of one phase on another are accounted for by interfacial friction and heat and mass transfer interaction terms in the equations. The conservation equations have the same form for each phase; only the constitutive relations and physical properties differ. Dividing the liquid phase into two fields is a convenient and physically accurate way of handling flows where the liquid can appear in both film and droplet form. The droplet field permits more accurate modeling of TH phenomena, such as entrainment, de-entrainment, fallback, liquid pooling, and flooding.

WCOBRA/TRAC also features a two-phase, one-dimensional hydrodynamics formulation. In this model, the effect of phase slip is modeled indirectly via a constitutive relationship that provides the phase relative velocity as a function of fluid conditions. Separate mass and energy conservation equations exist for the two-phase mixture and for the vapor.

The RV is modeled with the three-dimensional, three-field model, while the loops, major loop components, and safety injection points are modeled with the one-dimensional model.

All geometries modeled using the three-dimensional model are represented as a matrix of cells. The number of mesh cells used depends on the degree of detail required to resolve the flow field, the phenomena being modeled, and practical restrictions such as computing costs and core storage limitations.

The equations for the flow field in the three-dimensional model are solved using a staggered difference scheme on the Eulerian mesh. The velocities are obtained at mesh cell faces, and the state variables (e.g., pressure, density, enthalpy, and phasic volume fractions) are obtained at the cell center. This cell is the control volume for the scalar continuity and energy equations. The momentum equations are solved on a staggered mesh with the momentum cell centered on the scalar cell face.

The basic building block for the mesh is the channel, a vertical stack of single mesh cells. Several channels can be connected together by gaps to model a region of the RV. Regions that occupy the same level form a section of the vessel. Vessel sections are connected axially to complete the vessel mesh by specifying channel connections between sections. Heat transfer surfaces and solid structures that interact significantly with the fluid can be modeled with rods and unheated conductors.

One-dimensional components are connected to the vessel. The basic scheme used also employs the staggered mesh cell. The one-dimensional components consist of all the major components in the primary system, such as pipes, pumps, valves, SGs, and the pressurizer. The one-dimensional components are represented by a two-phase, five-equation, drift flux model. This formulation consists of two equations for the conservation of mass, two equations for the conservation of energy, and a single equation for the conservation of momentum. Closure for the field equations requires specification of the interphase relative velocities, interfacial heat and mass transfer, and other thermodynamic and constitutive relationships.

5.2 COMBUSTION ENGINEERING PLANT CATEGORY

The S-RELAP5 computer code was used to analyze the CE plant category. AREVA has developed S-RELAP5, a RELAP5-based TH system code, for performing realistic analyses of a large break LOCA

(LBLOCA) in PWRs as described in [ ]^{a,c}. The code is also suitable for analyzing PWR small break LOCA (SBLOCA) and non-LOCA transients. Most recently, AREVA has expanded the capability of S-RELAP5 for analyzing events and phenomena in boiling water reactors (BWRs).

RELAP5 is a light water reactor (LWR) transient analysis code developed at the Idaho National Engineering Laboratory (INEL) for the NRC. The series of RELAP5 codes released are RELAP5/MOD1, RELAP5/MOD2, and RELAP5/MOD3. S-RELAP5 incorporates features of RELAP5/MOD2 and RELAP5/MOD3, and AREVA's improvements. In general, the improvements and modifications included are those required to provide congruency with literature correlations and those required to obtain adequate simulation of key LOCA and non-LOCA experiments.

RELAP5 is a general-purpose code that, in addition to calculating the behavior of a RCS during a transient, can be used for simulation of a wide variety of hydraulic and thermal transients in both nuclear and non-nuclear systems involving mixtures of steam, water, non-condensable gas, and solute. The RELAP5 code is built on a non-homogeneous and non-equilibrium model for the two-phase system. The original objective of the RELAP5 development effort was to produce a code that includes important first order effects necessary for accurate prediction of system transients but that is sufficiently simple and cost effective so that parametric and sensitivity studies are feasible.

The base RELAP5 code includes hydrodynamic models, heat transfer and heat conduction models, a fuel model, a point reactor kinetics model, a control system and a trip system. It uses two-fluid, non-equilibrium, non-homogeneous field equations for transient simulation of the two-phase thermal-hydrodynamic behavior. The hydrodynamic models also include many generic component models such as pumps, valves, separators, jet pumps, turbines and accumulators, and some special-process models such as form-loss of abrupt area changes, critical flow and counter-current flow limit. The system mathematical models are solved by efficient numerical schemes to permit cost-effective computations. The code also includes many user conveniences such as extensive input checking capability to help users detect input errors and inconsistencies, free-format input, restart, renodalization, minor and major edits, and plot variables for interface with plotting tools.

The S-RELAP5 code evolved from AREVA ANF-RELAP code, a modified RELAP5/MOD2 version, used at AREVA for performing PWR plant licensing analyses including SBLOCA analysis, steam line break analysis, and PWR non-LOCA Chapter 15 event analyses. The code structure for S-RELAP5 was modified to be essentially the same as that for RELAP5/MOD3, with similar code-portability features. Since then, numerous improvements, new models and new capabilities have been implemented and incorporated into S-RELAP5 to support various methodologies.

5.3 BABCOCK AND WILCOX PLANT CATEGORY

The RELAP5/MOD2-B&W computer code [ ]^{a,c} was used to analyze the B&W plant category. RELAP5/MOD2 is an advanced system analysis computer code designed to analyze a variety of TH transients in LWR systems. It was developed by INEL under the NRC Advanced Code Program. RELAP5/MOD2 is advanced over its predecessors by its six-equation, full non-equilibrium, two-fluid model for the vapor-liquid flow field and partially implicit numerical integration scheme for more rapid execution. As a system code, it provides simulation capabilities for the reactor primary coolant system, secondary system, feedwater trains, control systems, and core neutronics. Special component models

include pumps, valves, heat structures, electric heaters, turbines, separators, and accumulators. Code applications include the full range of safety evaluation transients, LOCAs, and operating events.

The RELAP5/MOD2 hydrodynamic model is a one-dimensional, transient, two-fluid model for flow of a two-phase steam-water nature which can contain a non-condensable component in the steam phase and/or a nonvolatile component in the water phase. The major change from the RELAP5/MOD1 model is the addition of a second energy equation, which eliminates the need to constrain one phase at the saturated state. Other improvements include a revised interphase drag formulation, a new non-equilibrium wall heat transfer model, a revised wall friction partitioning model, a revised vapor generation model that includes wall heat transfer considerations, and the addition of several new special process/component models.

The RELAP5/MOD2 hydrodynamic model contains several options for simpler hydrodynamic models. These include homogeneous flow, thermal equilibrium, and frictionless-flow models. These options can be used independently or in combination. The homogeneous and equilibrium models were included primarily to be able to compare code results with results from the older homogeneous equilibrium model base codes.

The two-fluid equations of motion, which are used as the basis for the RELAP5/MOD2 hydrodynamic model, are formulated in terms of area- and time-average parameters of the flow. Phenomena that depend upon transverse gradients, such as friction and heat transfer, are formulated in terms of the bulk potentials using empirical transfer coefficient formulations. The system model is solved numerically using a semi-implicit finite difference technique. The basic two-fluid differential equations possess the property of complex characteristic roots, which gives the system a partially elliptic character and thus constitutes an ill-posed initial-boundary value problem. In RELAP5, the numerical problem is rendered well-posed by the introduction of artificial viscosity terms in the difference equation formulation, which dampen the high-frequency spatial components of the solution.

Heat structures provided in RELAP5 permit calculation of the heat transferred across solid boundaries of hydrodynamic volumes. Modeling capabilities of heat structures are general and include fuel pins or plates with nuclear or electrical heating, heat transfer across SG tubes, and heat transfer from pipe and vessel walls. Heat structures are assumed to be represented by one-dimensional heat conduction in rectangular, cylindrical, or spherical geometry. Surface multipliers are used to convert the unit surface of the one-dimensional calculation to the actual surface of the heat structure. Temperature-dependent thermal conductivities and volumetric heat capacities are provided in tabular or functional form either from built-in or user-supplied data.

Finite differences are used to advance the heat-conduction solutions. Each mesh interval may contain different mesh spacing and a different material, or both. The spatial dependence of the internal heat source may vary over each mesh interval. The time-dependence of the heat source can be obtained from reactor kinetics, one of several tables of power versus time, or a control system variable. Symmetry or insulated condition and tables of surface temperature versus time, heat transfer rate versus time, heat transfer coefficient versus time, or surface temperature are allowed. For heat structure surfaces connected to hydrodynamic volumes, a heat transfer package, containing correlations for convective, nucleate boiling, transition boiling, and film heat transfer from the wall to water and reverse transfer from water to wall, is provided.

RELAP5/MOD2 has been adopted and modified by AREVA for licensing and best estimate (BE) analyses of PWR transients in both the LOCA and non-LOCA categories. RELAP5/MOD2-B&W retains virtually all of the features of the original RELAP5/MOD2. Certain modifications have been made to enhance the predictive capabilities of the constitutive models and/or to improve code execution. More significant, however, are the AREVA additions to RELAP5/MOD2 models and features to meet the 10 CFR 50 Appendix K requirements for ECCS EMs. The Appendix K modifications are concentrated in the following areas: (1) critical flow and break discharge, (2) fuel pin heat transfer correlations and switching, and (3) fuel clad swelling and rupture for both zircaloy and zirconium-based alloy cladding types.

5.4 ANALYSIS OF WESTINGHOUSE DOWNFLOW PLANT CATEGORY USING S-RELAP5

During the initial development phase of this project, a simulation of the downflow plant category was completed by AREVA using S-RELAP5. The plant and transient condition analyzed was identical to that used by Westinghouse. The plant models used for each analysis were developed independently following different methods and techniques. The analysis completed by AREVA using S-RELAP5 produced results that compared reasonably well to those predicted by WCOBRA/TRAC, which are described in Section 9. This demonstrates that, irrespective of the computer codes and methods used, the resulting code predictions are expected to be consistent.

5.5 REFERENCES

5-1 NUREG/CR-3046, "COBRA/TRAC – A Thermal-Hydraulics Code for Transient Analysis of Nuclear Reactor Vessels and Primary Coolant Systems," 1983.

5-2 Thurgood, M. J., et al., "COBRA-TF Development," 8th Water Reactor Safety Information Meeting, 1980.

5-3 NUREG/CR-2054, "TRAC-PD2, An Advanced Best-Estimate Computer Program for Pressurized Water Reactor Loss-of-Coolant Accident Analysis," 1981.

5-4 WCAP-14747 (Non-Proprietary), "Code Qualification Document for Best-Estimate LOCA Analysis," 1998.

5-5 WCAP-16009-NP-A, "Realistic Large Break LOCA Evaluation Methodology Using the Automated Statistical Treatment of Uncertainty Method (ASTRUM)," January 2005.

5-6 [

]a,c

5-7 [

]a,c

6 DESCRIPTION OF PLANT MODELS

In this section, the plant models used to analyze each plant category are identified and described. The description includes major changes made to the base plant models to accommodate this scope of work, which includes changes to the AFP resistances to bound all plants in a specific category. The plant models are discussed for each of the four plant categories in the following subsections.

6.1 WESTINGHOUSE UPFLOW PLANT MODEL

The base plant model selected for the Westinghouse upflow analysis is a high-power, four-loop plant with a T-hot upper head configuration. The base plant model was developed for BE PCT and clad oxidation analysis. Since the base plant model was developed for BE analysis, many of the model non-critical inputs are set to nominal values. For this reason, some changes were made to bias the model toward an Appendix K analysis. Doing so has added conservatism to the model to account for uncertainties associated with the LTCC phase of the post-LOCA transient.

The major changes to the base plant model are discussed in further detail below:

- Break Location

For this analysis, a DEG HLB is modeled. Since the base plant model simulated a DEG cold leg break (CLB), the location had to be moved. This was completed by moving break components from the cold side of the broken loop to the hot side. The loop containing the pressurizer remained intact. This change also required that an accumulator and ECCS model be input into the broken loop such that ECCS flow from all loops was considered.

- Decay Heat Model

The BE decay heat model was replaced with the 1971 ANS infinite + 20% (Appendix K Standard).

- Core Region Interfacial Drag

It is known that the version of WCOBRA/TRAC utilized tends to over predict two-phase mixture level swell in the core under low pressure pool boiling conditions (Reference 6-1). To account for this, a multiplier on the core axial interfacial drag is applied consistent with the approach taken in Reference 6-1. The resulting reduced interfacial drag in the axial direction within the core region better predicts the void fraction and two-phase mixture level swell for low pressure boil-off conditions.

- ECCS Model

Since this analysis extends the simulation into the sump recirculation phase, additional trips and fills were added to the ECCS model to simulate switchover from RWST injection to sump recirculation.

- Barrel/Baffle Flow Resistance

In order to represent all Westinghouse upflow plants in operation in the U.S., a method was developed to calculate appropriate BB flow resistances for use in this analysis. The method and supporting calculations are contained in [ ]^{a,c}, which confirms that the BB flow resistances shown in Table 6-1 bound all Westinghouse upflow plants.

- Break Pressure Boundary Condition

The pressure boundary condition at the break was not changed for the short-term LOCA simulation. However, to extend the simulation beyond reflood, the pressure boundary was set to 14.7 psia to maximize break flow during the recirculation phase.

- Core Inlet Blockage

The dimensionless form-loss coefficient at the first core node was adjusted to simulate the build-up of debris during the recirculation phase of the transient. The flow area at the first core node is [ ]^{a,c} per FA which corresponds to the flow area through the [ ]^{a,c}. The value of the form-loss coefficient was varied from case-to-case. Tables 8-1 and 8-2 list the form-loss coefficient values applied for the various simulations.

The key inputs for this analysis are summarized in Table 6-1. These inputs are used for all simulations shown in Tables 8-1 and 8-2.

Table 6-1 Summary of Key Inputs – Westinghouse Upflow Barrel/Baffle Plant Design

Parameter	Analysis Value
Core Power including Uncertainty (MWt)	3658
Number of Loops	4
Number of Fuel Assemblies	193
Barrel/Baffle Total K/A^2 (ft^{-4})	[ ]^{a,c} (Max Resistance Cases) [ ]^{a,c} (Min Resistance Cases)
Upper Head Spray Nozzle Total K/A^2 (ft^{-4})	[ ]^{a,c}
Total Peaking (F_Q)	2.30
Radial Peaking ($F_{\Delta H}$)	1.80
Axial Peak Power Location	Top Axial Skew – 9 ft
ECCS Recirculation Flow Rate (gpm/FA)[1]	40, 30, 18, 12, 8
Containment Pressure during Recirculation Phase (psia)	14.7
ECCS Temperature after Sump Switchover (°F)	212
Sump Switchover Time (min)	20

Note: 1. Only the 40 and 18 gpm/FA flows are used for the max resistance cases.

6.2 WESTINGHOUSE DOWNFLOW PLANT MODEL

The base plant model selected for the Westinghouse downflow analysis is a high-power, three-loop plant with a T-hot upper head configuration. The base plant model was developed for BE PCT and clad oxidation analysis. Since the base plant model was developed for BE analysis, many of the model inputs are set to nominal values. For this reason, some changes were made to bias the model toward an Appendix K analysis. Doing so has added conservatism to the model to account for uncertainties associated with the LTCC phase of the post-LOCA transient.

The major changes to the base plant model are discussed in further detail below:

- Break Location

For this analysis, a DEG HLB is modeled. Since the base plant model simulated a DEG CLB, the location had to be moved. This was completed by moving break components from the cold side of the broken loop to the hot side. The loop containing the pressurizer remained intact. This change also required that an accumulator and ECCS model be input into the broken loop such that ECCS flow from all loops was considered.

- Decay Heat Model

The BE decay heat model was replaced with the 1971 ANS infinite + 20% (Appendix K Standard).

- Core Region Interfacial Drag

It is known that the version of WCOBRA/TRAC utilized tends to over predict two-phase mixture level swell in the core under low pressure pool boiling conditions (Reference 6-1). To account for this, a multiplier on the core axial interfacial drag is applied consistent with the approach taken in Reference 6-1. The resulting reduced interfacial drag in the axial direction within the core region better predicts the void fraction and two-phase mixture level swell for low pressure boil-off conditions.

- ECCS Model

Since this analysis extends the simulation into the sump recirculation phase, additional trips and fills were added to the ECCS model to simulate switchover from RWST injection to sump recirculation.

- Upper Head Spray Nozzle Flow Resistance

In order to represent all Westinghouse downflow plants in operation in the U.S., a method was developed to calculate appropriate UHSN flow resistances for use in this analysis. The method and supporting calculations are contained in [ ]^{a,c}, which confirms that the UHSN flow resistances shown in Table 6-2 bound all Westinghouse downflow plants.

- Break Pressure Boundary Condition

The pressure boundary condition at the break was not changed for the short-term LOCA simulation. However, to extend the simulation beyond reflood, the pressure boundary was set to 14.7 psia to maximize break flow during the recirculation phase.

- Core Inlet Blockage

The dimensionless form-loss coefficient at the first core node was adjusted to simulate the build-up of debris during the recirculation phase of the transient. The flow area at the first core node is [ ]^{a,c} per FA which corresponds to the flow area through the [ ]^{a,c}. The value of the form-loss coefficient was varied from case-to-case. Tables 9-1 and 9-2 list the form-loss coefficient values applied for the various simulations.

The key inputs for this analysis are summarized Table 6-2. These inputs are used for all simulations shown in Table 9-1 and Table 9-2.

Table 6-2 Summary of Key Inputs – Westinghouse Downflow Barrel/Baffle Plant Design

Parameter	Analysis Value
Core Power including Uncertainty (MWt)	2951
Number of Loops	3
Number of Fuel Assemblies	157
Barrel/Baffle Total K/A^2 (ft^{-4})	[ ]^{a,c}
Upper Head Spray Nozzle Total K/A^2 (ft^{-4})	[ ]^{a,c} (Max Resistance Cases) [ ]^{a,c} (Min Resistance Cases)
Total Peaking (F_Q)	2.30
Radial Peaking ($F_{\Delta H}$)	1.80
Axial Peak Power Location	Top Axial Skew – 9 ft
ECCS Recirculation Flow Rate (gpm/FA)[1]	40, 30, 18, 12, 8
Containment Pressure during Recirculation Phase (psia)	14.7
ECCS Temperature during Recirculation Phase (°F)	212
Sump Switchover Time (min)	20

Note: 1. Only the 40 and 12 gpm/FA flows are used for the max resistance cases.

6.3 COMBUSTION ENGINEERING PLANT MODEL

The base plant model selected for the CE analysis is a high-power CE plant design. The base plant model was developed for realistic PCT and clad oxidation analysis. Since the base plant model was developed for realistic analysis, many of the model inputs are set to nominal values. For this reason, some changes were made to bias the model toward an Appendix K analysis. Doing so has added conservatism to the model to account for uncertainties associated with the LTCC phase of the post-LOCA transient.

The major changes to the base plant model are discussed in further detail below:

- Break Location

For this analysis, a DEG HLB is modeled. Since the base plant model simulated a DEG CLB, the location had to be moved. This was completed by moving break components from the cold side of the broken loop to the hot side. This change also required that an accumulator and ECCS model be input into the broken loop such that ECCS flow from all loops was considered.

- Decay Heat Model

The realistic decay heat model was modified to bound the 1971 ANS infinite + 20% (Appendix K Standard) model.

- Downcomer Condensation Model

The condensation heat transfer coefficient in the downcomer was set to a maximum value to ensure saturated conditions at the core inlet.

- ECCS Model

Since this analysis extends the simulation into the sump recirculation phase, additional trips and fills were added to the ECCS model to simulate switchover from RWT injection to sump recirculation.

- Barrel/Baffle Flow Resistance

In order to represent all CE plants in operation in the U.S., a method was developed to calculate appropriate BB flow resistances for use in this analysis. The method and supporting calculations are contained in [ ]^{a,c} and [ ]^{a,c}, which confirms that the BB flow resistances shown in Table 6-3 bound all CE plants.

- Break Boundary Condition

The pressure boundary condition at the break was not changed for the short-term LOCA simulation. For the recirculation phase, the containment pressure was dynamically calculated; however, the conditions were biased to ensure a low pressure was calculated to maximize break flow during the recirculation phase.

- Core Inlet Blockage

The dimensionless form-loss coefficient at the first core node was adjusted to simulate the build-up of debris during the recirculation phase of the transient. The flow area at the first core node is [ ]^{a,c} per FA which corresponds to the nominal [ ]^{a,c}. The value of the form-loss coefficient was varied from case-to-case. Tables 10-1 and 10-2 list the form-loss coefficient values applied for the various simulations.

The key inputs for this analysis are summarized Table 6-3. These inputs are used for all simulations shown in Tables 10-1 and 10-2.

Table 6-3 Summary of Key Inputs – CE Plant Design	
Parameter	**Analysis Value**
Core Power including Uncertainty (MWt)	3458
Number of Fuel Assemblies	217
Barrel/Baffle Total K/A^2	[ ]^{a,c} (Max Resistance Cases) [ ]^{a,c} (Min Resistance Cases)
Total Peaking (F_Q)	2.37
Radial Peaking ($F_{\Delta H}$)	1.76
Axial Peak Power Location	Top Axial Skew
High Pressure Safety Injection (HPSI) Flow Rate	2400 gpm total or 11.1 gpm/FA[1] 1600 gpm total or 7.37 gpm/FA 800 gpm total or 3.69 gpm/FA
Low Pressure Safety Injection (LPSI) Flow Rate	0 gpm (Isolated on sump switchover)
Containment Pressure during Recirculation Phase (psia)	Dynamically Calculated
ECCS Temperature during Recirculation Phase (°F)	212
Recirculation Actuation Signal (min)	20
Notes: 1. The 2400 gpm case was only included in the minimum BB resistance analysis.	

6.4 BABCOCK AND WILCOX PLANT MODEL

The base plant model selected for the B&W analysis is a high-power B&W plant design. The base plant model was developed for Appendix K PCT and clad oxidation analysis. The analysis is based on the B&W SBLOCA EM described in [ ]^{a,c}. This model already conforms to Appendix K assumptions; however, certain changes were required.

The major changes to the base plant model are discussed in further detail below:

- Break Location

For the analysis, a 0.5 ft^2 break in the bottom of the hot leg was analyzed. The use of the 0.5 ft^2 HLB is appropriate for this analysis to represent the limiting DEG HLB for the following reasons:

- The time of interest for this evaluation is after the ECCS suction source has switched to the containment sump (which is assumed to be at 20 minutes).
- A 0.5 ft^2 break is large enough to depressurize the RCS below the low pressure injection (LPI) runout condition before this time, which is the behavior expected following a DEG break.
- Modeling this break size allows the use of the SBLOCA methodology, which is better developed for longer transients than the large HLB methodology resulting in more robust results.

Since the base plant model simulated a CLB, the location had to be moved. This was completed by moving break components from the cold side of the broken loop to the hot side. The loop containing the pressurizer remained intact. This change also required that an accumulator and ECCS model be input into the broken loop such that ECCS flow from all loops was considered.

- Decay Heat Model

The 1971 ANS infinite + 20% (Appendix K Standard) was already included in the base model; therefore, no changes were made to the decay heat model.

- Core Volumes

The core control volumes were switched from modeling equilibrium conditions (which is needed for calculating a short-term PCT) to non-equilibrium conditions. This change allowed the code to run for long periods of time in a pool boiling mode.

- ECCS Model

Since this analysis extends the simulation into the sump recirculation phase, additional trips and fills were added to the ECCS model to simulate switchover from BWST injection to sump recirculation.

- Barrel/Baffle Flow Resistance

The BB design for all B&W plants is the same and the BB flow resistances shown in Table 6-4 represents all B&W plants. The method and supporting calculations are contained in [ ]^{a,c}, which confirms the BB flow resistances shown in Table 6-3.

- Break Pressure Boundary Condition

The pressure boundary condition at the break was not changed for the short-term LOCA simulation. However, to extend the simulation beyond reflood the pressure boundary was set to 14.7 psia to maximize break flow during the recirculation phase.

- Core Inlet Blockage

The dimensionless form-loss coefficient at the first core node was adjusted to simulate the build-up of debris during the recirculation phase of the transient. The flow area at the first core node is [ ]^{a,c} per FA which corresponds to the nominal [ ]^{a,c}. The value of the form-loss coefficient was varied from case-to-case. Tables 11-1 and 11-2 list the form-loss coefficient values applied for the various simulations.

The key calculation inputs for this analysis are summarized in Table 6-4.

Table 6-4 Summary of Key Inputs – B&W Plant Design	
Parameter	**Analysis Value**
Core Power including Uncertainty (MWt)	3026
Number of Fuel Assemblies	177
Barrel/Baffle Total K/A[2]	[ ]a,c
Axial Peaking Factor	1.7
Peak Linear Heat Rate Limit (kW/ft)	17.3
Axial Peak Power Location	Top Axial Skew – 10.811 ft
Low Pressure Injection (LPI) Flow Rate[1]	Min = 1435 gpm[2] Max = 7275 gpm
Containment Pressure during Recirculation Phase (psia)	14.7
ECCS Temperature during Recirculation Phase (°F)	200
Sump Switchover Time (min)	20
Notes: 1. The minimum LPI flow rate was used to calculated K_{max} and t_{chem}. The maximum LPI flow rate was used to calculate K_{split} and m_{split}. 2. The LPI flow rate followed a pump curve in the analysis. The value shown is the flow at run-out conditions.	

6.5 REFERENCES

6-1 WCAP-15644-P, Rev. 2 (Proprietary) and WCAP-15644-NP Rev. 2 (Non-Proprietary), "AP1000 Code Applicability Report," March 2004.

6-2 [

]a,c

6-3 [

]a,c

6-4 [

]a,c

6-5 [

]a,c

7 REACTOR COOLANT SYSTEM STATE

The RCS state during the post-LOCA LTCC phase of the postulated accident is discussed in this section. Specifically, the RCS conditions prior to and after the arrival of debris are discussed. The RCS state prior to the arrival of debris describes the initial conditions of the system at the point of switchover to sump recirculation, while the RCS state after debris arrival describes the system response after the application of core inlet blockage.

The overall RCS state is observed to be similar for all plant categories and the discussion provided in this section is applicable to all plants considered in the analysis. The focus of this section is primarily on the RV and the flow patterns that are present during the post-LOCA transient. However, additional discussion is provided to also describe the SG state and RCS loops.

The discussion is broken into two segments; the RCS state and RV flow patterns present prior to the arrival of debris (no core inlet blockage) and the RCS state and RV flow patterns after the arrival of debris (core inlet blockage). The segment after the arrival of debris is further divided into two periods; the period prior to complete core inlet blockage and the period after complete core inlet blockage.

It is also necessary to define when the LTCC phase of the transient begins. For the purposes of this analysis, the LTCC phase begins after the core region has completely quenched and core temperatures have stabilized to acceptably low levels. The RWST is supplying coolant to the ECCS and injection is into the cold legs. Upon switchover to sump recirculation, it is assumed that debris-laden coolant begins to enter the ECCS, where it is transported to the RCS and begins to collect at the core inlet.

7.1 PRIOR TO DEBRIS ARRIVAL

Decay heat is at its highest during this segment. To satisfy DHR, fluid enters the downcomer, travels through the LP, core, UP, and exits out the break. As decay heat diminishes, so does boiling in the core region. As a result, the core void fraction decreases and the collapsed liquid level increases, as does the liquid inventory in the RV and the amount of liquid carryover out of the break. The BB channel continues to fill, consistent with the downcomer, and the upper head is mostly voided with no liquid being provided through the UHSNs since the upper downcomer has yet to fill. At this point, the loop piping and the SGs are mostly voided and steam generated in the core exits through the break.

The predicted flow patterns within the RV just prior to sump recirculation are depicted in Figure 7-1 for an upflow BB plant without pressure relief holes. As the figure shows, ECCS enters the cold legs, flows into the downcomer and enters the inner RV regions. At this point in time, the downcomer collapsed liquid level is most likely above the mid-plane of the active fuel but below the cold leg elevation. The exact location of the downcomer collapsed liquid level depends on the specific RCS and ECCS design, plant condition at the initiation of the postulated accident, and the time at which sump switchover occurs. For the purposes of this discussion, it is assumed that the downcomer collapsed liquid level is at the same elevation as the top of the active fuel.

Liquid enters the inner RV, flows through the LP and approaches the core inlet. In Figure 7-1, the core region is represented by a low-power (LP) region, an average-power (AVG) region, and a high-power (HA) region. In general, the high-power region is in the central part of the core and the low-power region is around the periphery of the core. As shown in the figure, flow through the core inlet is predominately

upward with a flow distribution that is skewed higher in the higher-power regions of the core. Core inlet flow at the core periphery can be oscillatory with periods of downward flow occurring. The exact flow distribution and mixing patterns at the core inlet are plant-dependent; however, it can generally be said that higher flows at the core inlet tend to result in more even flow distribution with fewer oscillations in the peripheral region, while lower core inlet flows result in a more uneven flow distribution and more oscillations at the core periphery.

The flow patterns within the core region, as shown in Figure 7-1, are predominately upward. As the transient progresses, decay heat decreases and a global circulation pattern can begin to form in the core region. At this point, periods of downward flow may exist in the lower-power peripheral regions. As decay heat further decreases, flow in the core periphery can become predominately downward.

A high void fraction flow regime exists at the core exit. Steam exiting the core tends to entrain liquid with it. A portion of the entrained liquid can exit the break, while another portion can deposit on structures contained in the UP. As liquid accumulates in the UP, it will drain back to the core region, especially around the periphery where the power and steaming rate are lower. This behavior can also impact the circulation patterns seen in the core region. Liquid from the UP drains into the lower-power periphery of the core, which promotes downflow. The excess liquid in the core periphery then feeds the hotter regions through cross flow.

The flow patterns in the BB region just prior to sump switchover depend on the collapsed liquid level in the BB channel. The BB collapsed liquid level is dependent on the downcomer collapsed liquid level and generally lags behind by several feet. For a condition in which the downcomer collapsed liquid level is at the top of the active fuel, the BB collapsed liquid level is likely to be somewhere below the top of the active fuel.

For an upflow BB plant, the flow behavior at the BB inlet is similar to that seen in the core periphery. Flow through the BB inlet is most likely oscillatory at this phase of the transient. Again, however, the exact flow pattern depends on the specific plant condition and is a function of the downcomer available driving head and the UP pressure. If the downcomer driving head is high enough to overcome the BB flow resistance and the UP pressure, flow through the BB inlet will be upward. Conversely, if the downcomer driving head is not high enough, liquid can flow from the UP region in the BB, resulting in downward flow through the channel. A more complex situation arises for plants with pressure relief holes, since communication exists between the BB and core periphery at intermediate elevations. For this case, there could be flow into the BB from the core periphery at some pressure relief hole elevations and flow out of the BB into the core at other elevations.

The situation is different for a downflow BB plant. In this design, there is no communication between the BB channel and the UP. Flow enters the top of the BB from the downcomer and flows downward to the core inlet, provided the downcomer collapsed liquid level is above the elevation of the holes in the core barrel that connect the two regions. If the downcomer collapsed liquid level is below this elevation, flow will enter the BB channel from the inlet until the downcomer collapsed liquid level rises to the necessary elevation.

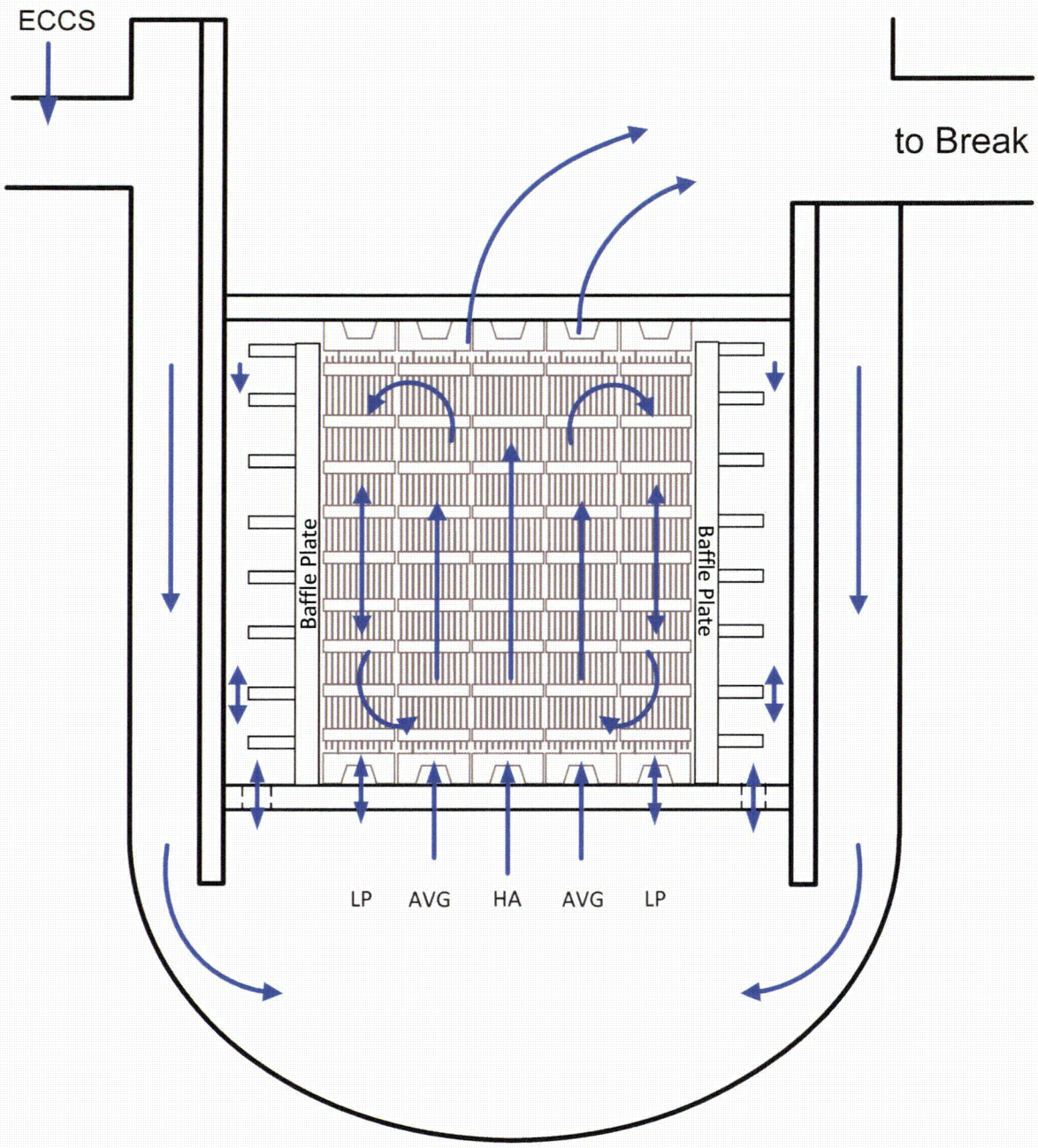

Figure 7-1 Core Flow Patterns with No Core Inlet Blockage

7.2 AFTER DEBRIS ARRIVAL

After switchover to sump recirculation, debris begins to transport through the ECCS and enters the RV, where it can collect at the core inlet. As debris collects at the core inlet, the resistance to flow through the core inlet increases, which allows the downcomer to fill to the cold leg elevation. At this point, a fraction of the ECCS flow begins to spill into the crossover legs and a fraction of the ECCS continues to enter the RV. The BB has completely flooded and, for an upflow plant, flow is predominately upward through the BB. Since the core inlet is only partially blocked, flow continues through the core inlet, but the flow rate is reduced due to the added resistance and the flow distribution across the core inlet is more uniform with upward flow in all channels. (This assumes uniform debris collection at the core inlet, as was assumed in the analysis.) If the debris collection across the core inlet is non-uniform, the flow distribution may also be non-uniform with higher flow in areas with less debris.

Figure 7-2 provides a depiction of the RV flow patterns predicted under conditions of partial core inlet blockage for an upflow BB plant without pressure relief holes. The presence of pressure relief holes changes the flow patterns in the BB channel. Instead of flow traversing the entire BB channel elevation, upward flow from the BB inlet only reaches the first elevation of pressure relief holes and enters the core. Flow above the first row of pressure relief holes may continue to be in the downward direction and is fed by liquid entering the BB from the UP. Figure 7-2 also illustrates that cross flow from the periphery of the core toward the central region is enhanced due to the increased liquid inventory entering the core periphery at the top from the BB channel and the reduction of flow through the core inlet.

As debris continues to accumulate at the core inlet, flow resistance continues to increase and the core inlet flow continues to decrease while the BB flow increases. Also, the crossover legs continue to fill with liquid. Once the crossover legs have filled, the upper downcomer begins to flood and liquid eventually reaches the UHSN elevation. It then flows through the UHSNs and floods the upper head, where it can drain into the UP and core region to provide additional liquid inventory for DHR.

As the transient progresses, debris continues to enter the RV. At some point, chemical products may be generated in the sump and transported to the RV. The arrival of chemical products to an established debris bed at the core inlet can result in complete core inlet blockage, which changes the RV flow patterns as depicted in Figure 7-3 for an upflow BB plant. As shown in the figure, the RV flow patterns are similar to those seen during partial blockage, except that flow through the core inlet has ceased and flow through the BB (or the UHSNs in the case of downflow BB plants) is the only liquid reaching the core region. This change also affects the flow patterns seen in the core region by increasing the downward flow in the periphery and the cross flow toward the central region of the core. Since the amount of liquid entering the core has decreased due to the loss of the core inlet flow path, boiling in the core becomes more vigorous. This leads to more chaotic void motion that tends to increase the overall mixing in the core by enhancing the cross flow radially across the core.

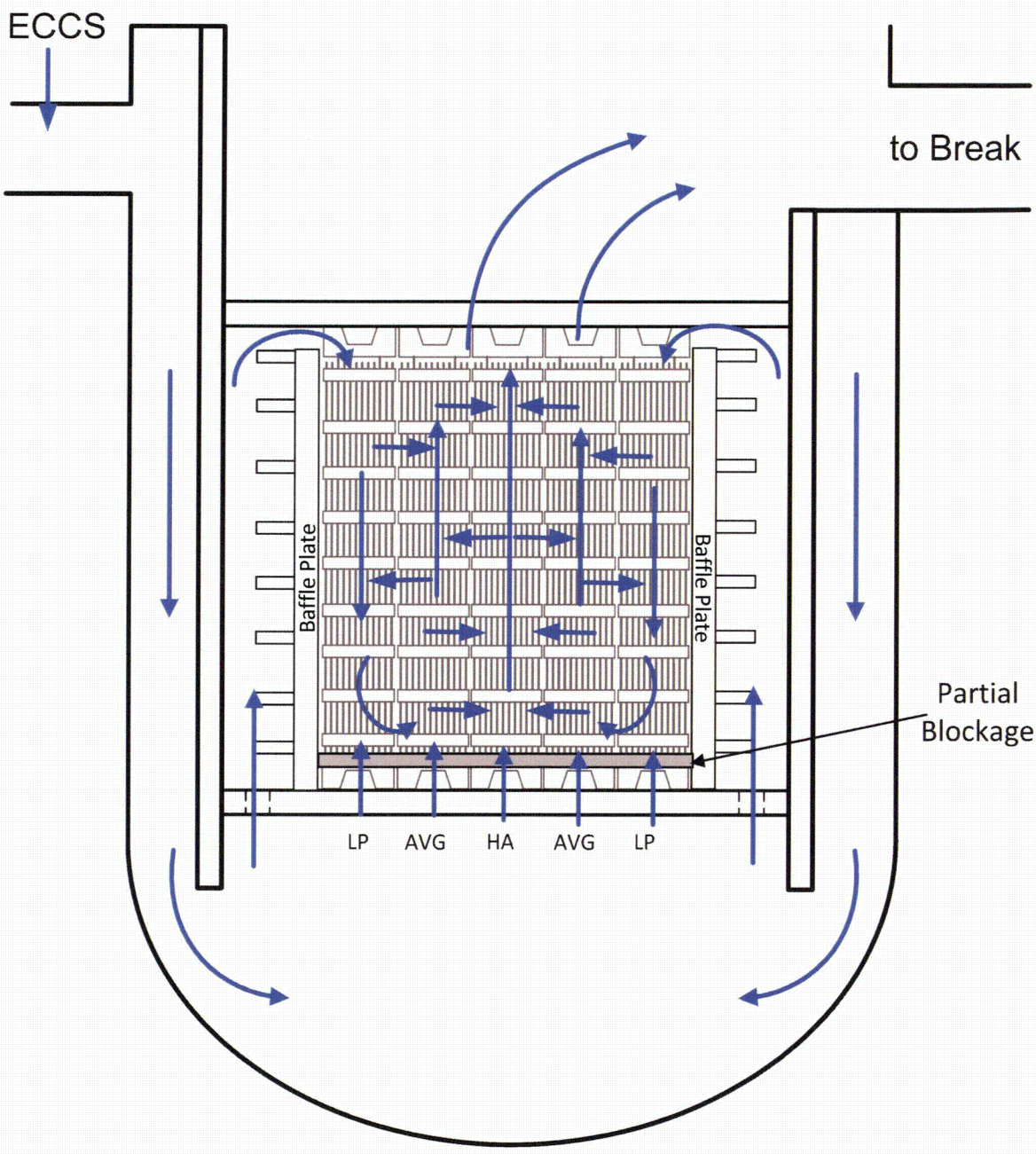

Figure 7-2 Core Flow Patterns with Partial Core Inlet Blockage

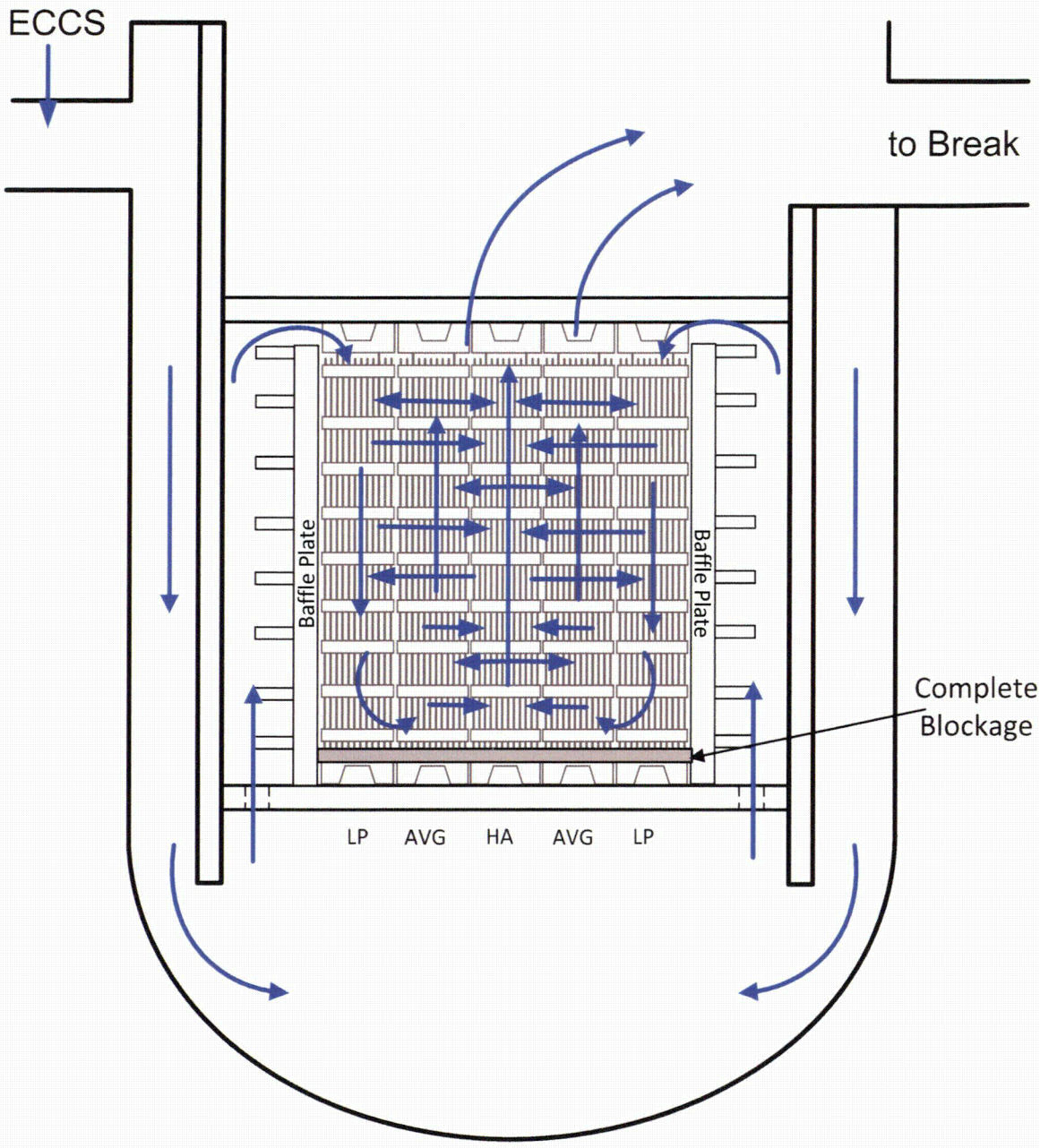

Figure 7-3 Core Flow Patterns with Complete Core Inlet Blockage

8 WESTINGHOUSE UPFLOW BARREL/BAFFLE DESIGNS

In this section, results from the Westinghouse upflow plant category are presented and discussed. The range of conditions and case matrix are provided in Section 8.1. Results from the analysis are presented in Section 8.2. This section is broken into several subsections and the material contained in each subsection is summarized as follows:

- In Section 8.2.1, results from a case that did not model debris build-up at the core inlet are used to describe the RCS state at the time of transfer to sump recirculation and the arrival of debris. Since all simulations are identical prior to that point in the transient, the discussion in this section is applicable to all cases. In the simulations, transfer to sump recirculation occurs 20 minutes after the postulated LOCA.

- In Section 8.2.2, results from the case used to determine t_{block} are presented. This case did not apply partial blockage to the core inlet prior to the application of complete core inlet blockage. Complete core inlet blockage was applied instantaneously at time t_{block} and was applied uniformly across all core channels.

- In Section 8.2.3, results from the case used to determine a value for K_{max} are presented. This case applied partial blockage to the core inlet prior to the application of complete core inlet blockage. The partial blockage was applied instantaneously at the point of transfer to sump recirculation and was applied uniformly across all core channels. Complete core inlet blockage was also applied instantaneously at time t_{block} and was applied uniformly across all core channels.

- In Section 8.2.4, results from additional cases used to determine K_{split} and m_{split} are presented. For these cases, a linear ramp in resistance was applied uniformly across the core inlet and complete core inlet blockage was not simulated. Since these cases were used to assess the timing of the activation of the BB channel, the build-up of core inlet resistance was applied more slowly compared to the cases used to determine K_{max}. As a result, the RCS response to core inlet blockage was much slower in that the downcomer fill rate and the activation of the BB channel occurred over a longer period of time. These simulations are more realistic with regard to the timing at which debris is expected to arrive at the core inlet.

Section 8.3 summarizes and discusses the key analysis results.

8.1 RANGE OF CONDITIONS AND CASE MATRIX

The simulation matrix used to determine t_{block} and K_{max} is shown in Table 8-1. For these cases, a maximum BB flow resistance was used. In the table, the loss coefficient column identifies the core inlet losses applied at the designated initiation times to simulate the collection of debris. All cases that modeled core inlet blockage applied a step change or a timewise-linear ramp to the loss coefficient applied at the core inlet. Cases 0A and 0B did not model core inlet blockage; Cases 1A, 1B, 2A, and 2B applied step changes; and Cases 3A and 3B applied linear ramps. The core inlet resistances applied for these cases are presented graphically in Figure 8-1, Figure 8-2, and Figure 8-3.

Step changes in loss coefficients are applied over a 60 second interval and are referred to as instantaneous ramps. For example, in Case 2A, a step change from 0 to $7.5x10^5$ is applied from 1200 to 1260 seconds, and an additional step change from $7.5x10^5$ to $1x10^9$ is applied from 4800 to 4860 seconds. The second ramp leads to complete core inlet blockage. For simulations that applied a linear ramp, the loss coefficient starts at zero and ramps to a value of $4x10^6$. Complete core inlet blockage is not applied to the simulations that apply a linear ramp. For Case 3A, the linear ramp occurs over a one-hour period and for Case 3B, it occurs over a two-hour period. For all simulations, the sump recirculation flow rate is applied 1200 seconds after the initiation of the event.

The simulation matrix used to determine K_{split} and m_{split} is shown in Table 8-2. For these cases, a minimum BB flow resistance was used. In the table, the loss coefficient column identifies the core inlet losses applied starting at the designated initiation time and ending at the designated end time. For example, in Case 1, a linear ramp of the loss coefficient at a rate of 6000 /hr is applied starting at 1200 seconds and ending at 12,000 seconds. The ending value of the loss coefficient is 18,000. Complete core inlet blockage is not applied to these cases. For all simulations, the sump recirculation flow rate is applied 1200 seconds after the initiation of the event.

Table 8-1 Simulation Matrix for t_{block} and K_{max} – Westinghouse Upflow Plant Design

Case	Sump Recirculation Flow Rate (gpm/FA)	Debris Bed Model	
		Loss Coefficient	Initiation Time (sec)
0A	40	NONE	N/A
0B	18	NONE	N/A
1A	40	$1x10^9$	4800
1B	18	$1x10^9$	8580
2A	40	$7.5x10^5/1x10^9$	1200/4800
2B	18	$5x10^5/1x10^9$	1200/8580
3A	40	$4x10^6$/hr	1200
3B	18	$2x10^6$/hr	1200

Table 8-2 Simulation Matrix for K_{split} and m_{split} – Westinghouse Upflow Plant Design

Case	Sump Recirculation Flow Rate (gpm/FA)	Debris Bed Model (Linear Ramp)		
		Loss Coefficient	Initiation Time (sec)	End Time (sec)
1	40	6000/hr	1200	12,000
2	30	6000/hr	1200	12,000
3	18	6000/hr	1200	12,000
4	12	6000/hr	1200	12,000
5	8	6000/hr	1200	26,400

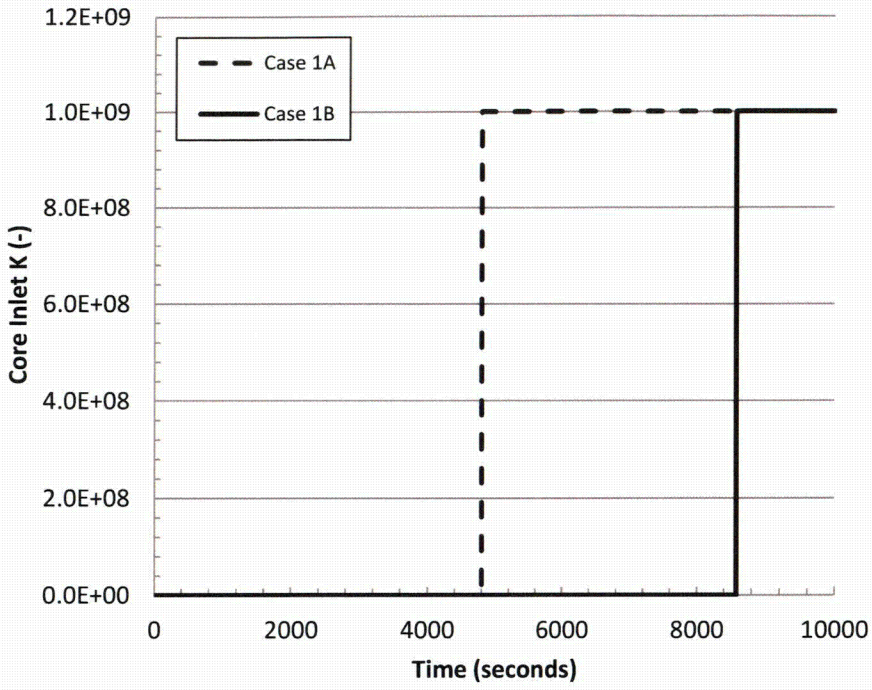

Figure 8-1 Core Inlet Resistance Transient Applied to Case 1 Simulations from Westinghouse Upflow Analysis

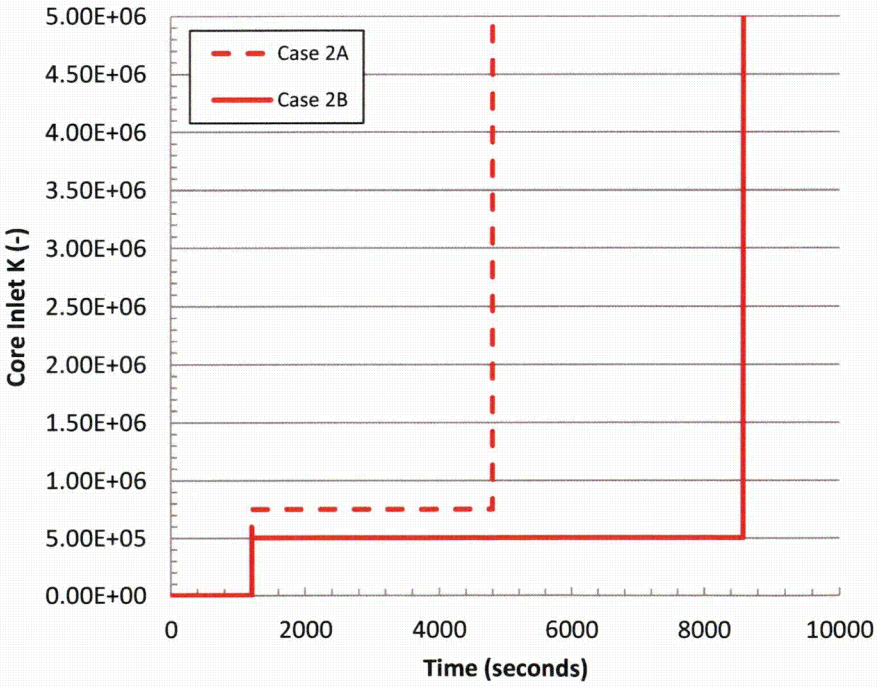

Figure 8-2 Core Inlet Resistance Transient Applied to Case 2 Simulations from Westinghouse Upflow Analysis

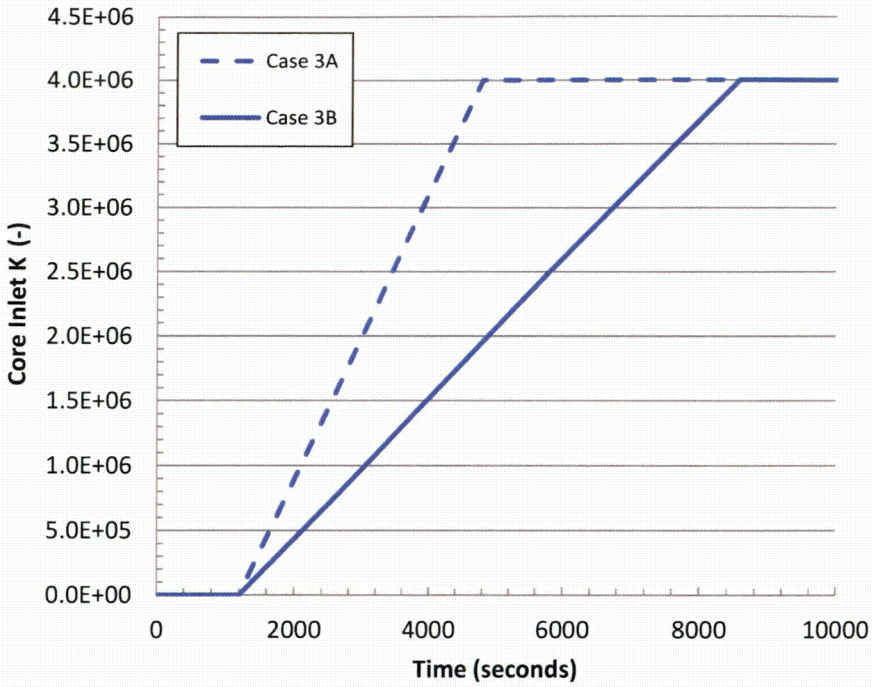

Figure 8-3 Core Inlet Resistance Transient Applied to Case 3 Simulations from Westinghouse Upflow Analysis

8.2 RESULTS OF ANALYSIS

Key results from the t_{block} and K_{max} simulations are summarized in Table 8-3. Cases 0A and 0B have no core inlet blockage applied and serve as baseline cases for comparison to the blockage cases. Cases 1A and 1B apply complete core inlet blockage and determine the minimum time that complete blockage can be tolerated. Cases 2A through 3B apply resistances to the core inlet prior to reaching complete core inlet blockage and are used to determine the maximum resistance that can be tolerated prior to reaching complete blockage.

Based on the results presented in Table 8-3, it is concluded that LTCC can be maintained if complete core inlet blockage occurs 143 minutes (8580 sec), or later, after the initiation of the LOCA event. This time is taken from the minimum ECCS recirculation flow case (Case 1B) and bounds the range of recirculation flows investigated. Prior to reaching complete core inlet blockage, a maximum supportable K_{max} value of $5x10^5$, corresponding to a pressure drop of 14.4 psid across the core inlet, is determined to be the limiting value when a uniform resistance is applied instantaneously upon entering sump recirculation. These values are taken from the minimum ECCS recirculation flow case (Case 2B) and bound the range of recirculation flows investigated.

In addition, the results from Cases 3A and 3B, which apply a linear ramp in resistance over time, demonstrate that the instantaneous cases bound any slower build-up of resistance due to the collection of debris at the core inlet. In the prototypic system, it is unrealistic to expect all the debris to arrive at the core inlet instantaneously. It is expected that the arrival of debris will occur over some finite period of time that is on the order of hours. Since the exact timing of debris arrival is complex and will vary from plant-to-plant, the approach for determining K_{max} via application of an instantaneous ramp simplifies the

approach by taking the timing of debris arrival out of the solution. Taking this approach inherently leads to a conservative K_{max} value. This is demonstrated by comparing K_{max} to the final form-losses applied to the Series 3 cases. From Table 8-3, the final form-loss applied to the Series 3 cases was $4x10^6$, which almost an order of magnitude higher than K_{max}.

With regard to BAPC, all cases demonstrate that, after core inlet blockage, the break exit quality remains sufficiently low such that boron is flushed from the core and concentrations are expected to remain well below the solubility limit. Further, all cases demonstrate that the core mixing patterns are such that the core can be considered well-mixed and no localized regions containing higher boron concentration are expected to form.

Key results from the K_{split} and m_{split} simulations are summarized in Table 8-4. The K_{split} values shown in the table are used in conjunction with the ECCS sump recirculation flow rates to generate the curve shown in Figure 8-4. The time that K_{split} occurs is determined by examination of the BB exit flow rate. The first timestep in which the BB exit flow rate becomes positive is defined as the K_{split} time. If flow oscillations (positive BB exit flow followed by a reversal to negative flow) occur, the time of K_{split} is selected after the flow oscillations stop and the BB exit flow remains positive. The fraction of ECCS flow through the core inlet and BB shown in Table 8-4 are taken at the end of the core inlet form-loss ramp. The transient flow split between the core inlet and BB is shown in Figure 8-5 for the five ECCS recirculation flow rates investigated. The flow split is represented as the fraction of total ECCS recirculation flow through the BB and is plotted as a function of the core inlet resistance following K_{split}.

Table 8-3 Summary of Results for t_{block} and K_{max} – Westinghouse Upflow Plant Design

Case	Time Core Inlet Resistance Applied	Core Inlet Loss Coefficient (K)	Core Inlet Average Mass Flow Rate per FA	Core Inlet Average Velocity	Pressure Drop across Debris Bed	Break Exit Quality	PCT
---	seconds	---	lbm/sec	ft/s	psid	---	°F
0A	N/A	N/A	5.3	0.54	-	0.05	< 260
0B	N/A	N/A	2.4	0.22	-	0.20	< 260
1A	4800	$1x10^9$	5.3	0.54	-	0.25	< 500
1B	8580	$1x10^9$	2.4	0.22	-	0.25	< 800
2A	1200/4800	$7.5x10^5/1x10^9$	0.56	0.057	15.7	0.20	< 700
2B	1200/8580	$5x10^5/1x10^9$	0.66	0.067	14.4	0.25	< 800
3A	1200 - 4800	$0 – 4x10^6$	0.26	0.026	17.5	0.20	< 525
3B	1200 - 8580	$0 – 4x10^6$	0.26	0.026	17.5	0.25	< 500

Table 8-4 Summary of Results for K_{split} and m_{split} – Westinghouse Upflow Plant Design

Case	Time of K_{split}	K_{split}	Fraction of ECCS Flow through Core Inlet	Fraction of ECCS Flow through Barrel/Baffle	Final Pressure Drop across Debris Bed
---	seconds	---	---	---	psid
1	1819	1032	0.55	0.45	9.6
2	2763.5	2606	0.57	0.43	6.4
3	5307	6845	0.68	0.32	3.3
4	10,304	15,173	0.92	0.08	2.4
5	19,297.5	30,163	0.78	0.22	2.4

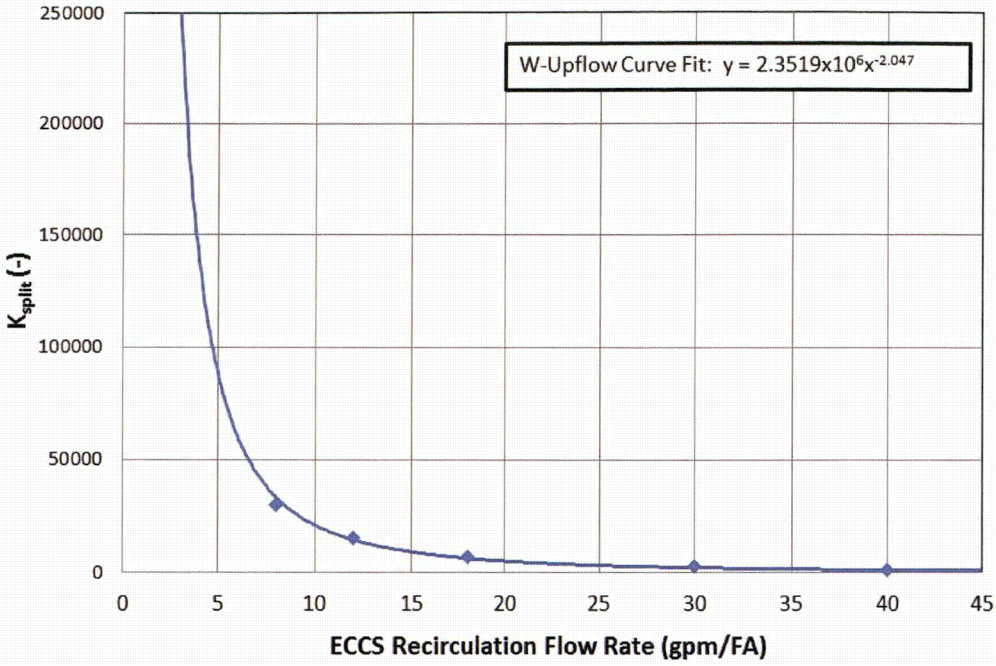

Figure 8-4 K_{split} as a Function of ECCS Recirculation Flow Rate from Westinghouse Upflow Analysis

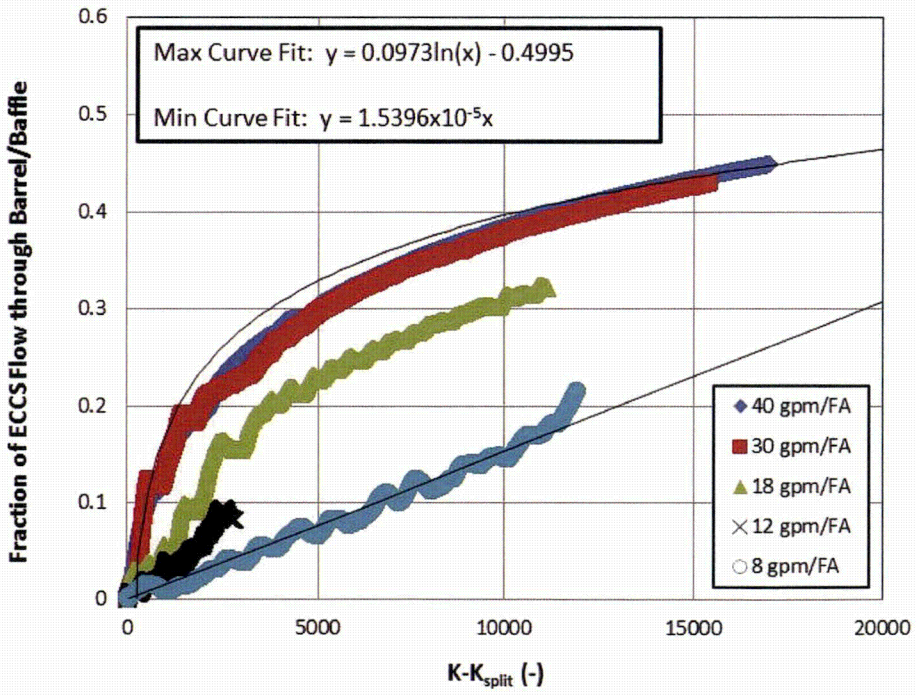

Figure 8-5 Fraction of ECCS Recirculation Flow through the BB following K_{split} from Westinghouse Upflow Analysis

8.2.1 All Cases – Before Debris Introduction

The results from Case 0A are used to describe the RCS state at the point of transfer to sump recirculation and the arrival of debris. Since all simulations are identical prior to that point in the transient, the discussion in this section is applicable to all cases. In the simulations, transfer to sump recirculation occurs 20 minutes after the postulated LOCA.

Just before transfer to sump recirculation, the RCS loop piping and SGs are mostly voided. The entire core has quenched and the cladding temperatures are just above saturation temperature, as shown in Figure 8-6. The core region is covered with a two-phase mixture and the core collapsed liquid level is roughly six feet into the active fuel region. Figure 8-7 shows the hot assembly collapsed liquid level and Figure 8-8 shows the downcomer and BB channel collapsed liquid levels. Comparison of the two figures indicates that the BB channel collapsed liquid level is comparable to the hot assembly collapsed liquid level, while the downcomer collapsed level is several feet higher. The difference between the collapsed liquid level in the downcomer and the inner RV is expected given the additional two-phase pressure losses in the boiling core. It is also noted that the downcomer collapsed liquid level is well below the cold leg elevation, which limits the available driving head at the start of sump recirculation.

As the pumped ECCS flow enters the cold legs, coolant can either travel toward the RV or it can go through the RCP and spill into the crossover legs of the RCS loop piping. For times prior to sump recirculation, and the arrival of debris, the ECCS flow split behavior is similar in the broken and intact loops. Figure 8-9 shows the integrated ECCS flow split on the broken loop. As shown in the figure, the slope of the integrated flow going in the direction of the RV is similar to the slope of the integrated total pumped ECCS flow while the slope of the integrated flow going toward the RCP remains fairly flat. This behavior indicates that the majority of the total pumped ECCS flow is traveling to the RV. This behavior is expected given that the resistance to flow from the injection point to the unfilled downcomer is less than the resistance through the RCPs to the crossover legs.

Figure 8-10 and Figure 8-11 show the integrated mass flow rates at the core inlet for each of the four core channels. A positive slope indicates positive flow into the core. Just prior to sump recirculation, all of the slopes are positive, indicating flow from the LP into the four core channels (i.e., upflow). Figure 8-12 shows the integrated mass flow rate near the core outlet. The integrated outlet flow from the core is the summation of the hot assembly and two average core channels, all of which have positive flow out of the core, while the integrated outlet flow in the peripheral channel has downward flow from the UP to the peripheral channel. Figure 8-13 shows the axial liquid velocities in the BB region. The figure shows that the top of the BB channel experiences flow into the channel from the UP, similar to the peripheral core channel.

The integrated break mass flow is shown in Figure 8-14. The figure shows that all of the break flow is from the RV side, which indicates no liquid carryover through the broken loop SG to the break. The break exit quality is shown in Figure 8-15. The figure shows that the nominal break exit quality is less than 20% upon transfer to sump recirculation, which indicates a substantial amount of liquid carryover out the break. Due to the large amount of liquid carryover prior to sump recirculation, BAP is controlled and boron concentration levels in the RV upon entry to sump recirculation are expected to be comparable to the ECCS source concentration.

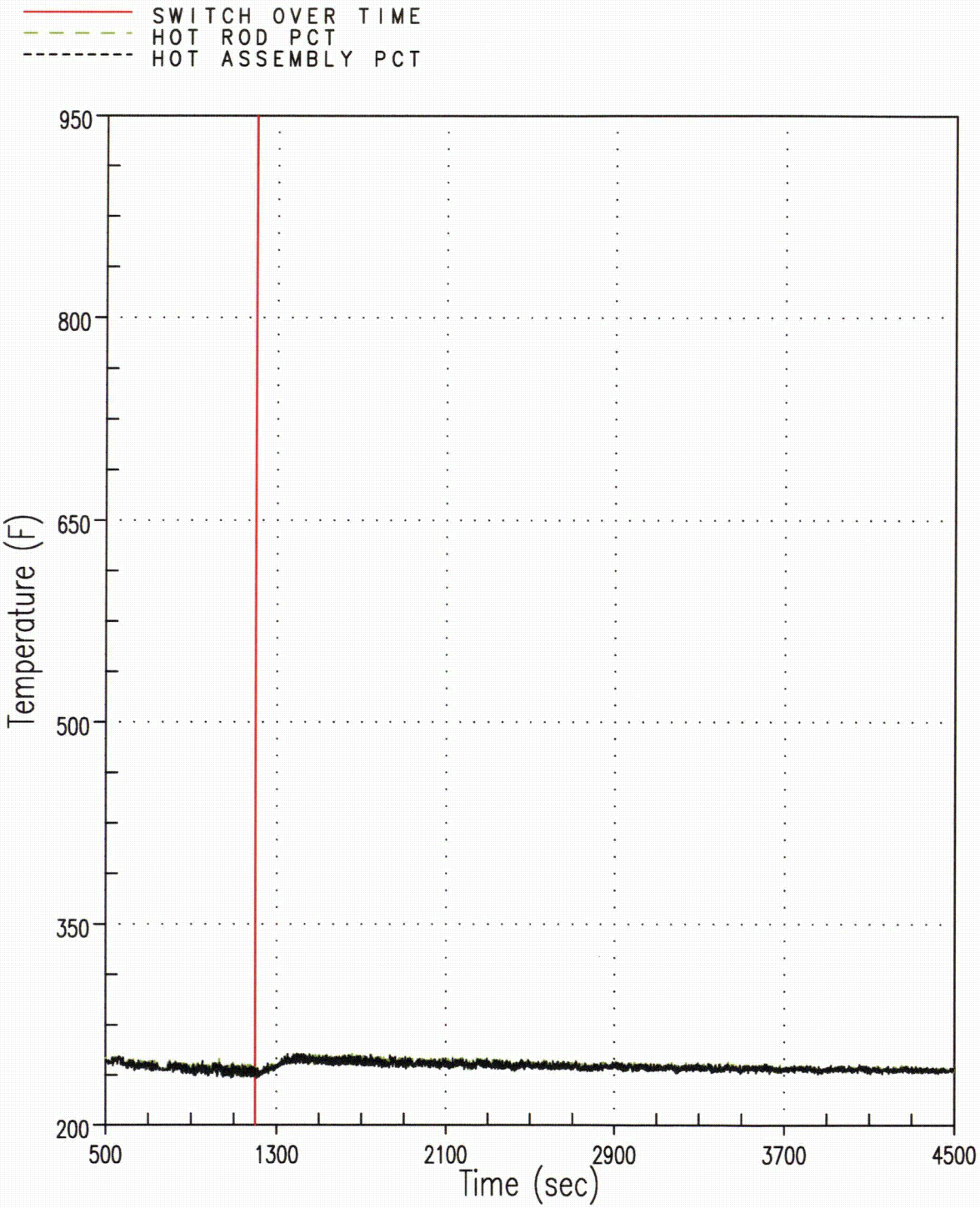

Figure 8-6 Case 0A – Hot Rod and Hot Assembly Peak Cladding Temperatures

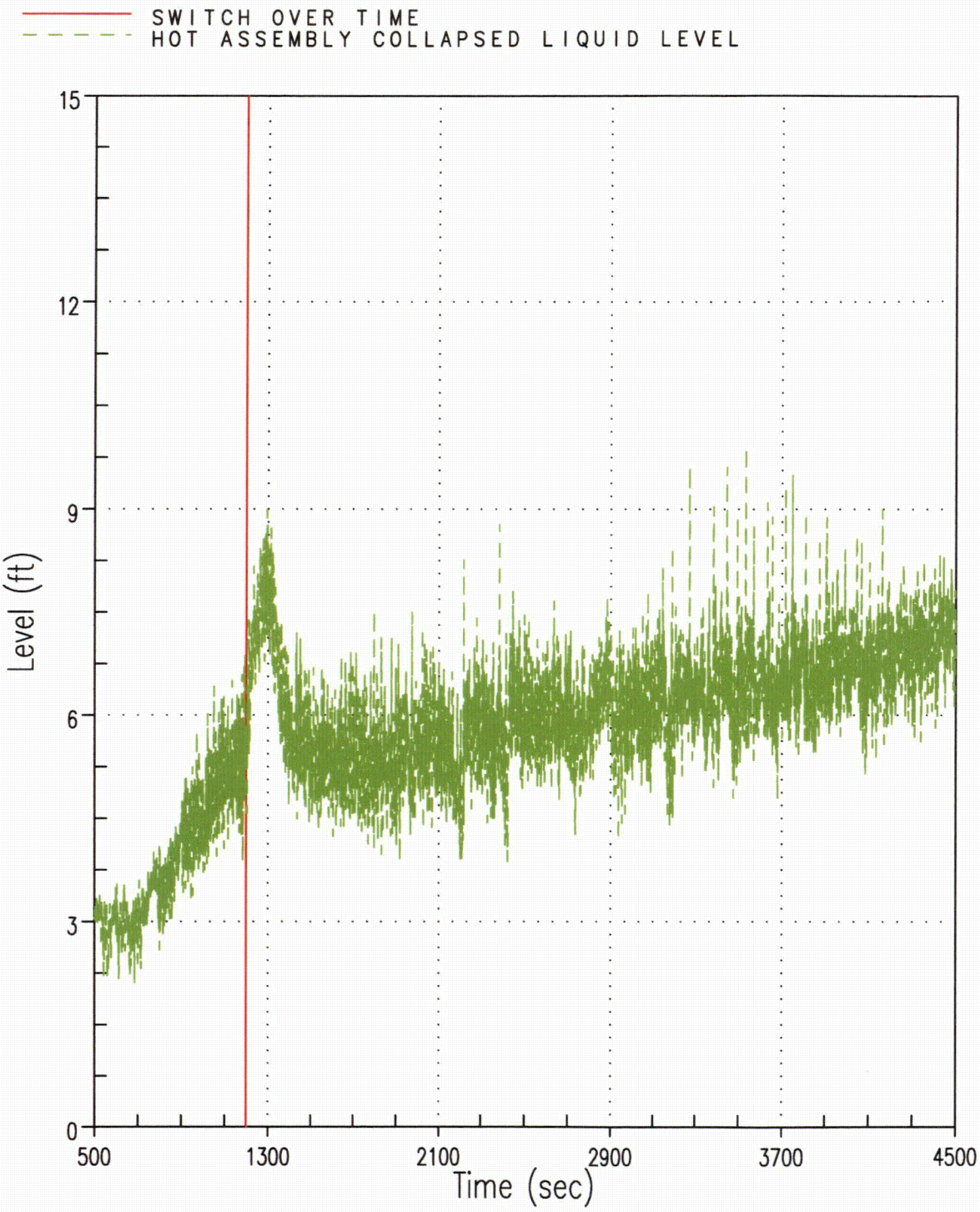

Figure 8-7 Case 0A – Hot Assembly Collapsed Liquid Level

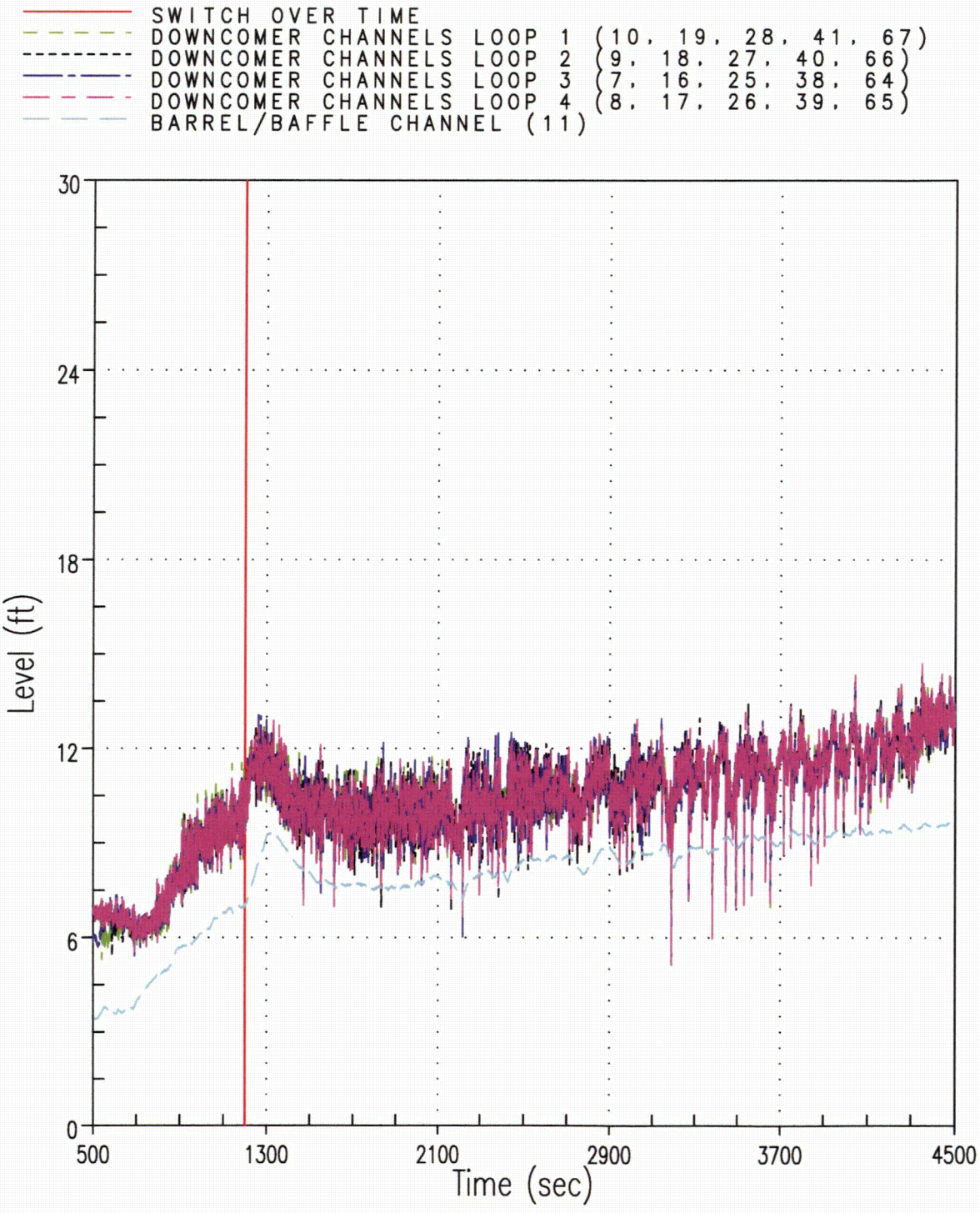

Figure 8-8 Case 0A – Downcomer and Barrel/Baffle Collapsed Liquid Levels

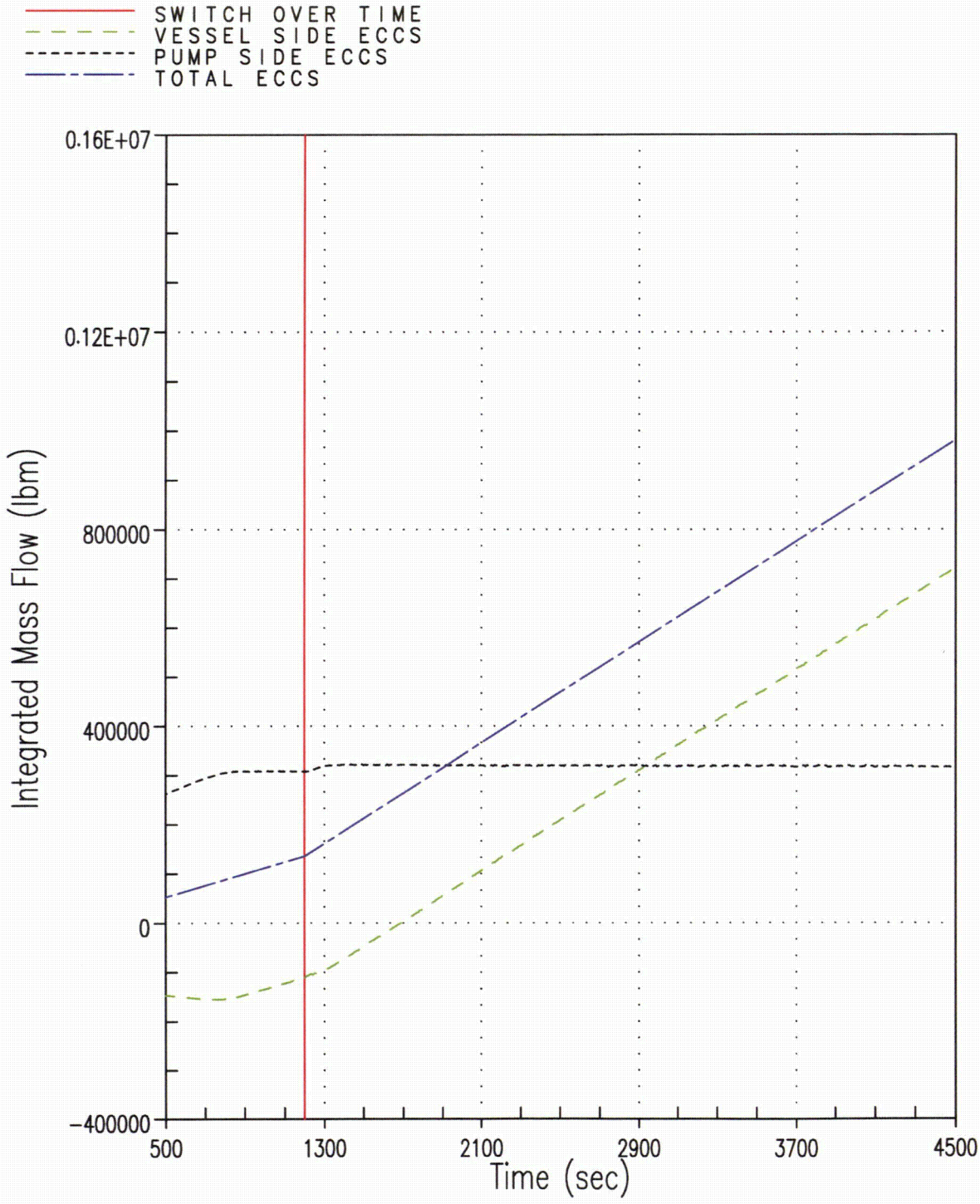

Figure 8-9 Case 0A – Integrated ECCS Flow Split in Broken Loop

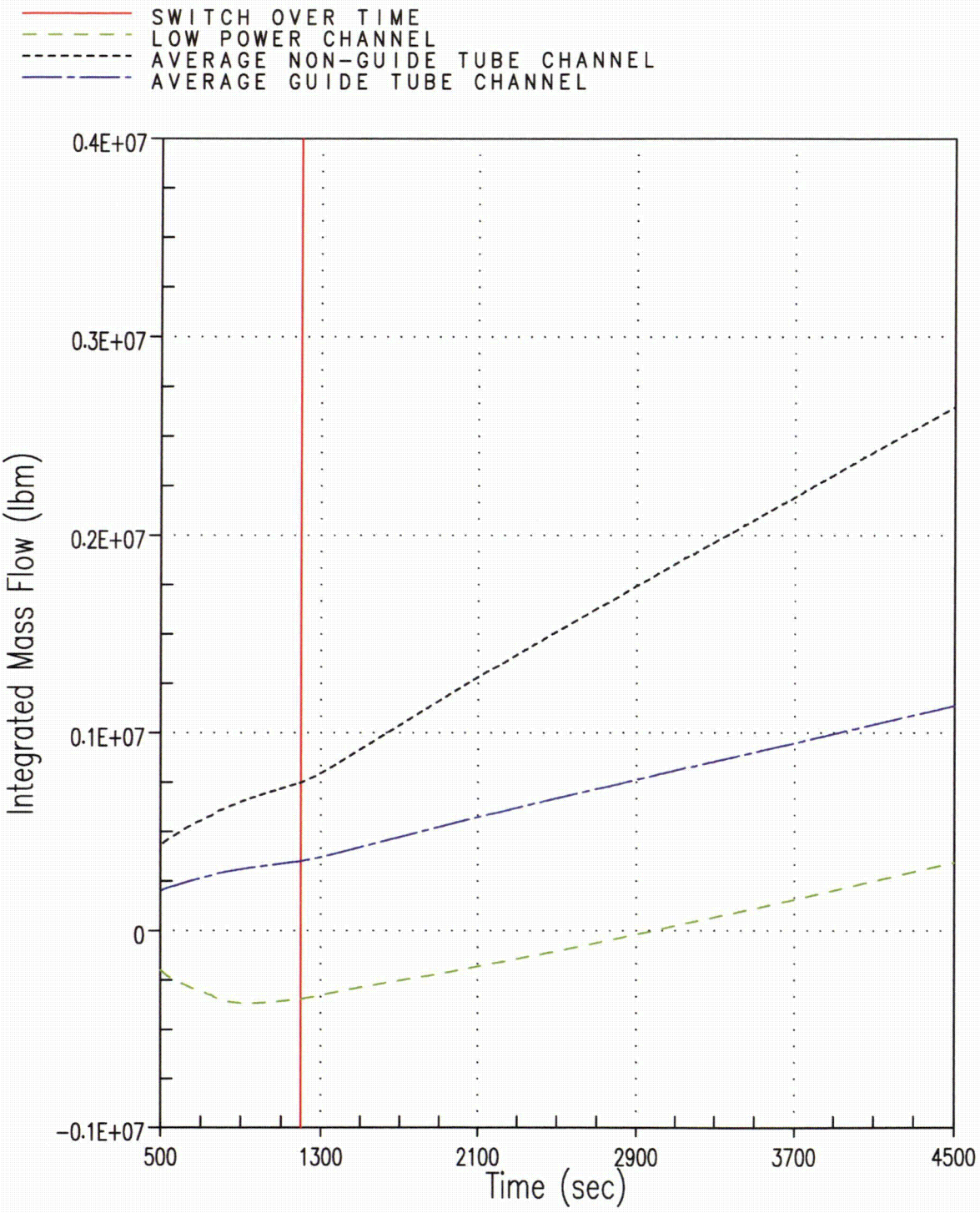

Figure 8-10 Case 0A – Integrated Core Inlet Mass Flow from Average and Peripheral Channels

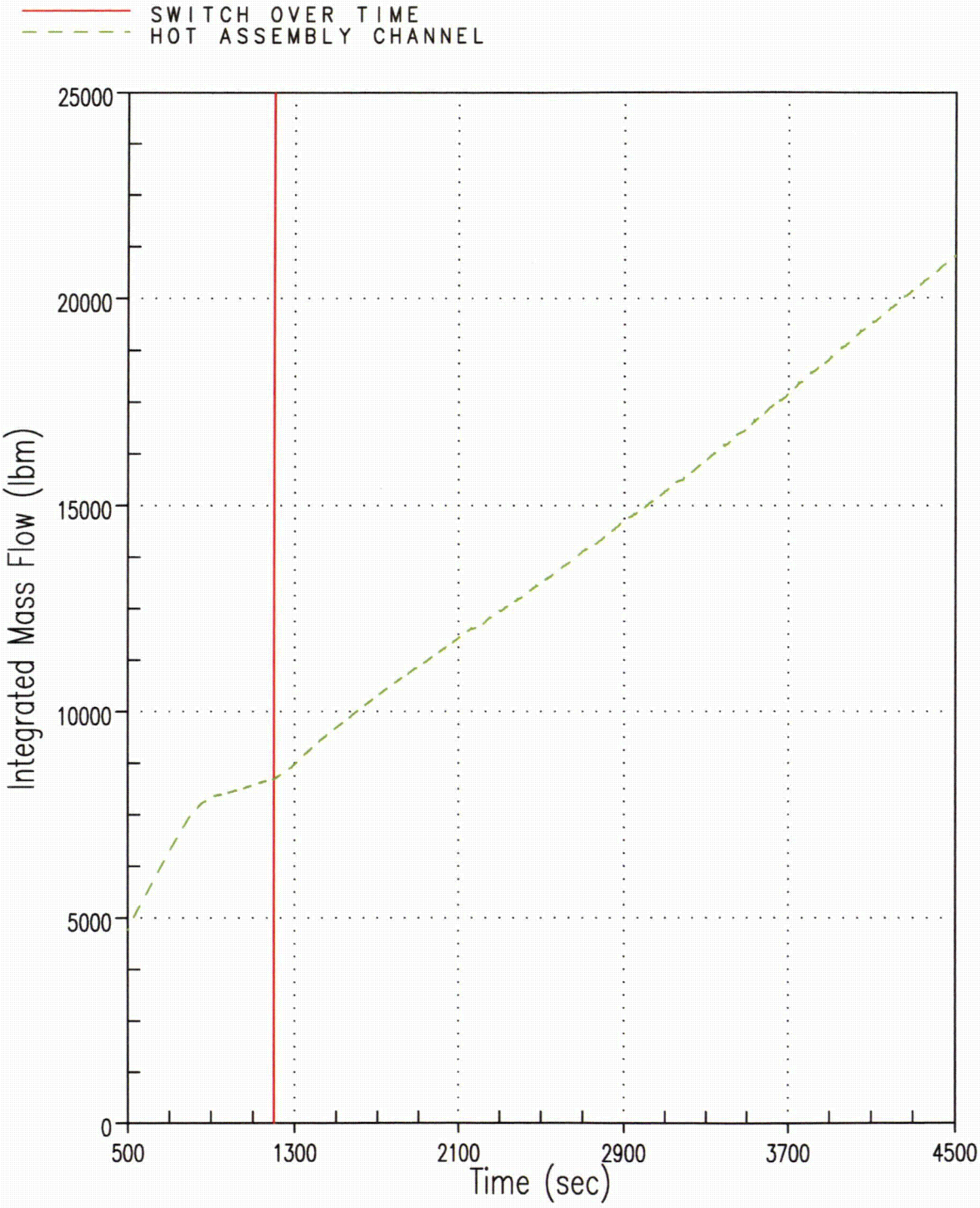

Figure 8-11 Case 0A – Integrated Core Inlet Mass Flow from Hot Assembly Channel

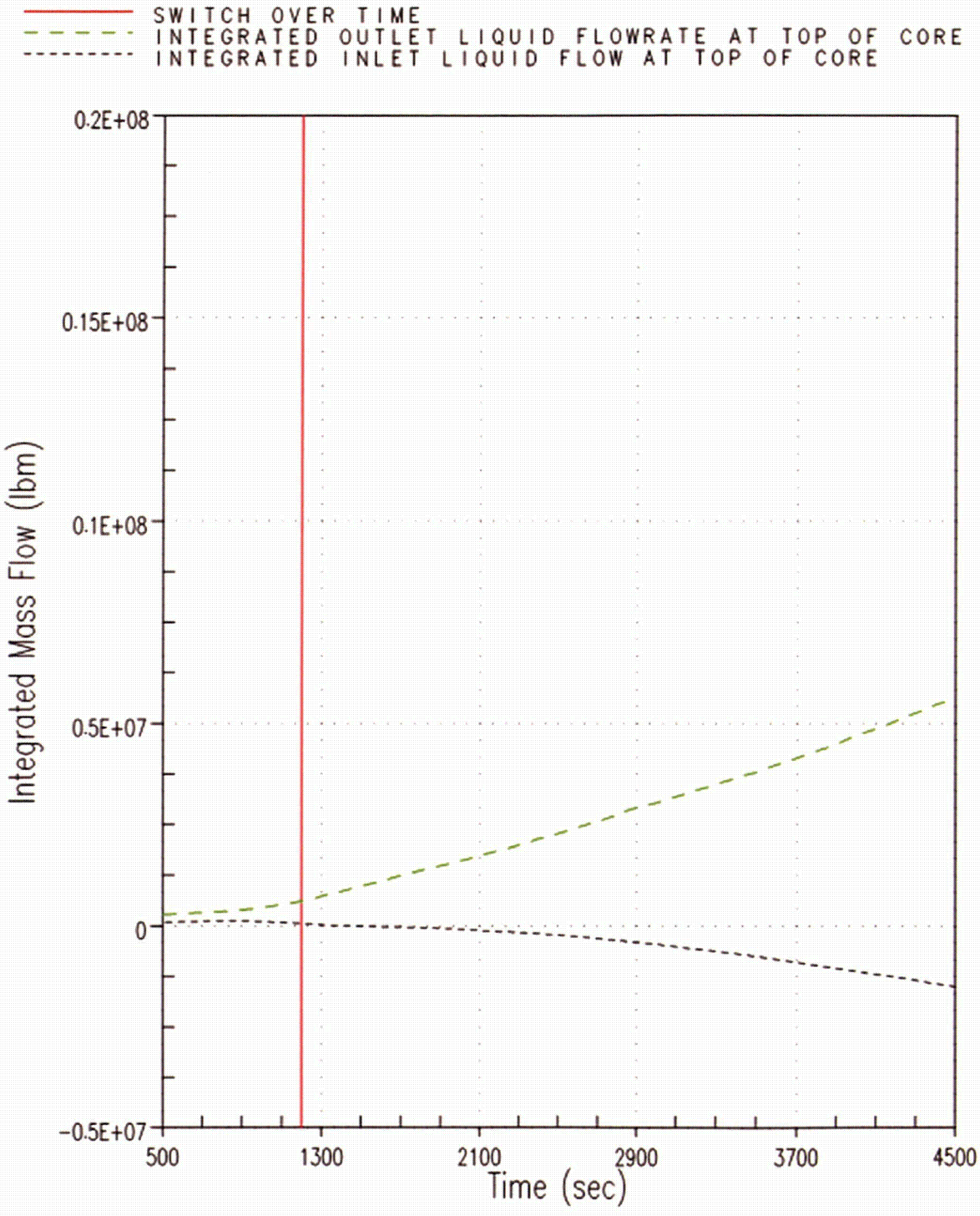

Figure 8-12 Case 0A – Integrated Core Exit Mass Flow

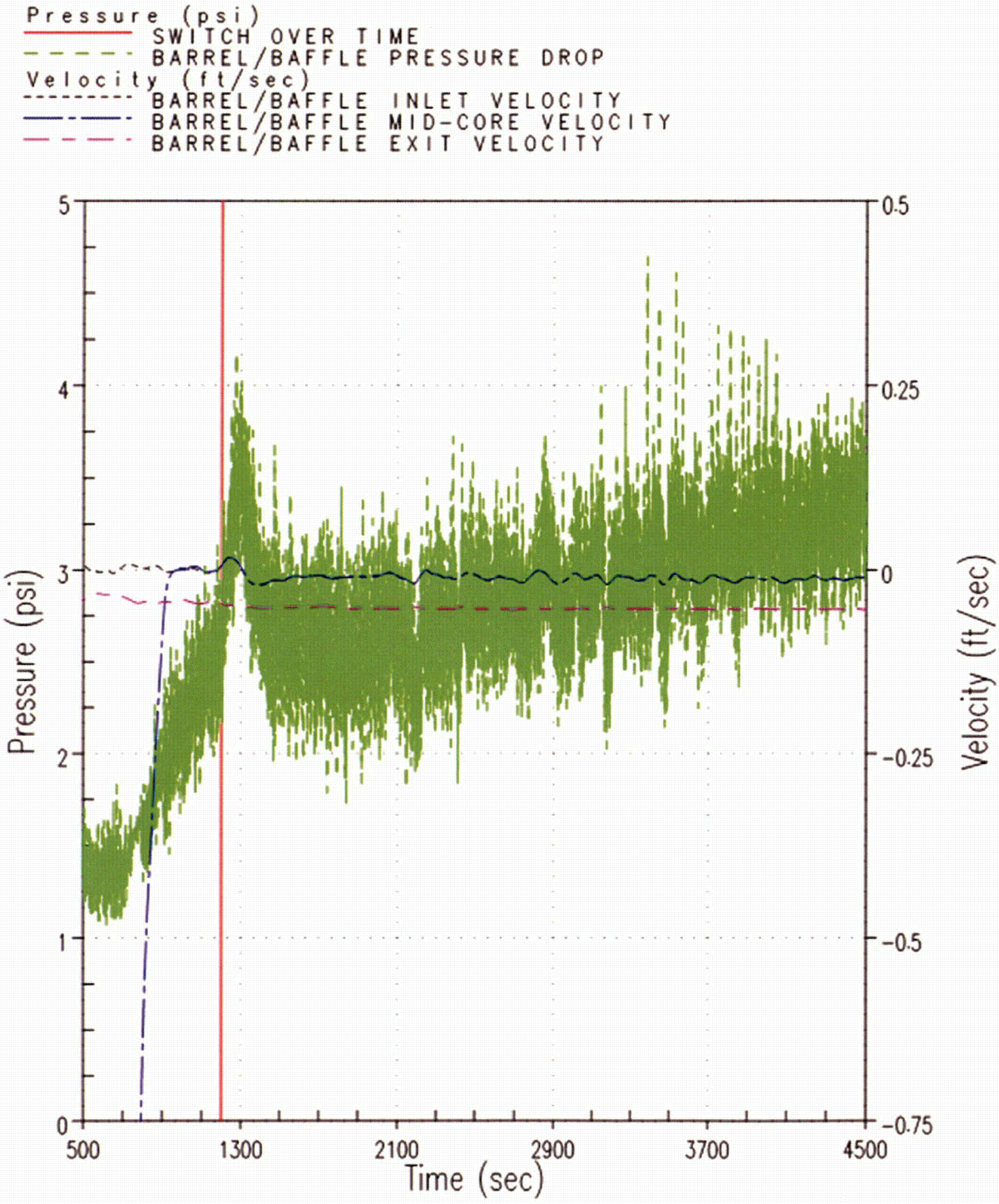

Figure 8-13 Case 0A – Barrel/Baffle Channel Pressure Drop and Liquid Velocities

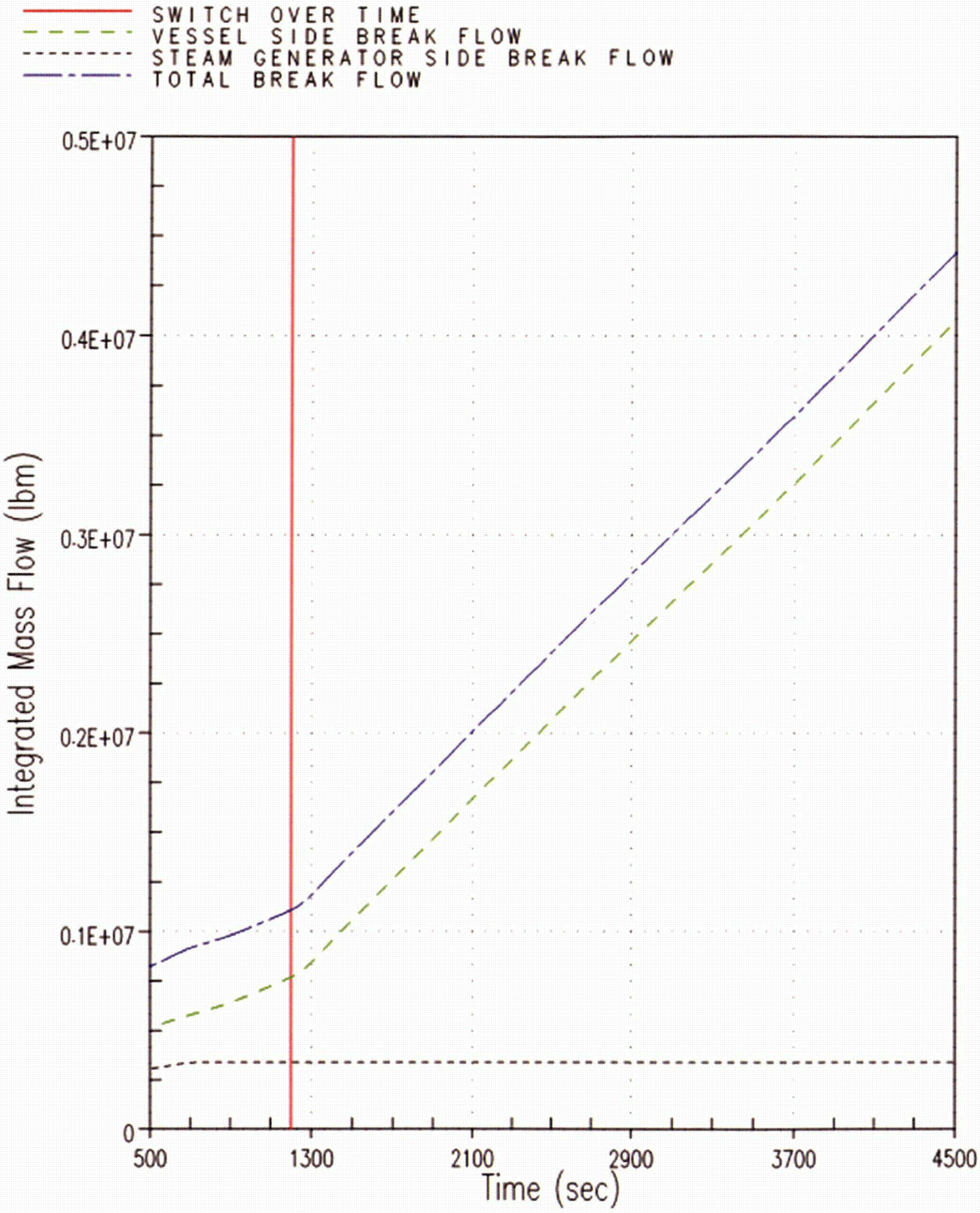

Figure 8-14 Case 0A – Integrated Mass Flow from the Break

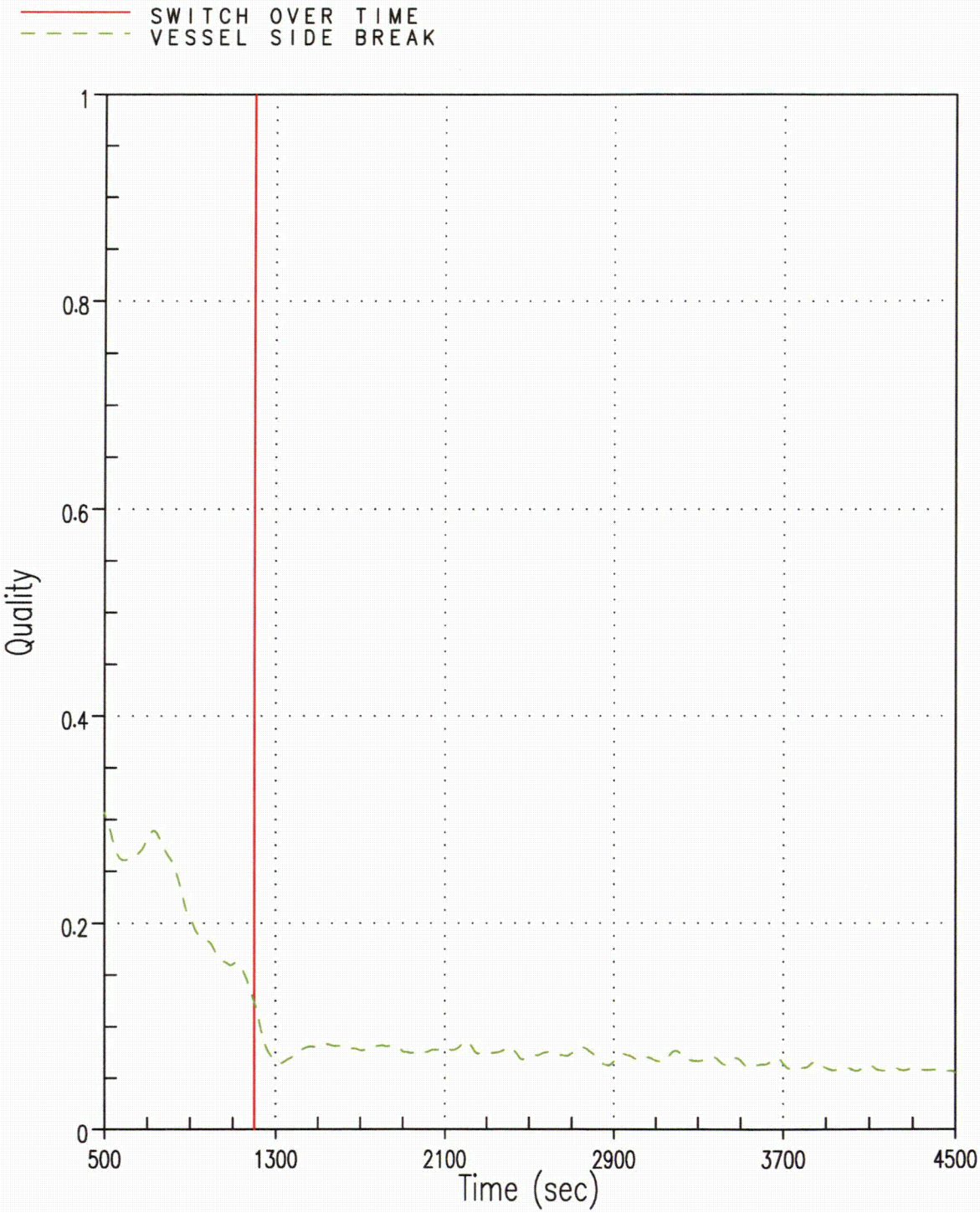

Figure 8-15 Case 0A – Break Exit Quality

8.2.2 After Debris Introduction – Calculation of t_{block}

Cases 1A and 1B are used to determine t_{block}. These cases do not apply partial blockage to the core inlet prior to the application of complete core inlet blockage. Case 1B produces the latest t_{block} time and will be discussed in this section.

Throughout the duration of the transient, more-than-adequate core cooling flow is provided through the ECCS to the cold legs. Complete core inlet blockage is applied at 143 min (8580 seconds). After this time, coolant from the ECCS backs-up and fills the downcomer until adequate driving head is achieved such that flow can be provided to the core via the exit of the BB channel. Figure 8-16 shows that the core experiences a short-duration temperature excursion after application of complete core inlet blockage; however, PCT remains below 800°F. The temperature excursion occurs at the top of the core and is due to the delay time associated with filling the downcomer to provide adequate driving head such that coolant can flow through the BB channel to the top of the core. No coolant is being provided to the core while the downcomer is filling, which leads to dryout and core uncovery. Once the downcomer fills such that the BB channel is active in providing coolant to the top of the core, the two-phase mixture level in the core is recovered, as is the cladding temperature.

The RV fluid mass is shown in Figure 8-17. When complete core inlet blockage is applied, the RV inventory increases quickly, which can be credited to filling of the downcomer. Once the downcomer fills and the BB channel becomes an active flow path, the RV fluid mass eventually stabilizes and remains fairly constant for the remainder of the transient. These trends are consistent with the behavior of the core collapsed liquid level as shown in Figure 8-18, which shows the hot assembly collapsed liquid level. The collapsed liquid levels in the other core channels show similar trends. The downcomer and BB channel collapsed liquid levels are shown in Figure 8-19. When the blockage is applied, the downcomer collapsed liquid level quickly increases due to the blockage at the core inlet. As a result, the BB channel is filled with coolant and flow through the channel provides coolant to the top of the core.

The core inlet mass flow rate and the BB exit flow rate are compared to boil-off in Figure 8-20. The figure indicates that flow into the core is well in excess of boil-off prior to the application of complete core inlet blockage. After the blockage is applied, flow through the core inlet ceases and flow in excess of boil-off from the BB exit enters the top of the core and provides coolant for DHR.

The majority of the flow that exits the BB flows into the peripheral core channel and the flow direction is predominately downward. Figure 8-21 shows the liquid velocities in the top third of the peripheral core channel and Figure 8-22 shows the liquid velocities in the bottom third of the low-power channel. These plots indicate that the flow of liquid is predominately downward along the entire length of the peripheral core channel.

With the bulk of the liquid exiting the BB channel and flowing downward in the periphery of the core, cross flow provides liquid to the average channels and hot assembly channel. This behavior is illustrated in Figure 8-23, which shows the cross flow velocity in the top third of the core from the average core channel to the hot assembly channel. The positive velocities in the figure indicate that flow is going into the hot assembly channel from the average assembly channel. Similar cross flows are observed predominately from the peripheral channel into the average channels along the entire axial elevation of the core.

The break exit quality is shown in Figure 8-24. This figure shows that, prior to the application of complete core inlet blockage, the quality remains below 20%. After the application of blockage, the case shows a spike in the break quality (consistent with the core uncovery), which quickly recovers and stabilizes just above 20%. Due to the large amount of liquid carryover out the break before and after complete core inlet blockage, BAP is controlled and boron concentrations in the RV will remain well below the solubility limit for the duration of the transient.

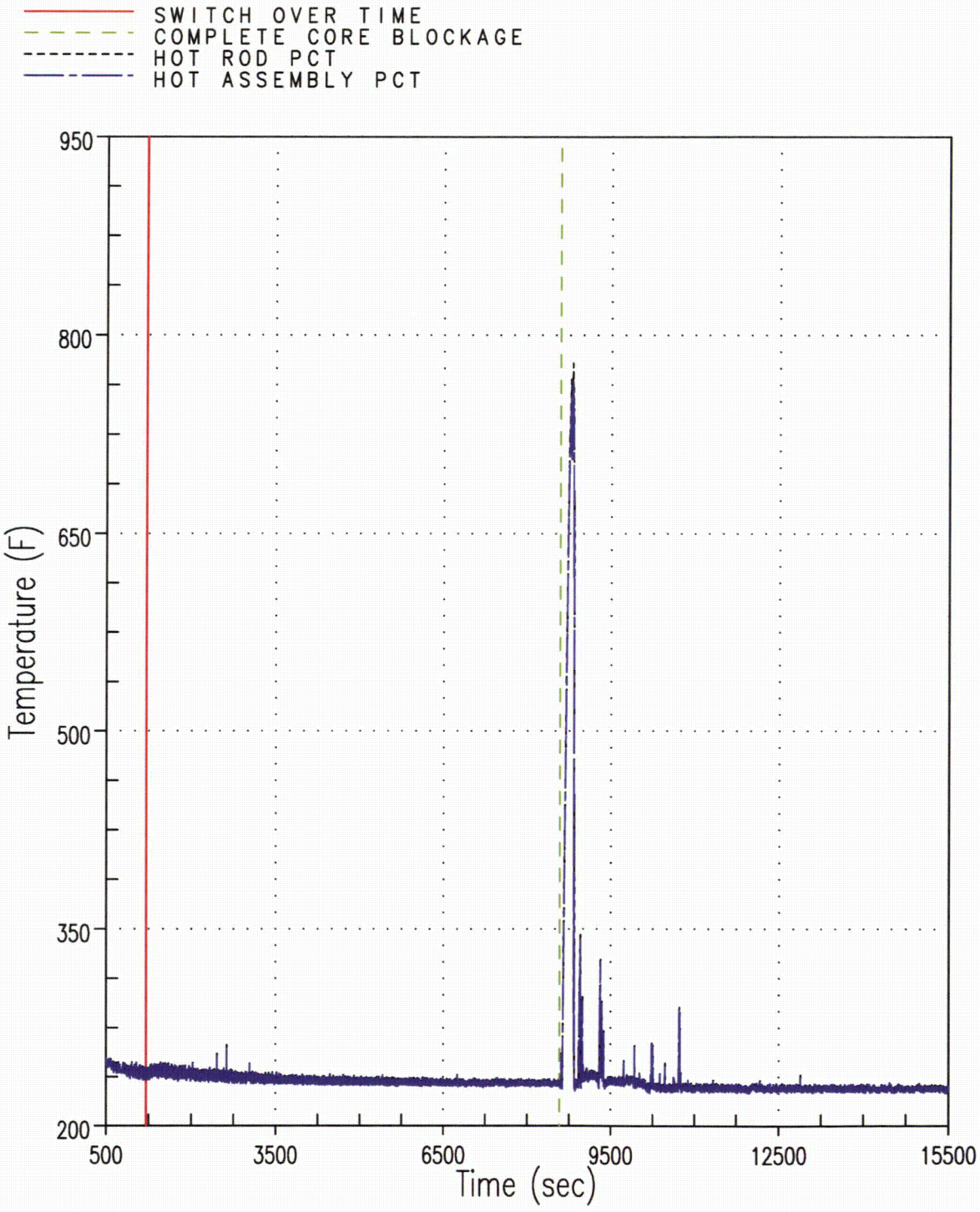

Figure 8-16 Case 1B – Hot Rod and Hot Assembly Peak Cladding Temperatures

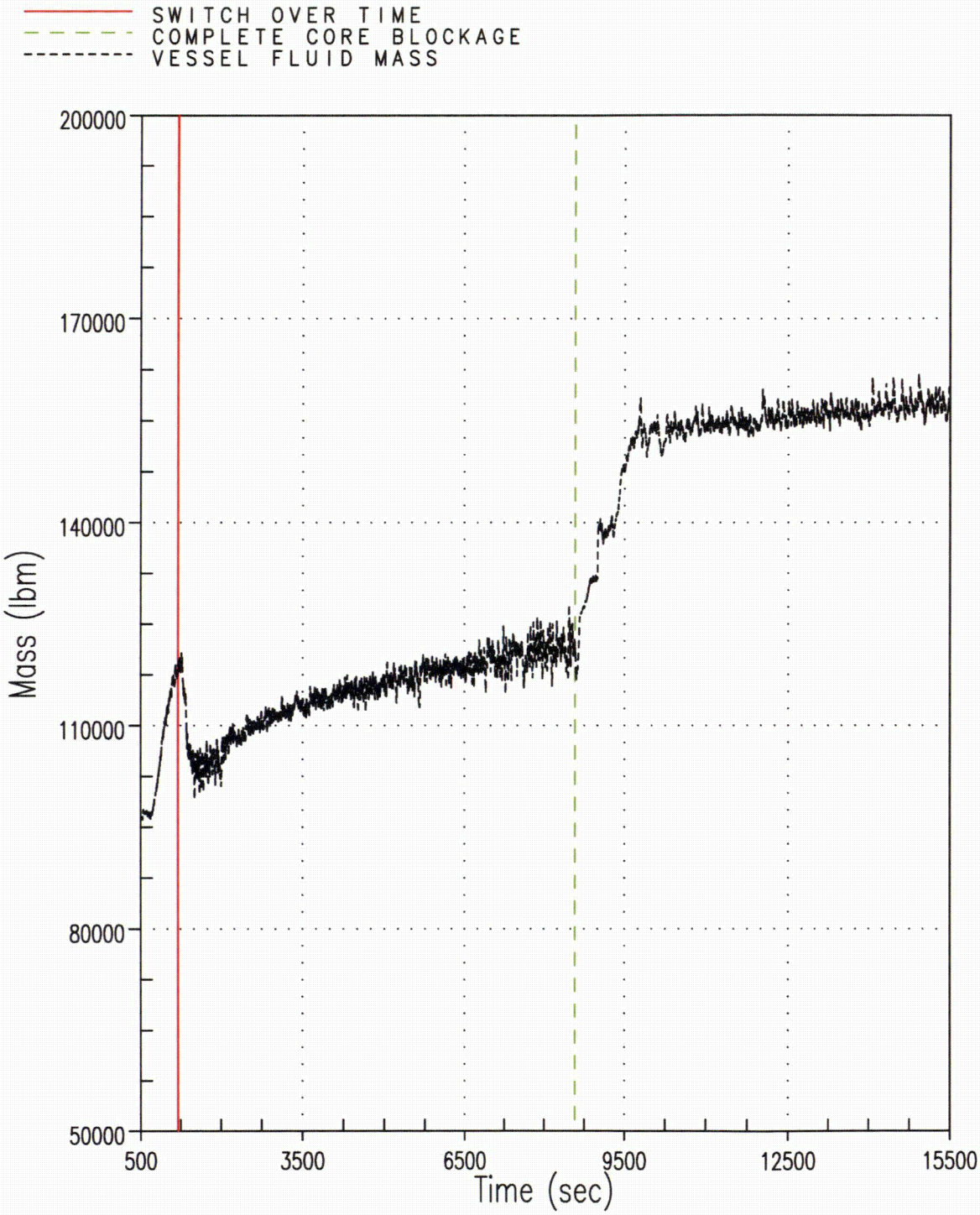

Figure 8-17 Case 1B – Reactor Vessel Fluid Mass

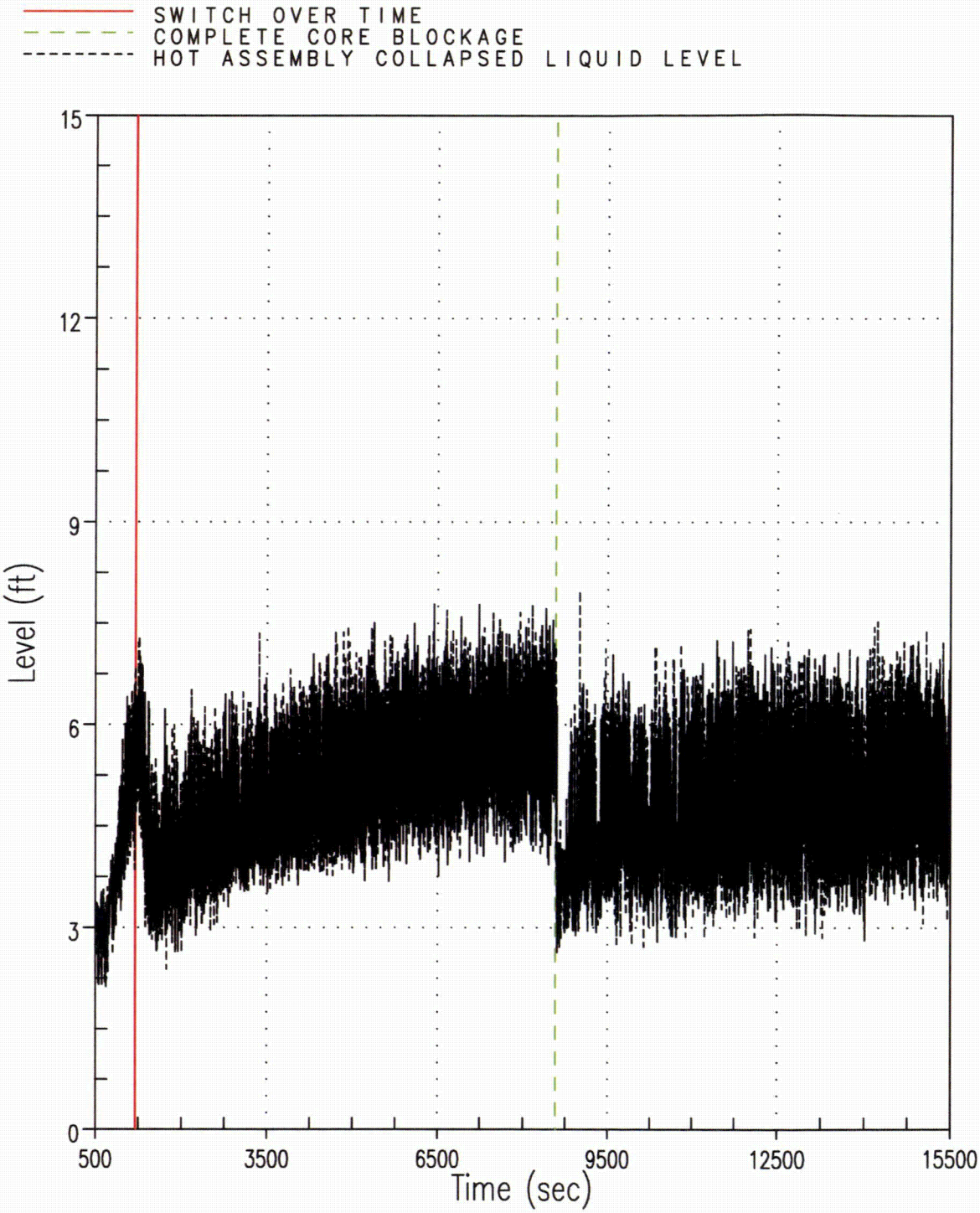

Figure 8-18 Case 1B – Hot Assembly Collapsed Liquid Level

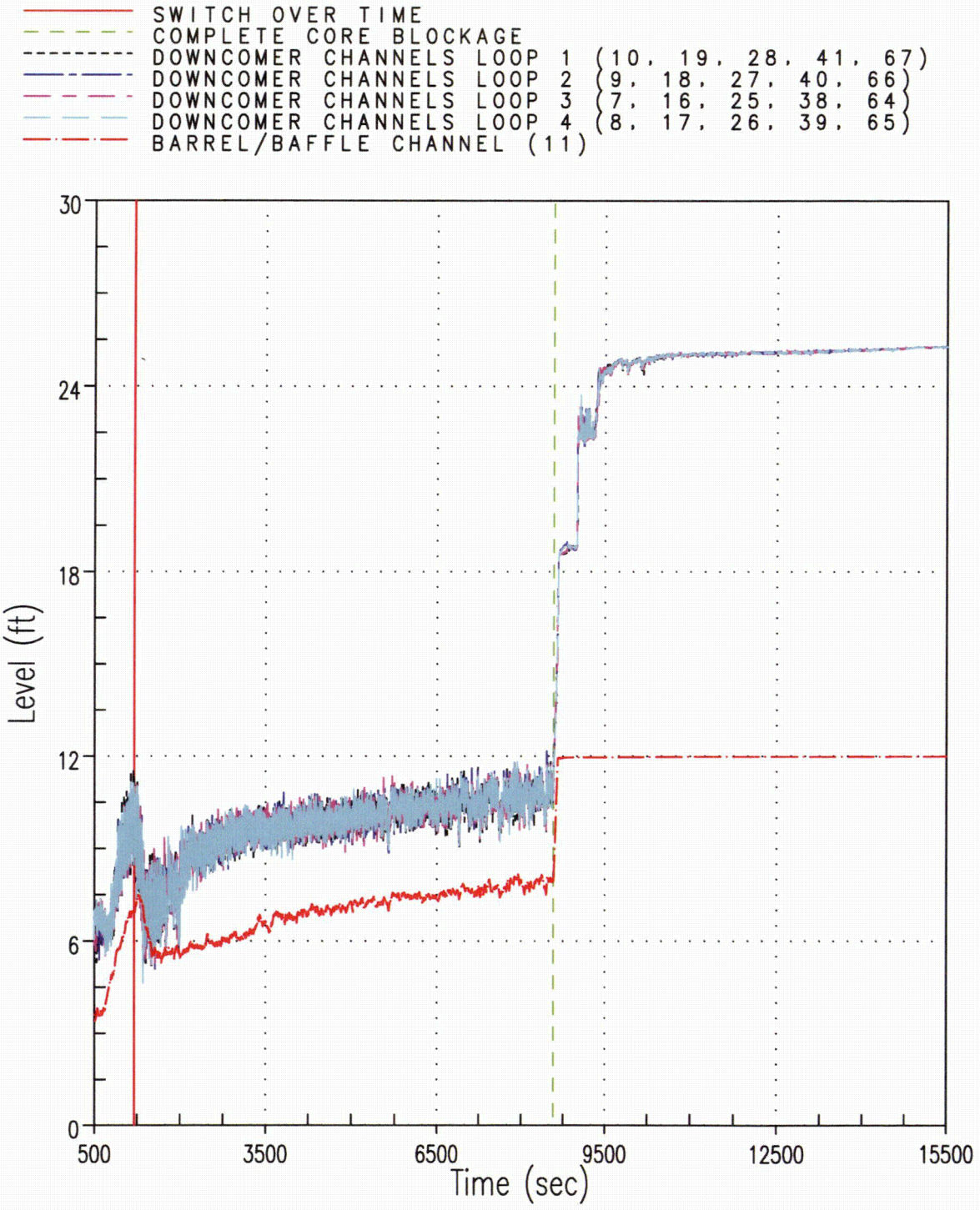

Figure 8-19 Case 1B – Downcomer and Barrel/Baffle Channel Collapsed Liquid Levels

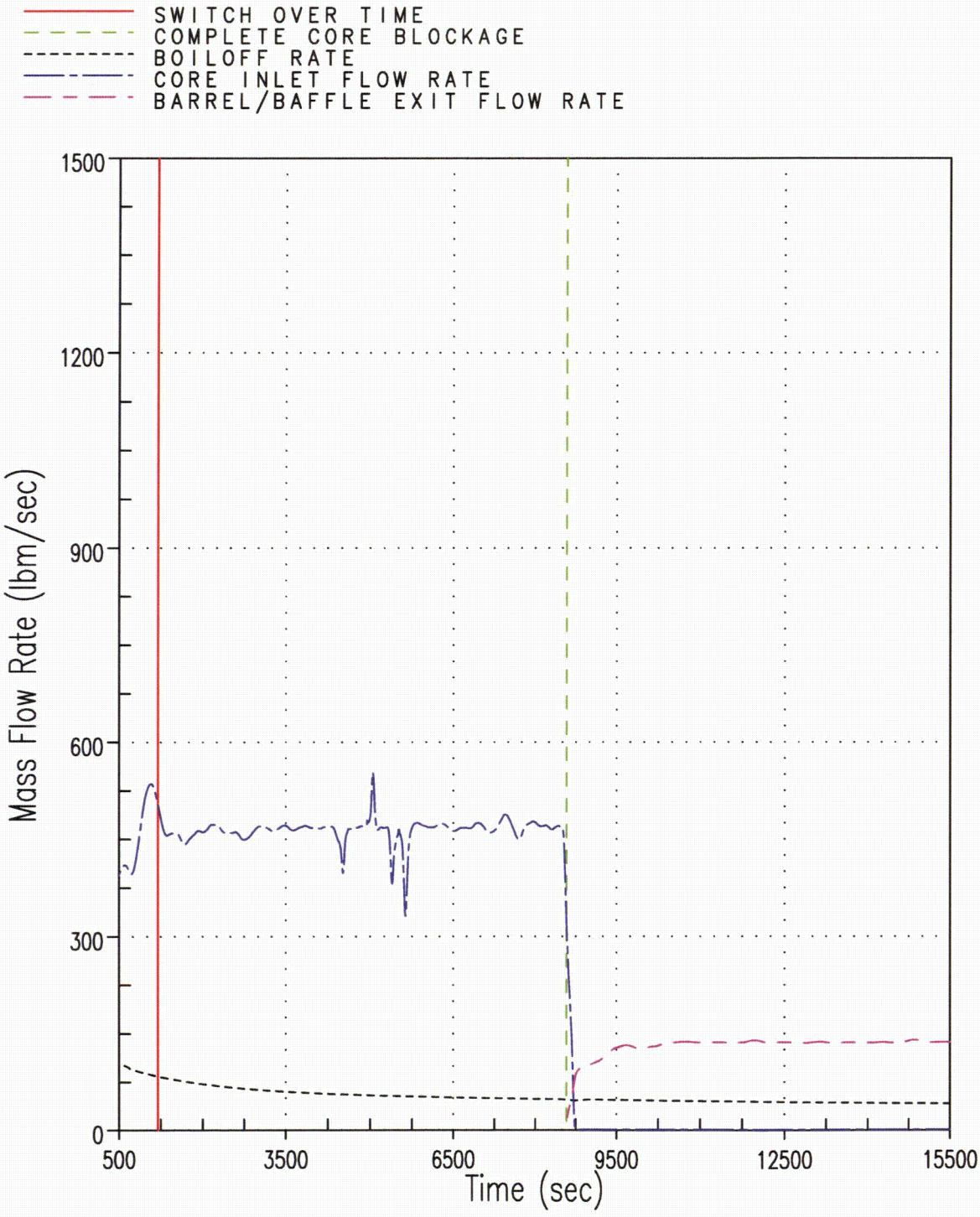

Figure 8-20 Case 1B – Core Inlet and Barrel/Baffle Channel Exit Flow Rate Compared to Boil-off

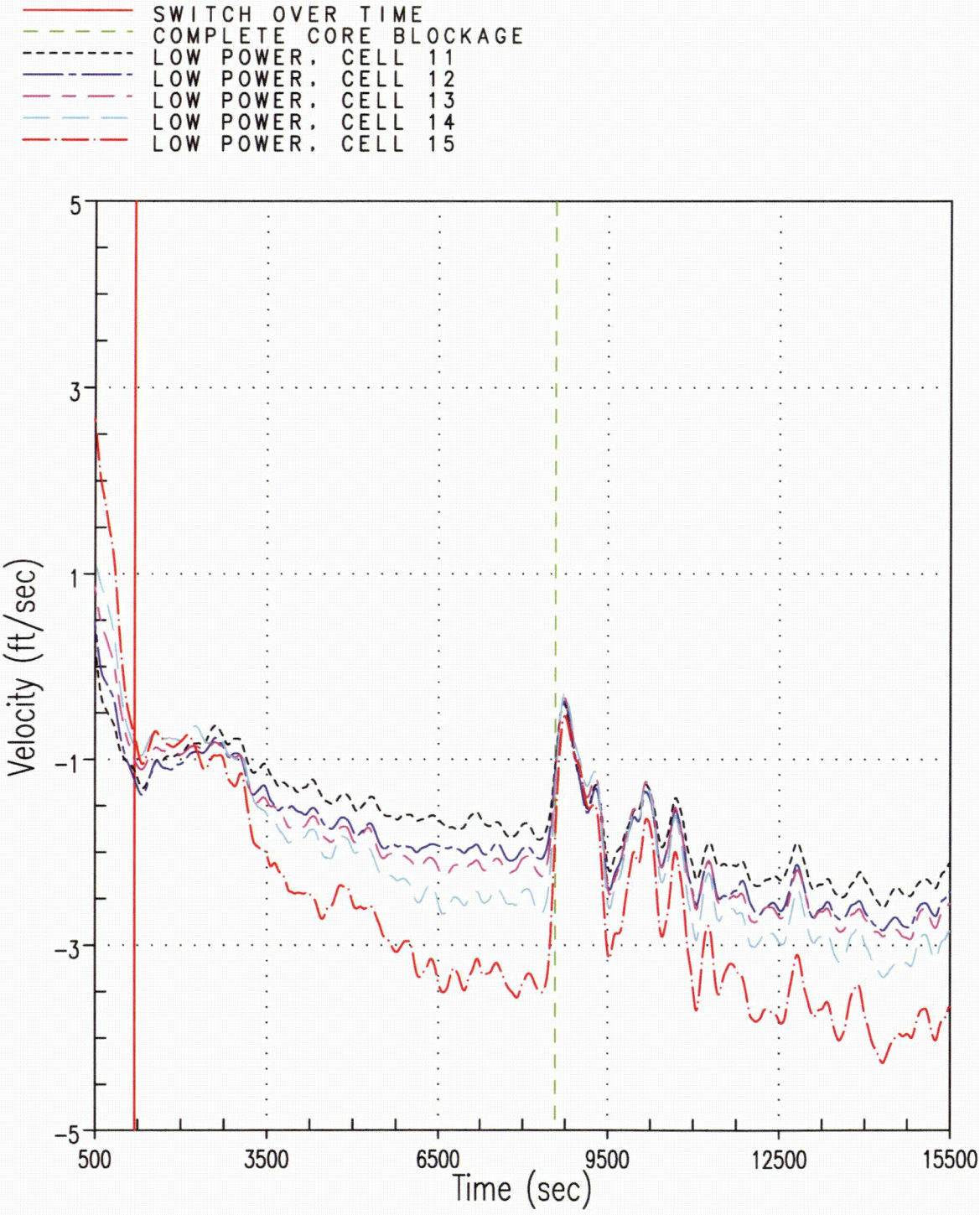

Figure 8-21 Case 1B – Liquid Velocity at the Top of the Peripheral Core Channel

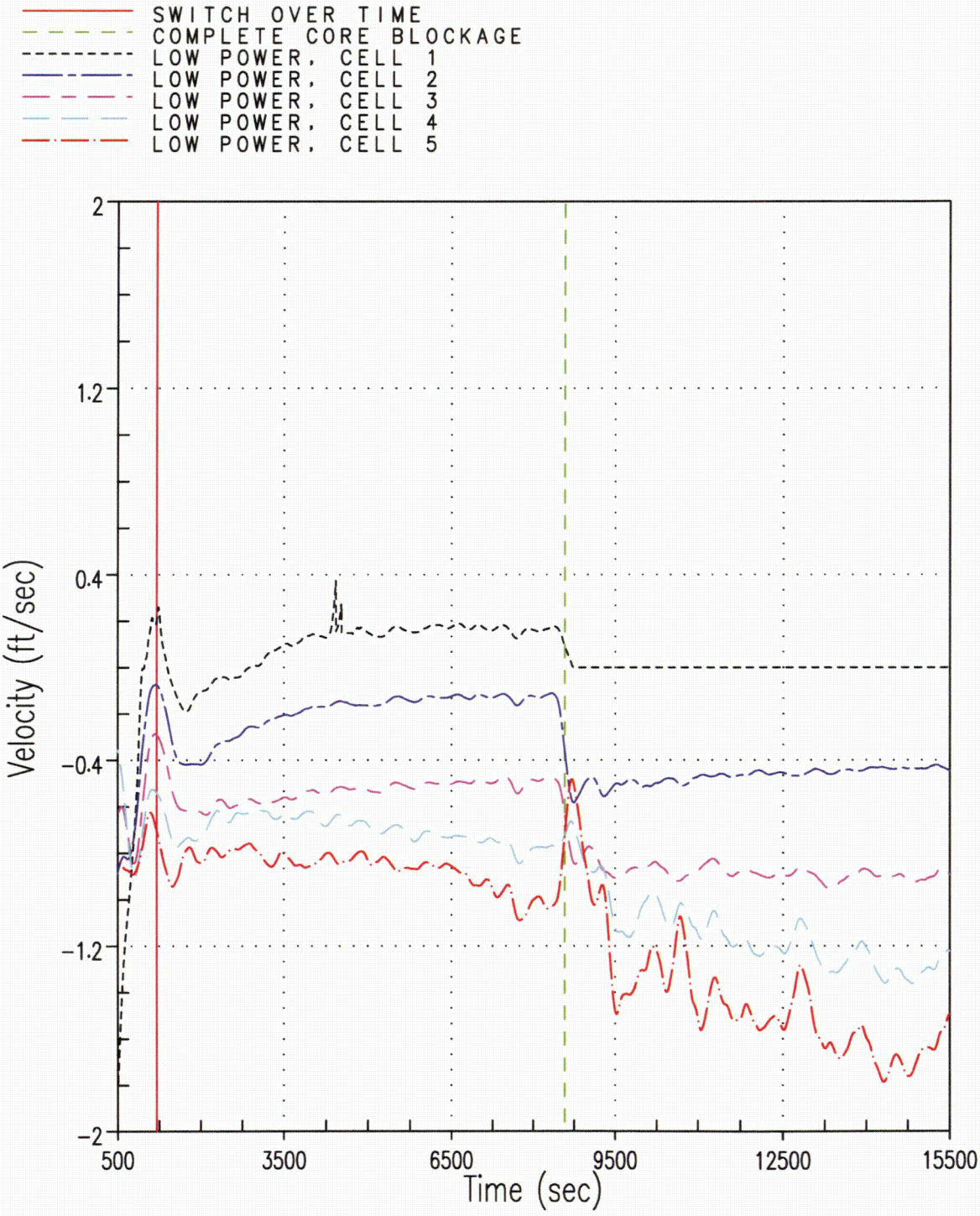

Figure 8-22 Case 1B – Liquid Velocity at the Bottom of the Peripheral Core Channel

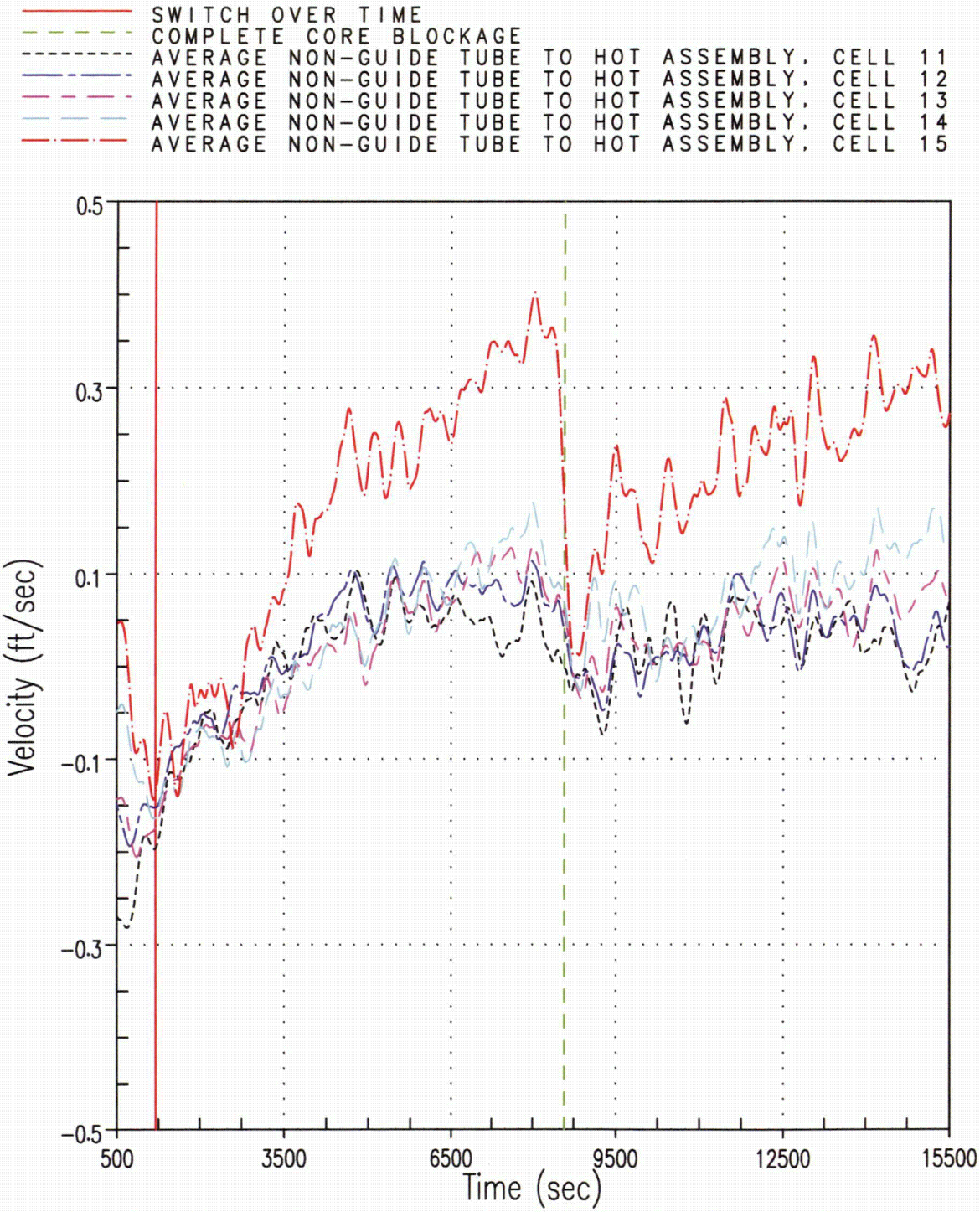

Figure 8-23 Case 1B – Cross Flow from Average Non-Guide Tube Core Channel to Hot Assembly Core Channel at the Top of the Core

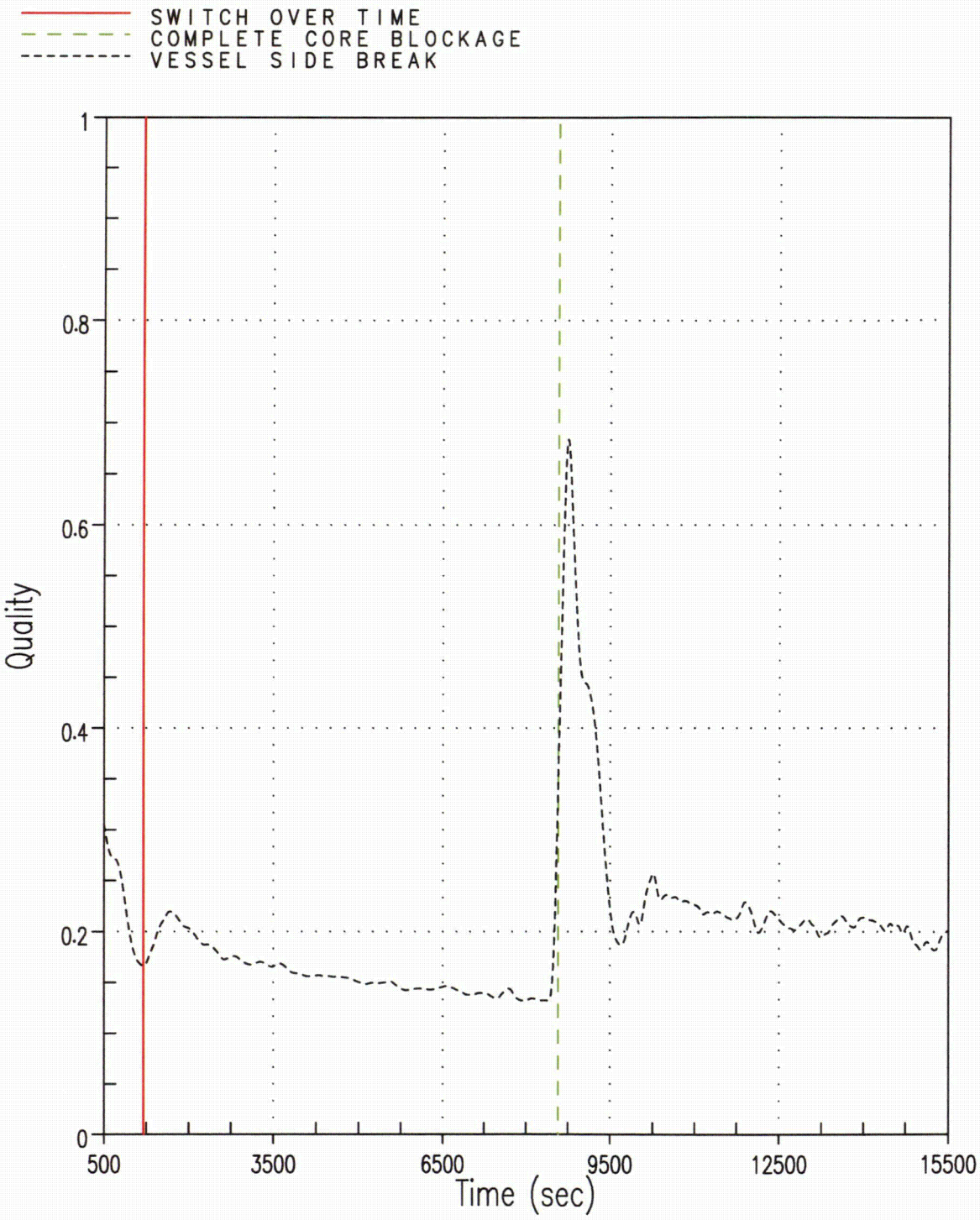

Figure 8-24 Case 1B – Break Exit Quality

8.2.3 After Debris Introduction – Calculation of K_{max}

Cases 2A and 2B are used to determine a value for K_{max}. These cases apply partial blockage to the core inlet prior to the application of complete core inlet blockage. These partial blockages are applied instantaneously at the point of transfer to sump recirculation and are applied uniformly across all core channels. Case 2B produces the lowest K_{max} value and will be discussed in this section.

Throughout the duration of the transient, more-than-adequate core cooling flow is provided through the ECCS to the cold legs. The partial blockage is applied at 20 min (1200 seconds) and complete core inlet blockage is applied at 143 min (8580 seconds). After the partial blockage is applied, the RCS response is very similar to the response seen after complete core inlet blockage as described in Section 8.2.2 except that flow continues through the core inlet at a reduced rate. Coolant from the ECCS backs-up and fills the downcomer until adequate driving head is achieved such that flow through the BB channel begins. From this point forward, the total flow entering the LP is split between the core inlet and the BB channel. Figure 8-25 shows that the core experiences a short-duration temperature excursion after the application of partial core inlet blockage; however, PCT remains below 800°F. DHR is maintained via a combination of flow through the core inlet and flow through the BB channel to the top of the core.

The RV fluid mass is shown in Figure 8-26. When partial core inlet blockage is applied, the RV inventory increases quickly, which can be credited to filling of the downcomer. Once the downcomer fills and the BB channel becomes an active flow path, the RV fluid mass eventually stabilizes and remains fairly constant for the remainder of the transient. The application of complete core inlet blockage later in the transient has minimal impact on the RV fluid inventory. These trends are consistent with the behavior of the core collapsed liquid level as shown in Figure 8-27, which show the hot assembly collapsed liquid. The collapsed liquid levels in the other core channels show similar trends. The downcomer and BB channel collapsed liquid levels are shown in Figure 8-28. When the blockage is applied, the downcomer collapsed liquid level quickly increases due to the increased resistance to flow through the core inlet. As a result, the BB channel is filled with coolant and flow through the channel provides coolant to the top of the core.

The core inlet mass flow rate and the BB exit flow rate are compared to boil-off in Figure 8-29. The figure indicates that flow into the core is well in excess of boil-off after the application of partial and complete core inlet blockage. Figure 8-30 shows the pressure drop across the debris bed and the core inlet liquid velocities. The figure confirms that flow through the core inlet continues after the application of partial blockage and ceases after the application of complete core inlet blockage.

The majority of the flow that exits the BB flows into the peripheral core channel and the flow direction is predominately downward. Figure 8-31 shows the liquid velocities in the top third of the peripheral core channel and Figure 8-32 shows the liquid velocities in the bottom third of the low-power channel. These plots indicate that the flow of liquid is predominately downward along the entire length of the peripheral core channel similar to what was seen after complete core inlet blockage in the Series 1 cases.

With the bulk of the liquid exiting the BB channel and flowing downward in the periphery of the core, cross flow provides liquid to the average channels and hot assembly channel. This behavior is illustrated in Figure 8-33, which shows the cross flow velocity in the top third of the core from the average core channel to the hot assembly channel. The positive velocities in the figures indicate that flow is going into

the hot assembly channel from the average assembly channel. Similar cross flows are observed from the peripheral channel into the average channels at the top elevations of the core. It is noted that the cross flows between core channels near the bottom of the core are less vigorous given that flow continues through the core inlet.

The break exit quality is shown in Figure 8-34. This figure shows that the quality prior to the application of partial core inlet blockage remains below 20%. After the application of partial blockage the case shows a spike in the break quality (consistent with the core uncovery), which slowly recovers and stabilizes just below 20% prior to the application of complete core inlet blockage. When complete core inlet blockage is applied, the break exit quality increases slightly to a value just above 20%. Due to the large amount of liquid carryover out the break during the transient, BAP is controlled and boron concentrations in the RV will remain well below the solubility limit.

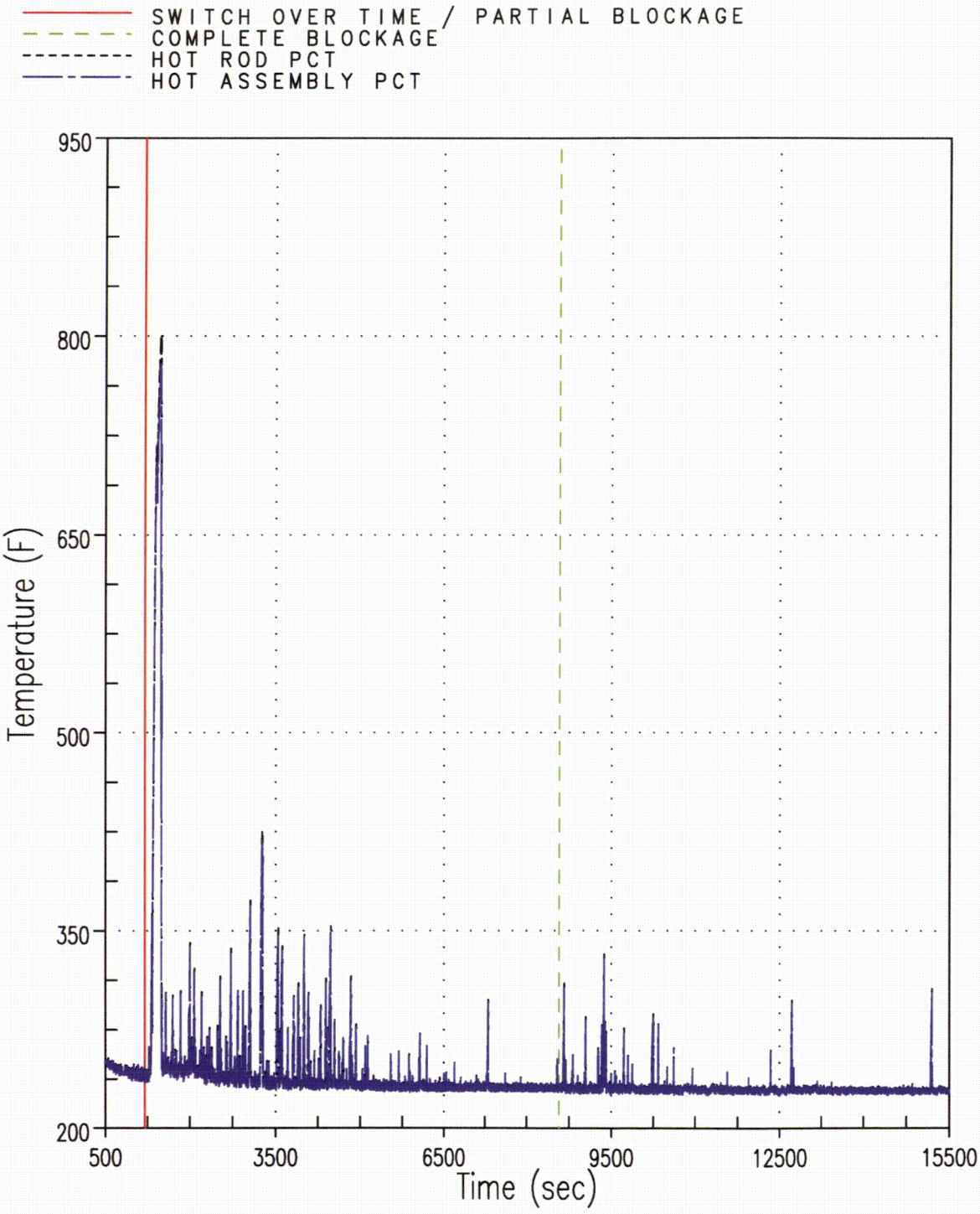

Figure 8-25 Case 2B – Hot Rod and Hot Assembly Peak Cladding Temperatures

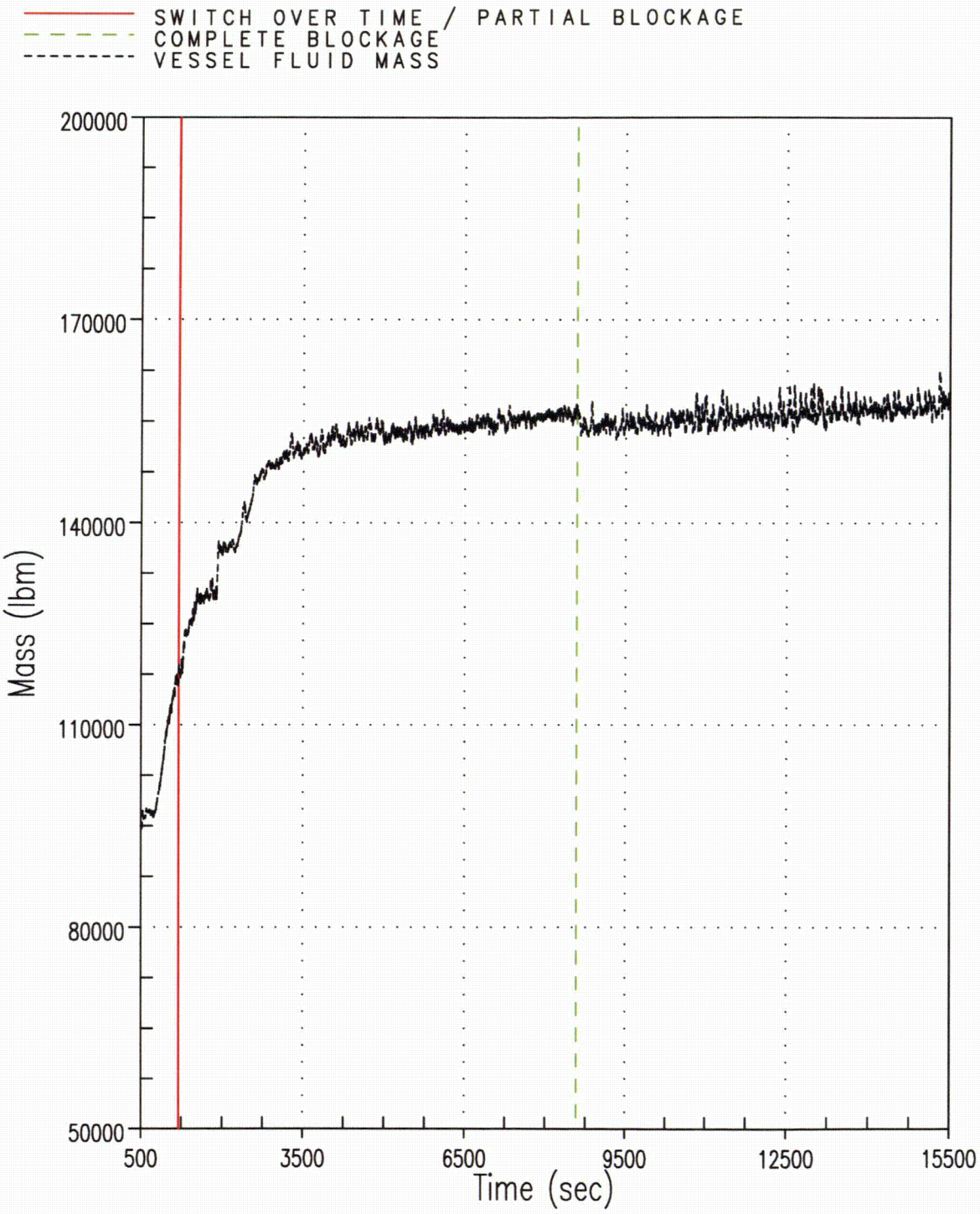

Figure 8-26 Case 2B – Reactor Vessel Fluid Mass

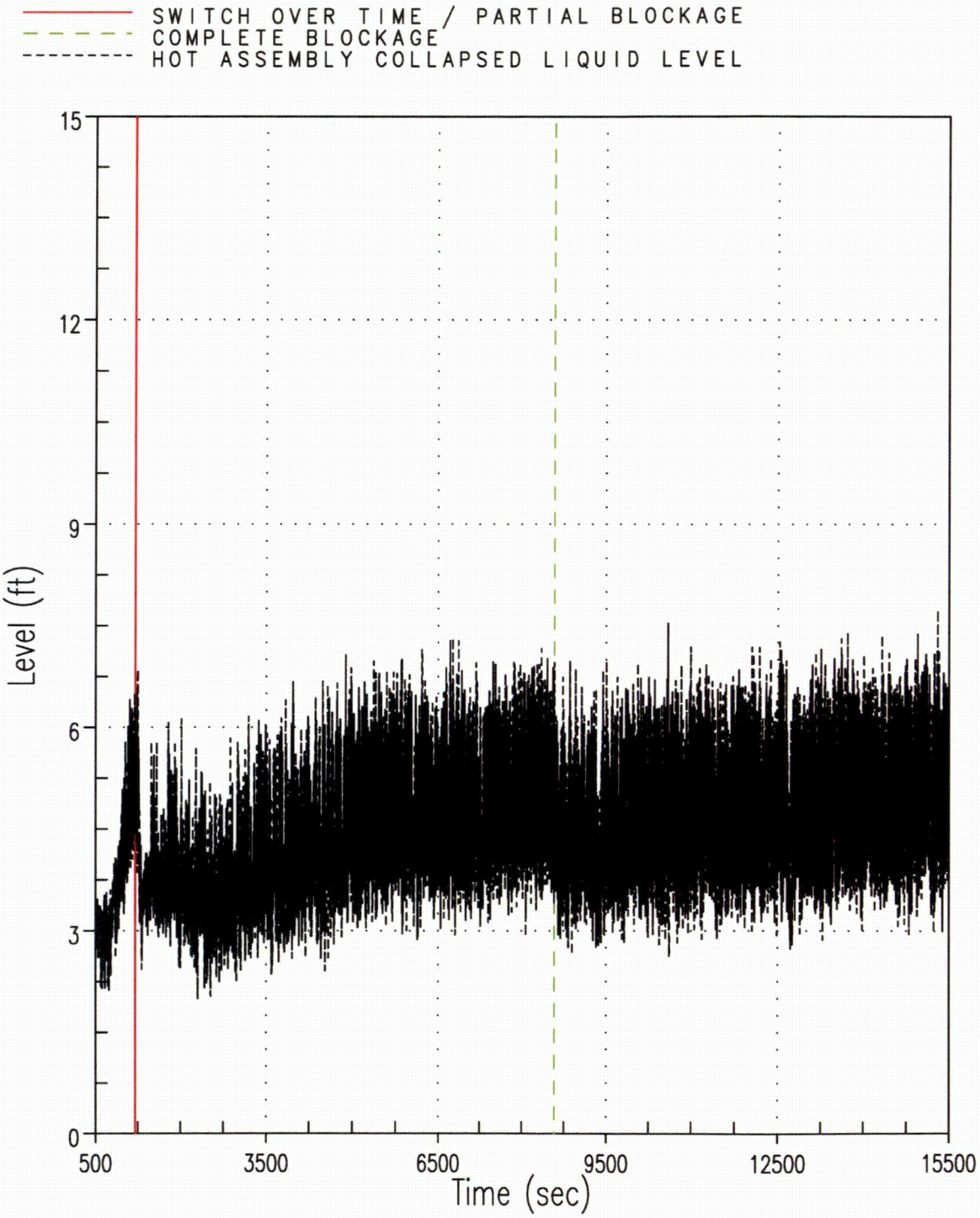

Figure 8-27 Case 2B – Hot Assembly Collapsed Liquid Level

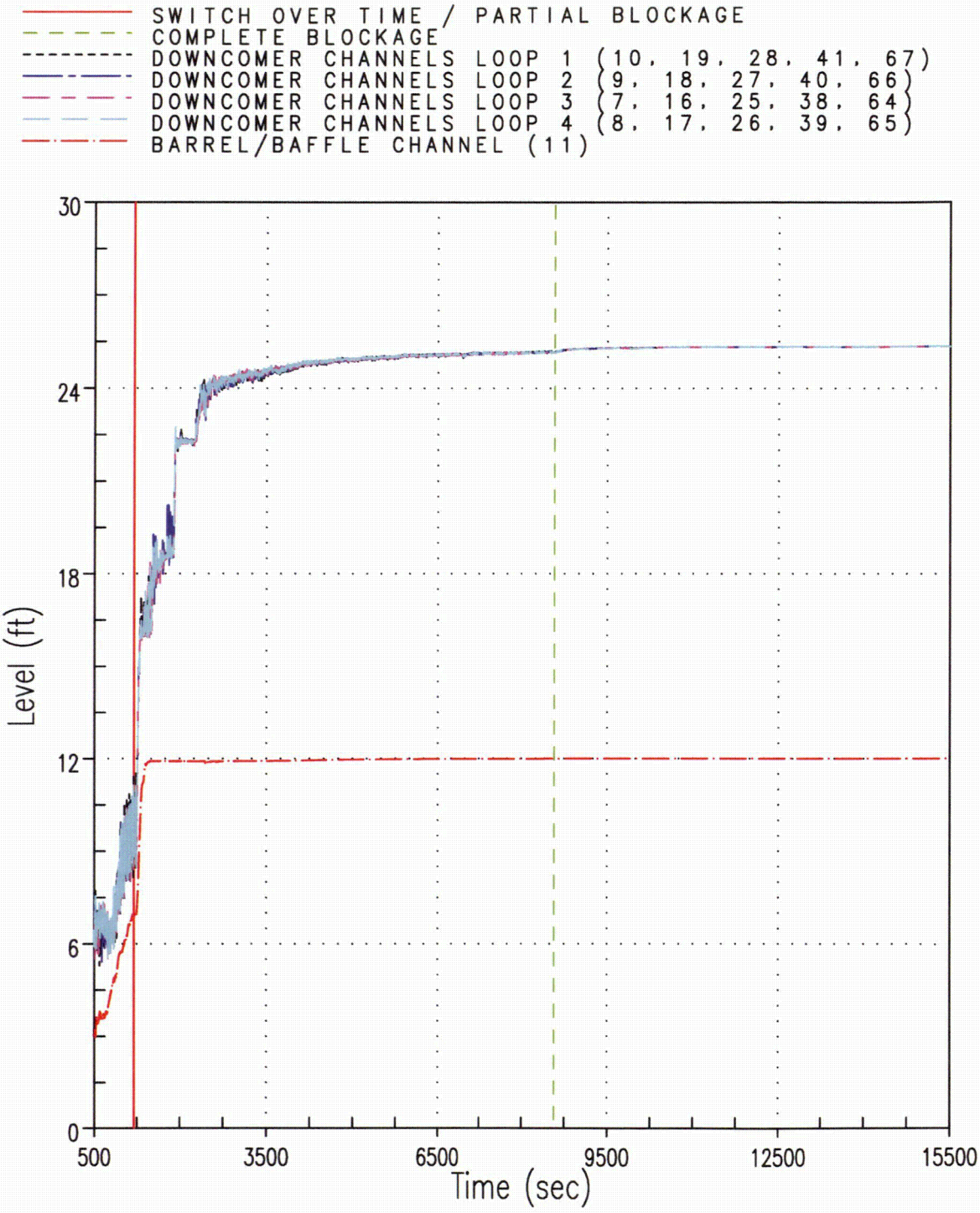

Figure 8-28 Case 2B – Downcomer and Barrel/Baffle Channel Collapsed Liquid Levels

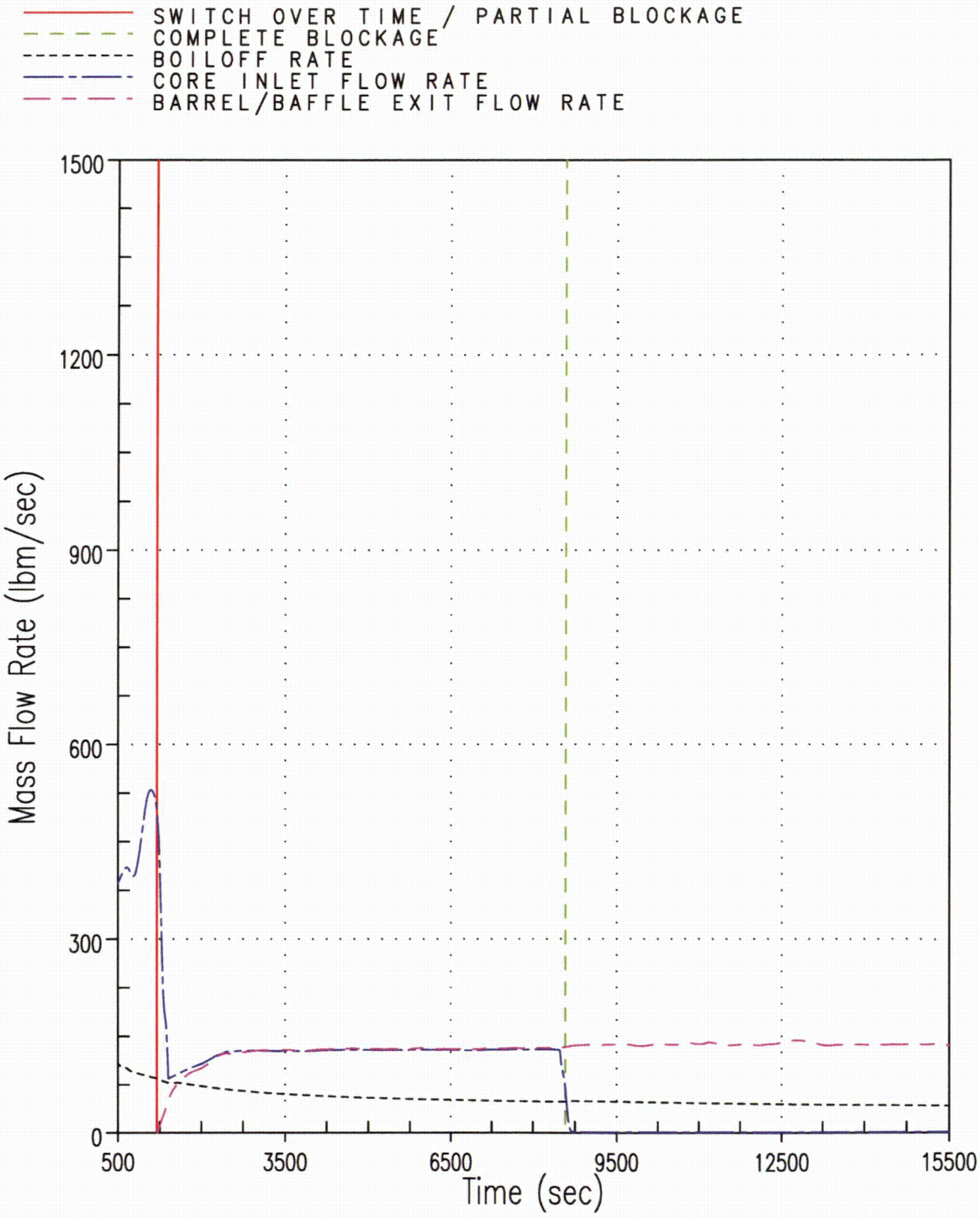

Figure 8-29 Case 2B – Core Inlet and Barrel/Baffle Channel Exit Flow Rate Compared to Boil-off

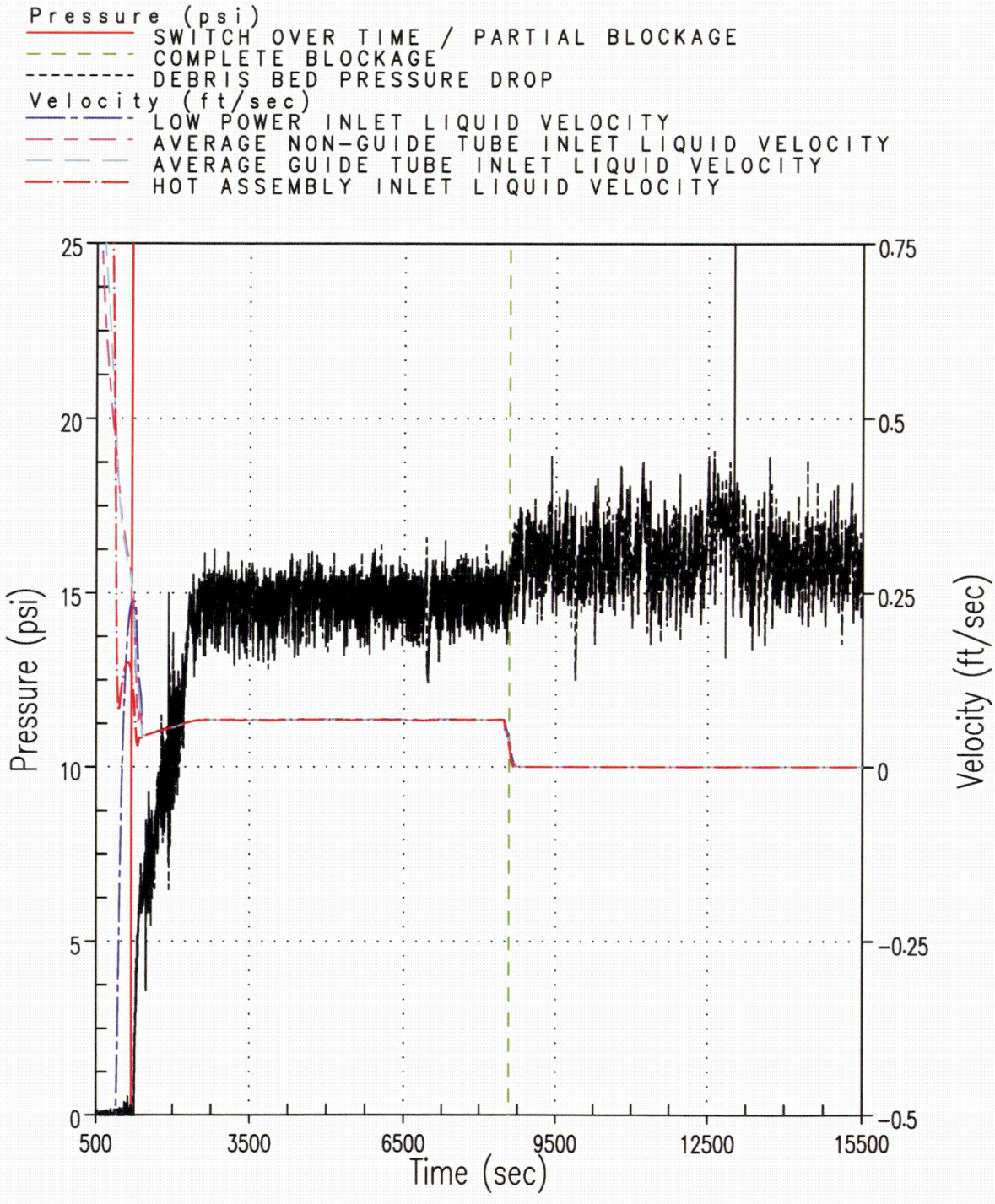

Figure 8-30 Case 2B – Pressure Drop across Debris Bed and Core Inlet Liquid Velocities

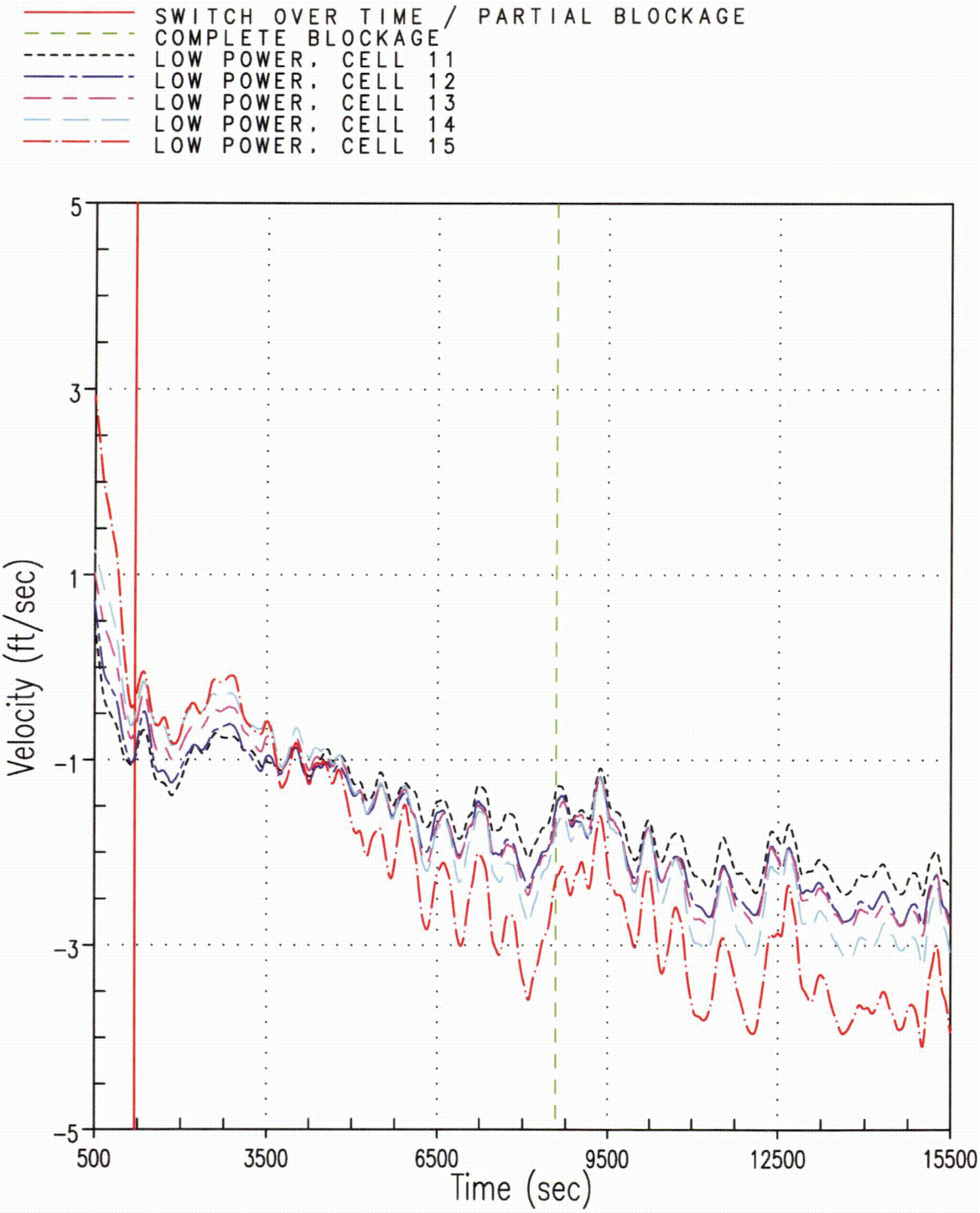

Figure 8-31 Case 2B – Liquid Velocity at the Top of the Peripheral Core Channel

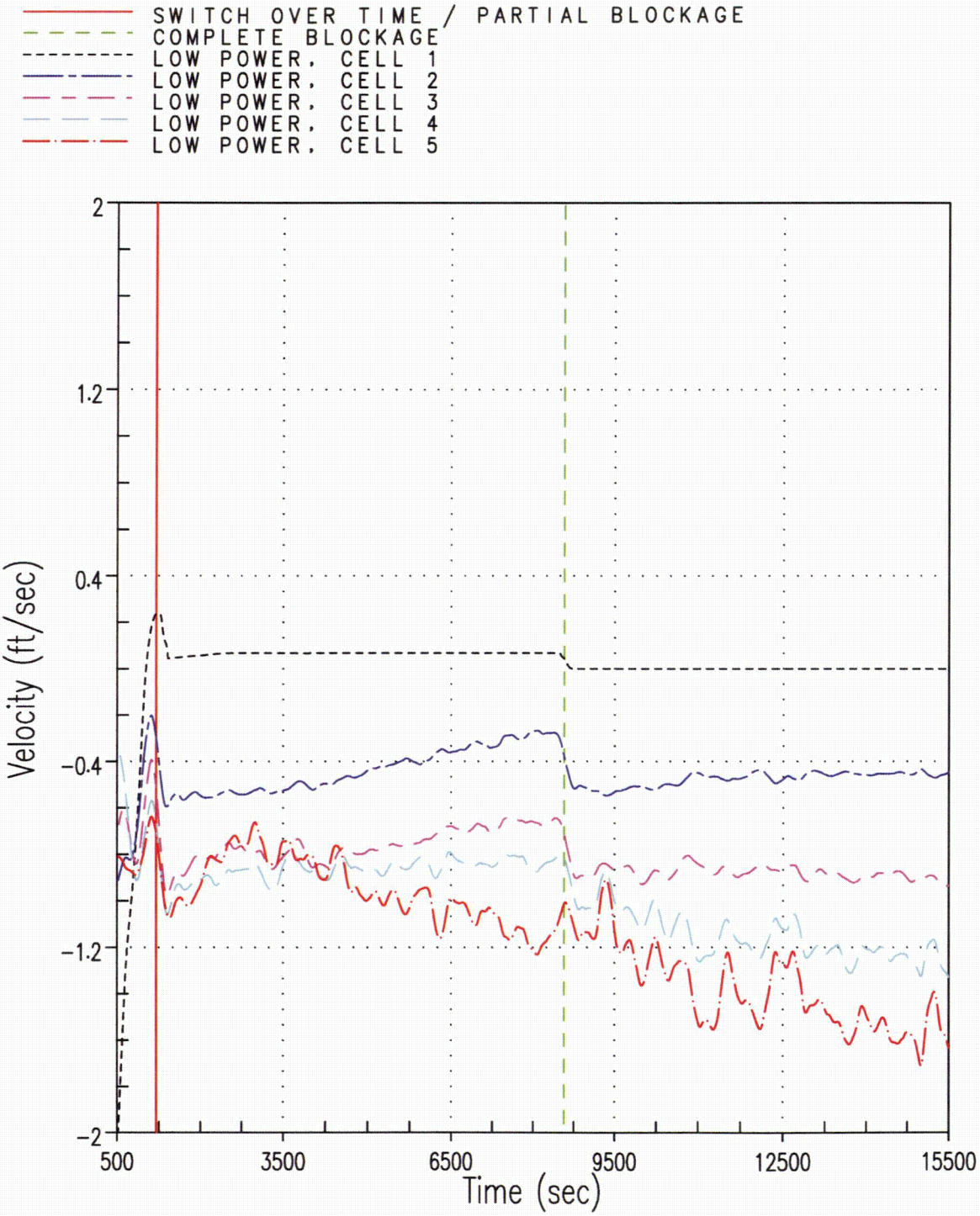

Figure 8-32 Case 2B – Liquid Velocity at the Bottom of the Peripheral Core Channel

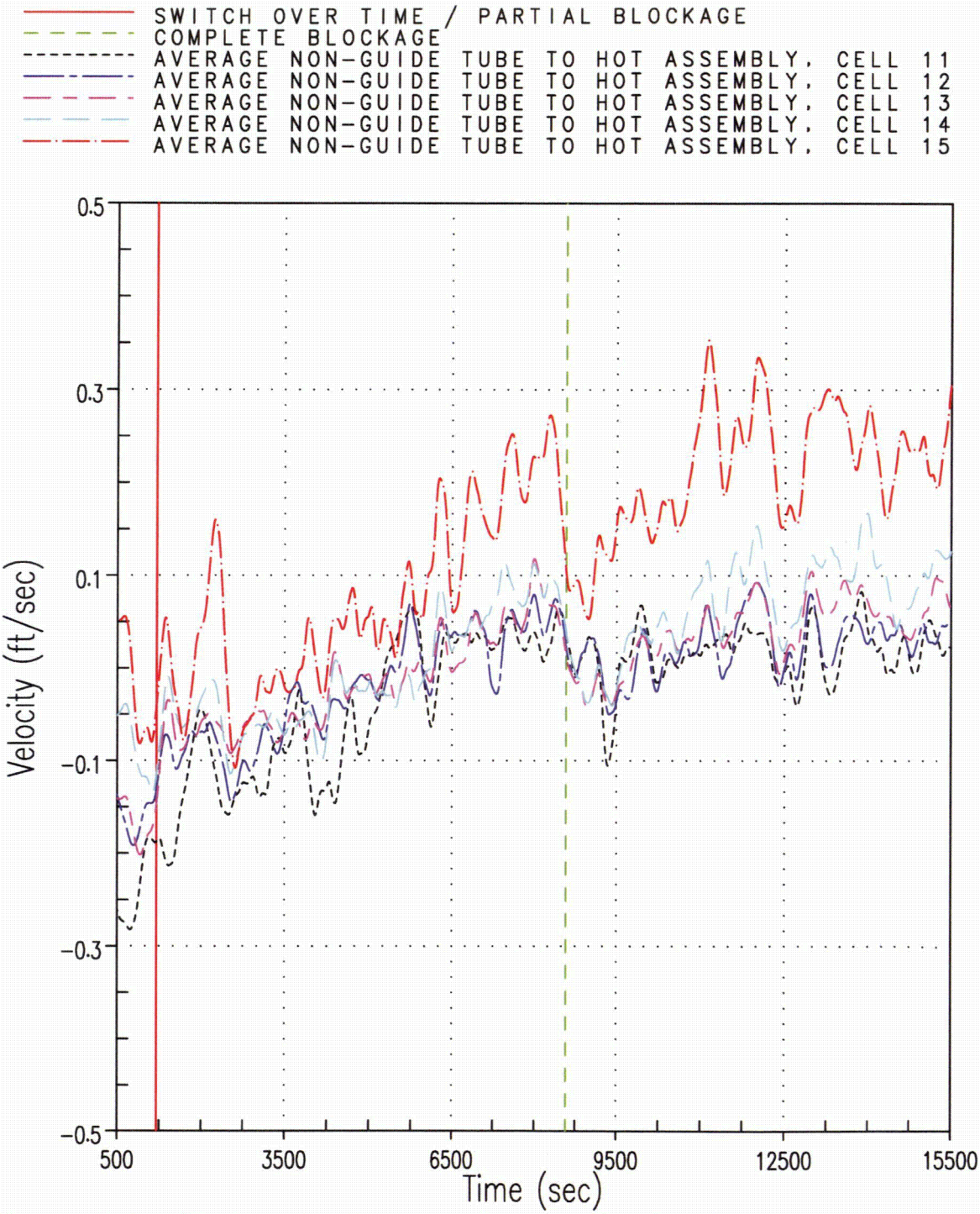

Figure 8-33 Case 2B – Cross Flow from Average Non-Guide Tube Core Channel to Hot Assembly Core Channel at the Top of the Core

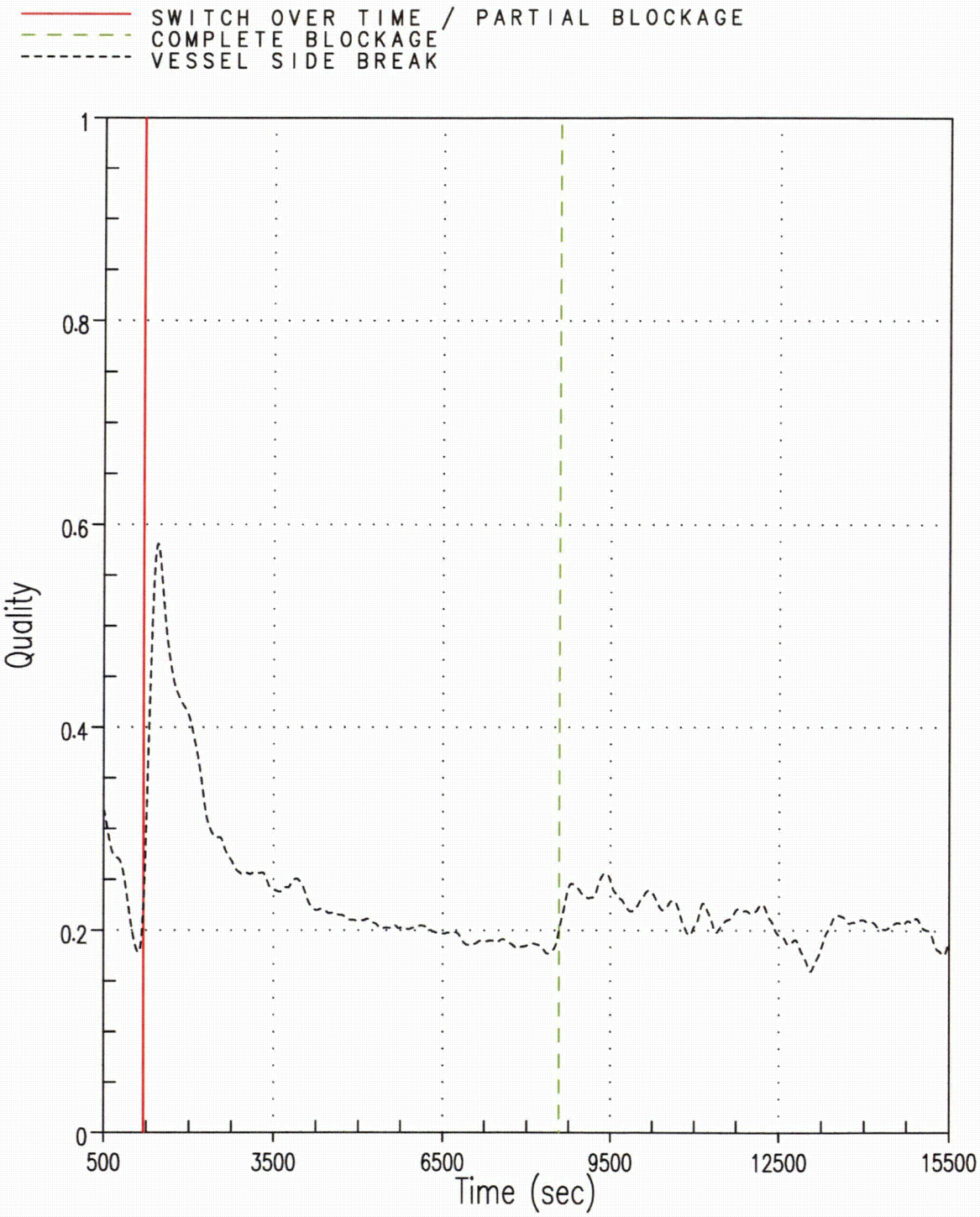

Figure 8-34 Case 2B – Break Exit Quality

8.2.4 After Debris Introduction – Calculation of K_{split} and m_{split}

Five additional cases were run to determine K_{split} and m_{split}. For these cases, a linear ramp in resistance was applied at the core inlet and complete core inlet blockage was not simulated. Since these cases were used to assess the timing of the activation of the BB channel, the build-up of core inlet resistance was applied more slowly compared to the cases used to determine K_{max}. As a result, the RCS response to core inlet blockage was much slower in that the downcomer fill rate and the activation of the BB channel occurred over a longer period of time. It is noted that these simulations are more realistic with regard to the timing at which debris is expected to arrive at the core inlet.

Even though five simulations were completed to cover the full range of ECCS flows expected during sump recirculation, only the high-, mid-, and low-flow cases were selected for discussion in this section. Similar trends were observed in the two cases not discussed.

8.2.4.1 Case 1 – 40 gpm/FA

Select transient plots from Case 1 are shown in Figures 8-35 through 8-38. The RCS response to core inlet blockage was expected and is generally consistent with the transient response discussed in Section 8.2.3. Figure 8-35 shows the core inlet and BB exit flow rates compared to boil-off. The figure demonstrates that flow to the core is well above boil-off during the entire transient. The flow response to core inlet blockage is also shown by the figure. As core inlet blockage is applied, the pressure drop across the core inlet increases. Once K_{split} is reached, the BB exit flow rate becomes positive and increases as the magnitude of core inlet blockage increases. As a result, the core inlet flow rate decreases consistent with the rate that the BB flow rate increases.

Figure 8-36 shows the transient downcomer and BB collapsed liquid levels. As core inlet blockage is applied, both the downcomer and BB collapsed liquid levels increase as expected. When K_{split} is reached, the BB collapsed liquid level indicates that the BB channel is completely flooded and the downcomer collapsed liquid level is several feet higher. As core inlet blockage continues to increase, the downcomer continues to flood and eventually reaches the UHSN elevation.

The PCT transient is shown in Figure 8-37. The figure indicates that the PCT remains well below 800°F, and the lack of any significant heatups indicates that the core never uncovers after application of core inlet resistance.

Figure 8-38 shows the pressure drop across the core inlet and the core inlet liquid velocity. As expected, the core inlet velocity decreases as the pressure drop across the simulated debris bed increases.

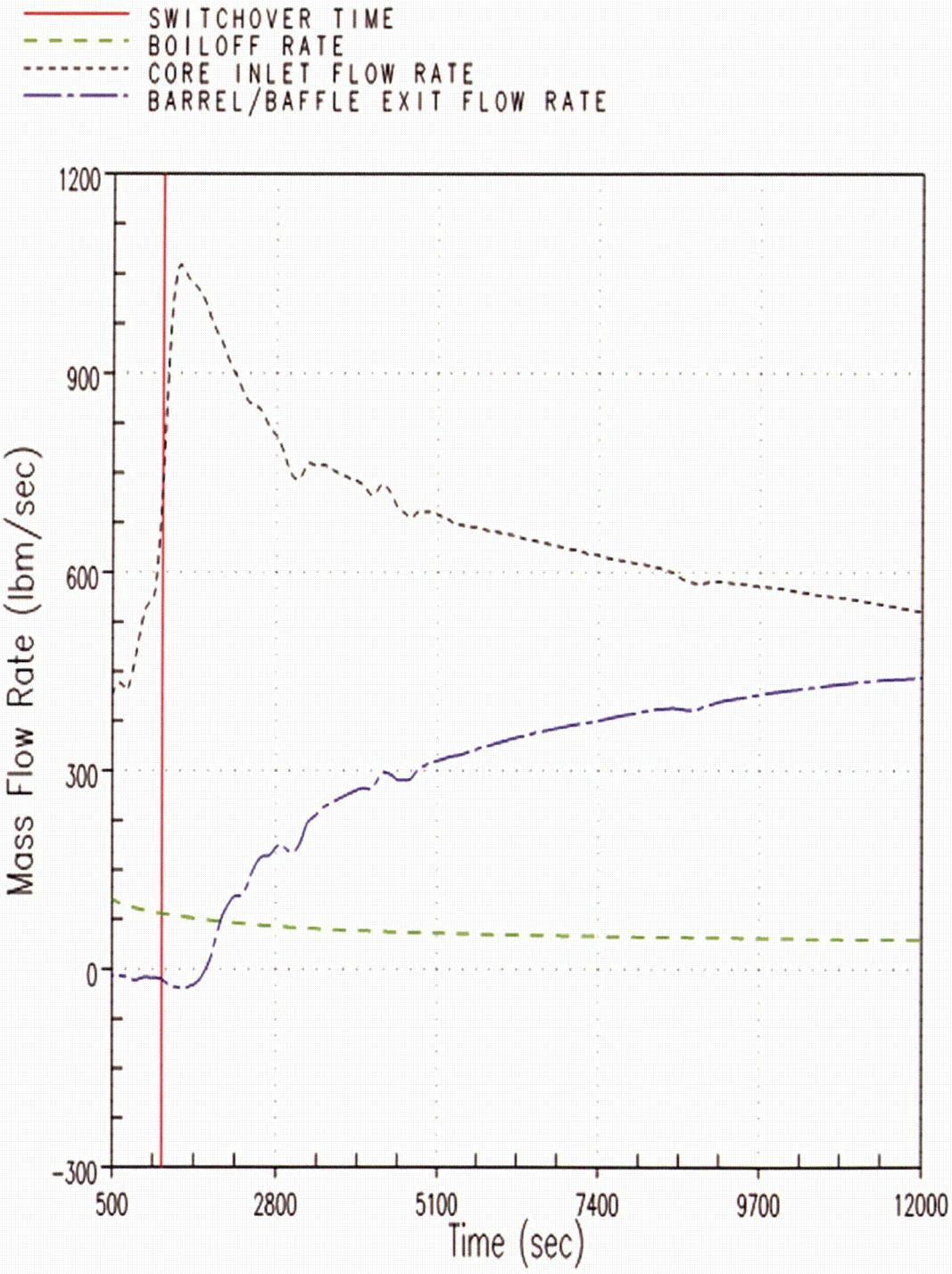

Figure 8-35 K_{split} Case 1 – Core Inlet and Barrel/Baffle Exit Flow Rates Compared to Boil-off

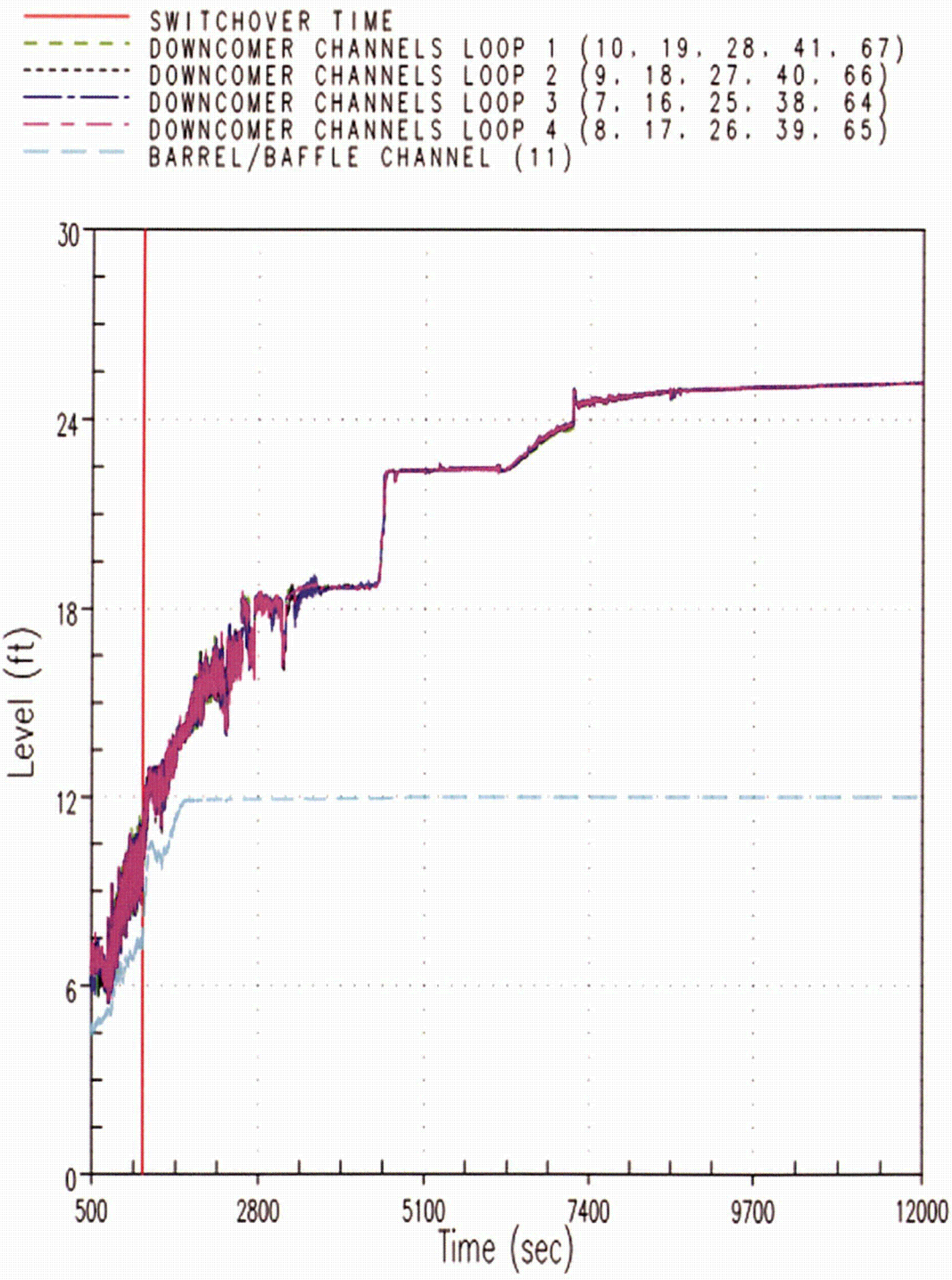

Figure 8-36 K_{split} Case 1 – Downcomer and Barrel/Baffle Collapsed Liquid Levels

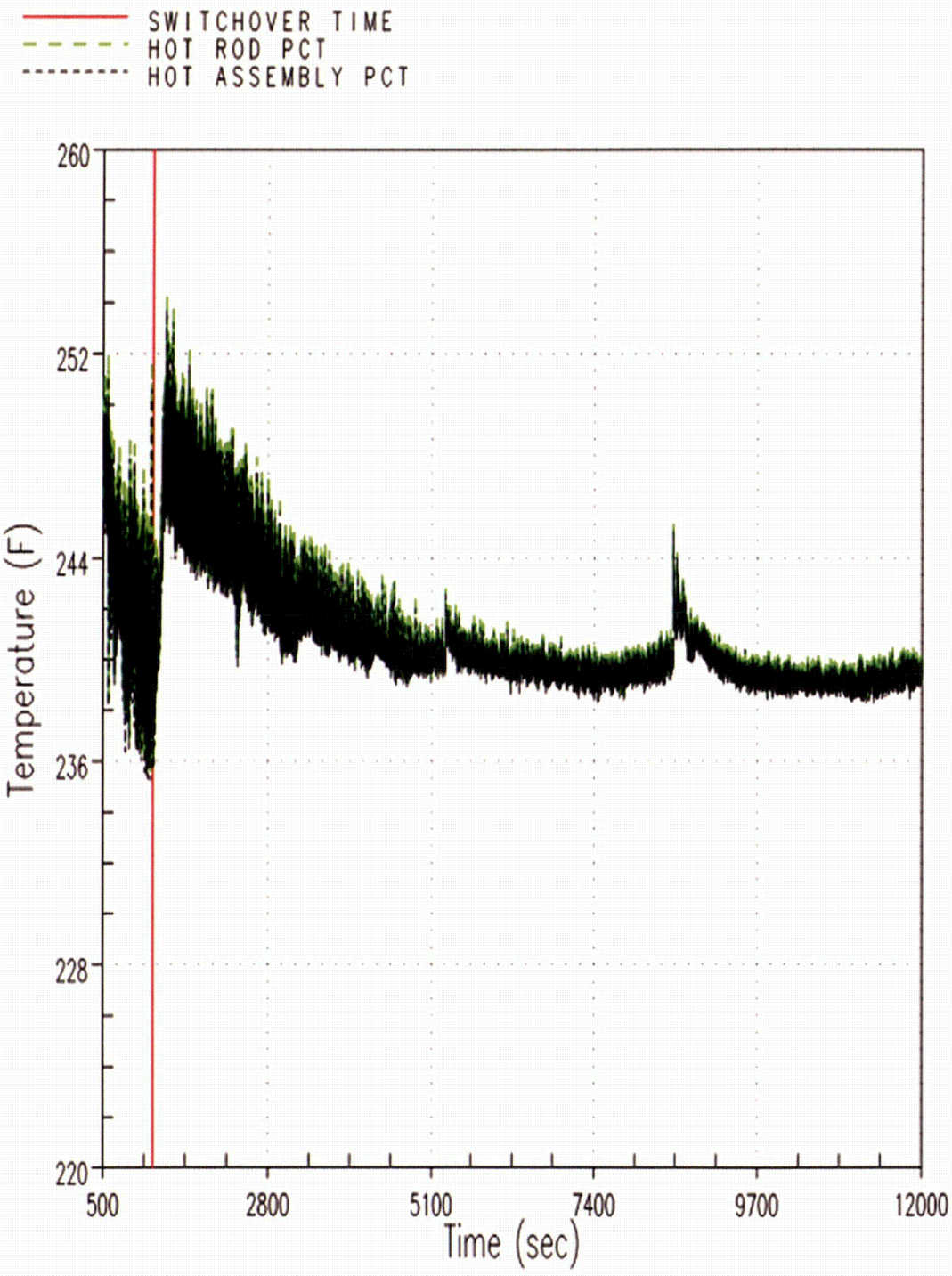

Figure 8-37 K_{split} Case 1 – Hot Rod and Hot Assembly Peak Cladding Temperatures

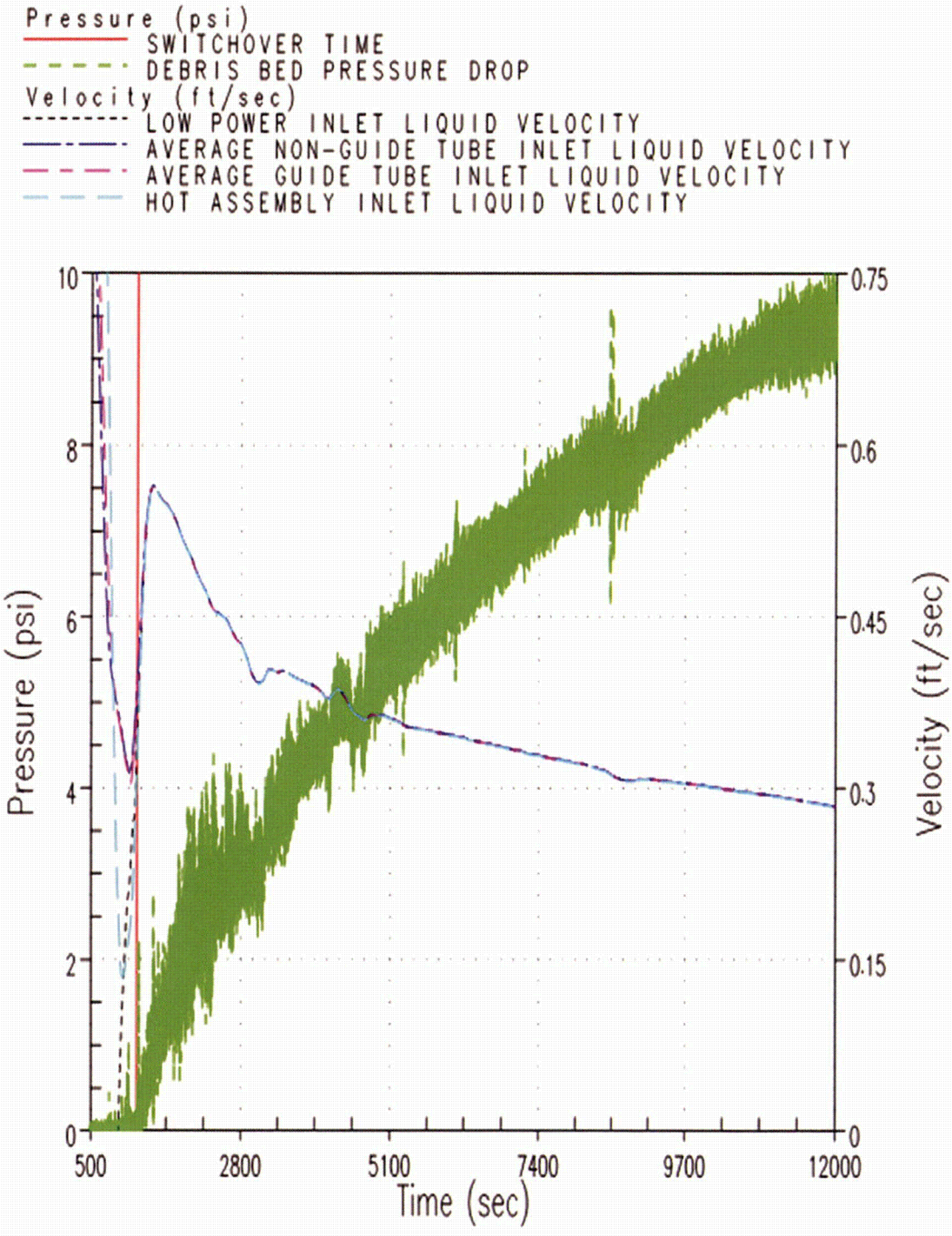

Figure 8-38 K_{split} Case 1 – Debris Bed Pressure Drop and Core Inlet Liquid Velocity

8.2.4.2 Case 3 – 18 gpm/FA

Select transient plots from Case 3 are shown in Figures 8-39 through 8-42. The RCS response to core inlet blockage was expected and is generally consistent with the transient response discussed in Section 8.2.3. Figure 8-39 shows the core inlet and BB exit flow rates compared to boil-off. The figure demonstrates that flow to the core is well above boil-off during the entire transient. The flow response to core inlet blockage is also shown by the figure. As core inlet blockage is applied, the pressure drop across the core inlet increases. Once K_{split} is reached, the BB exit flow rate becomes positive and increases as the magnitude of core inlet blockage increases. As a result, the core inlet flow rate decreases consistent with the rate that the BB flow rate increases. Comparing this flow response to the high-flow case described previously, it can be seen that reducing the ECCS flow results in a longer time period to reach K_{split}.

Figure 8-40 shows the transient downcomer and BB collapsed liquid levels. As core inlet blockage is applied, both the downcomer and BB collapsed liquid levels increase as expected. When K_{split} is reached, the BB collapsed liquid level indicates that the BB channel is completely flooded and the downcomer collapsed liquid level is several feet higher. For this case, the ECCS flow rate is not high enough to completely flood the downcomer to the UHSN elevation during the simulation.

The PCT transient is shown in Figure 8-41. The figure indicates that the PCT remains well below 800°F, and the lack of any heatups indicates that the core never uncovers after application of core inlet resistance.

Figure 8-42 shows the pressure drop across the core inlet and the core inlet liquid velocity. As expected, the core inlet velocity decreases as the pressure drop across the simulated debris bed increases.

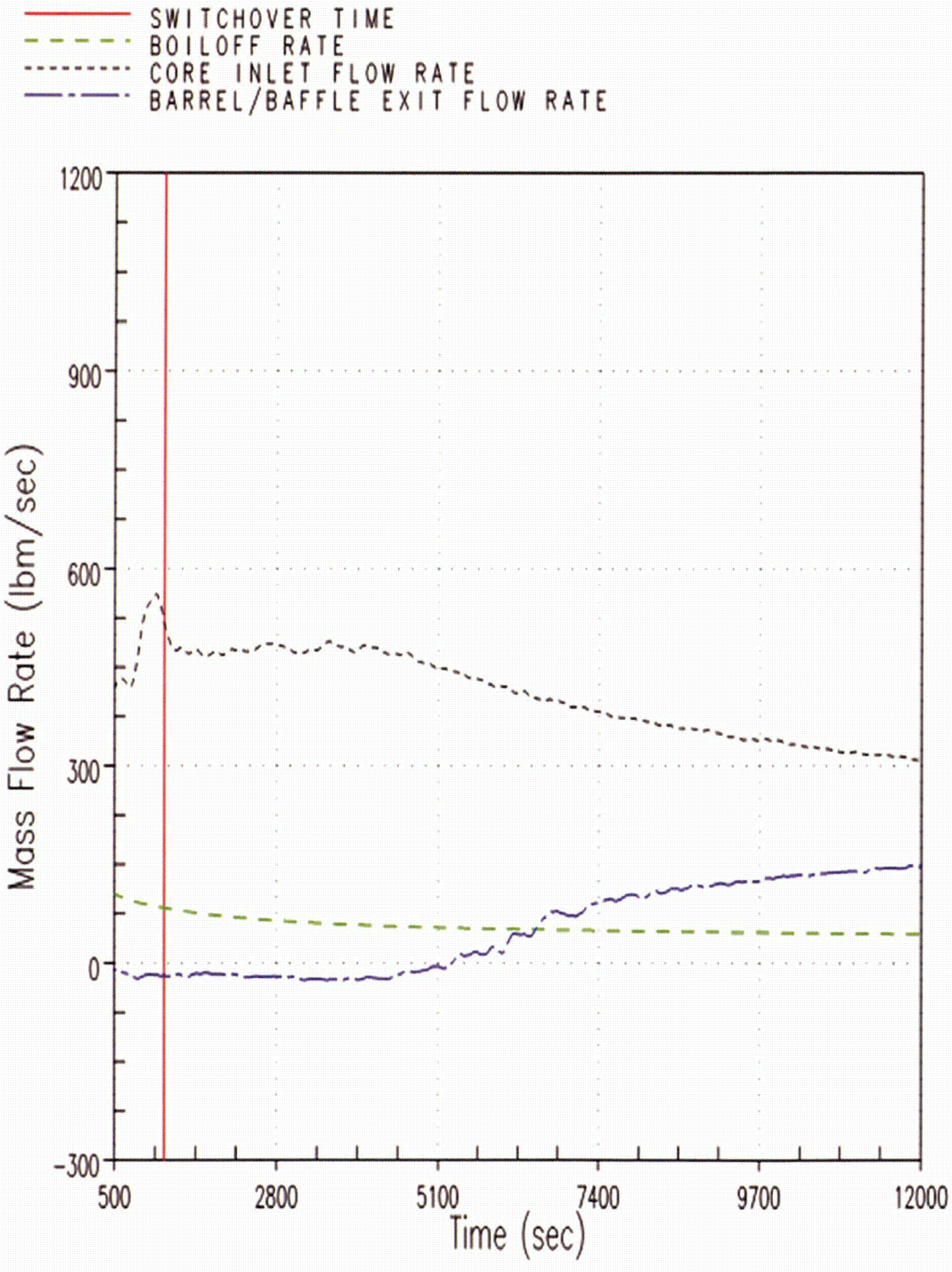

Figure 8-39 K_{split} Case 3 – Core Inlet and Barrel/Baffle Exit Flow Rates Compared to Boil-off

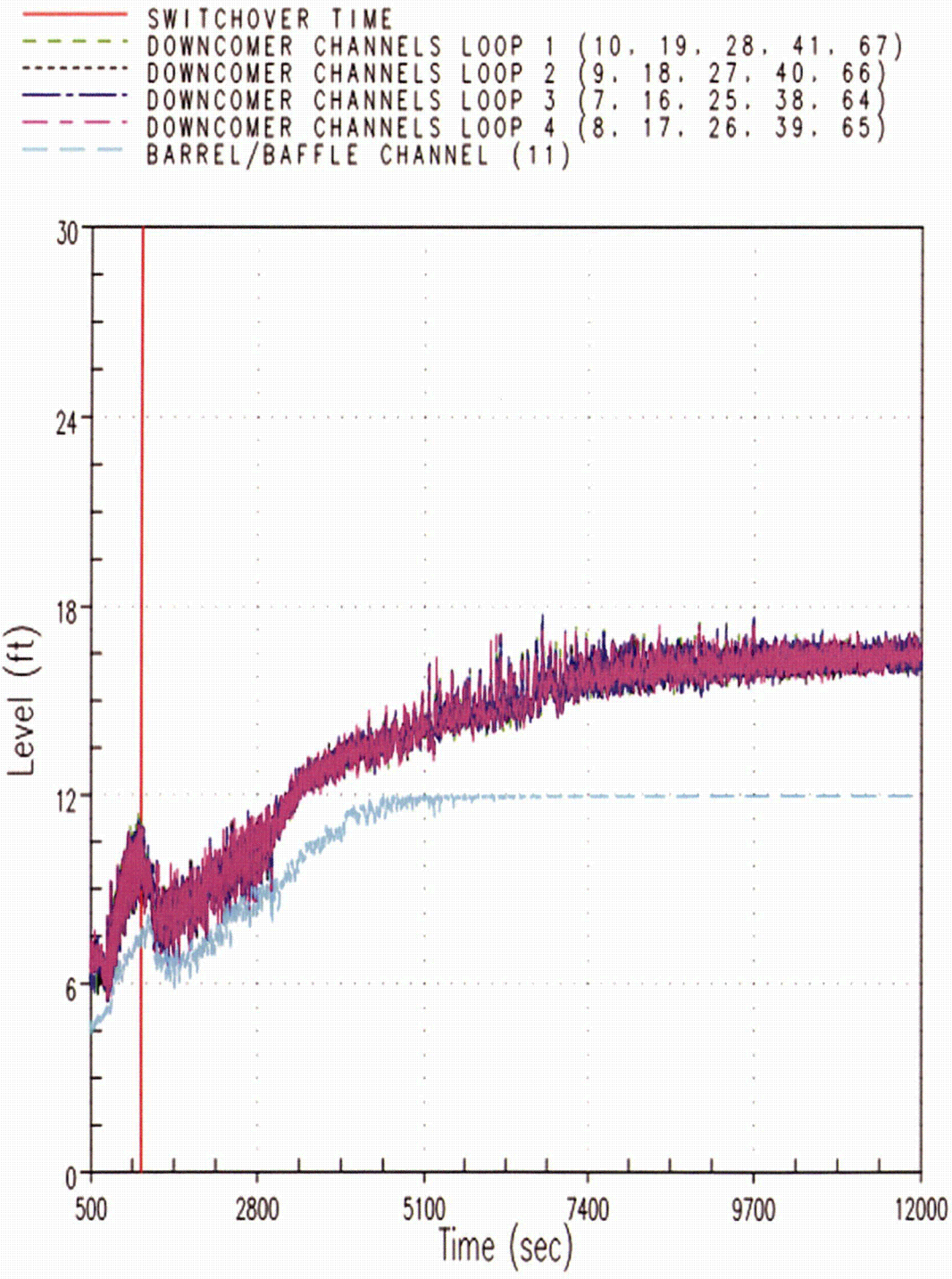

Figure 8-40 K_{split} Case 3 – Downcomer and Barrel/Baffle Collapsed Liquid Levels

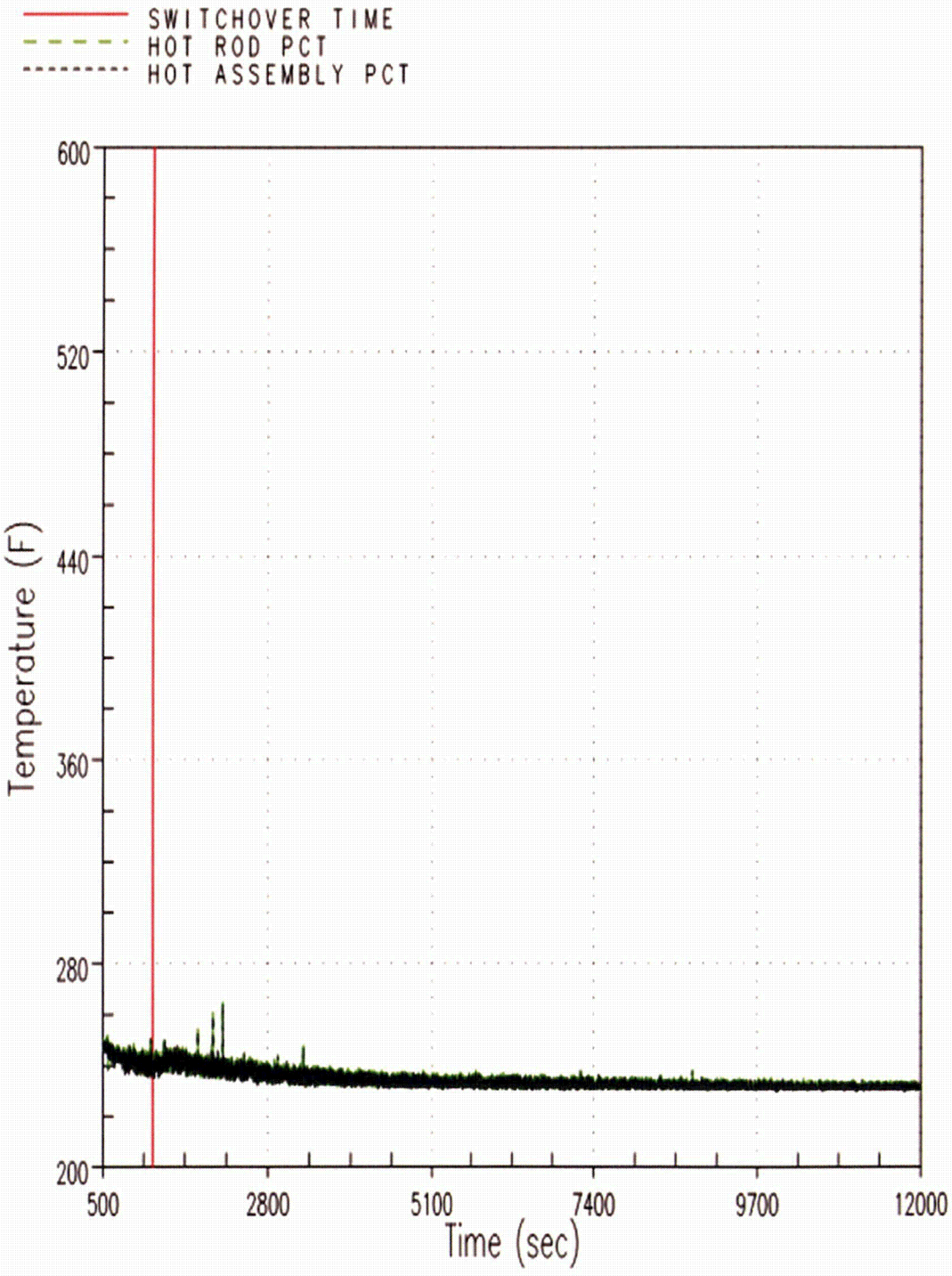

Figure 8-41 K_{split} Case 3 – Hot Rod and Hot Assembly Peak Cladding Temperatures

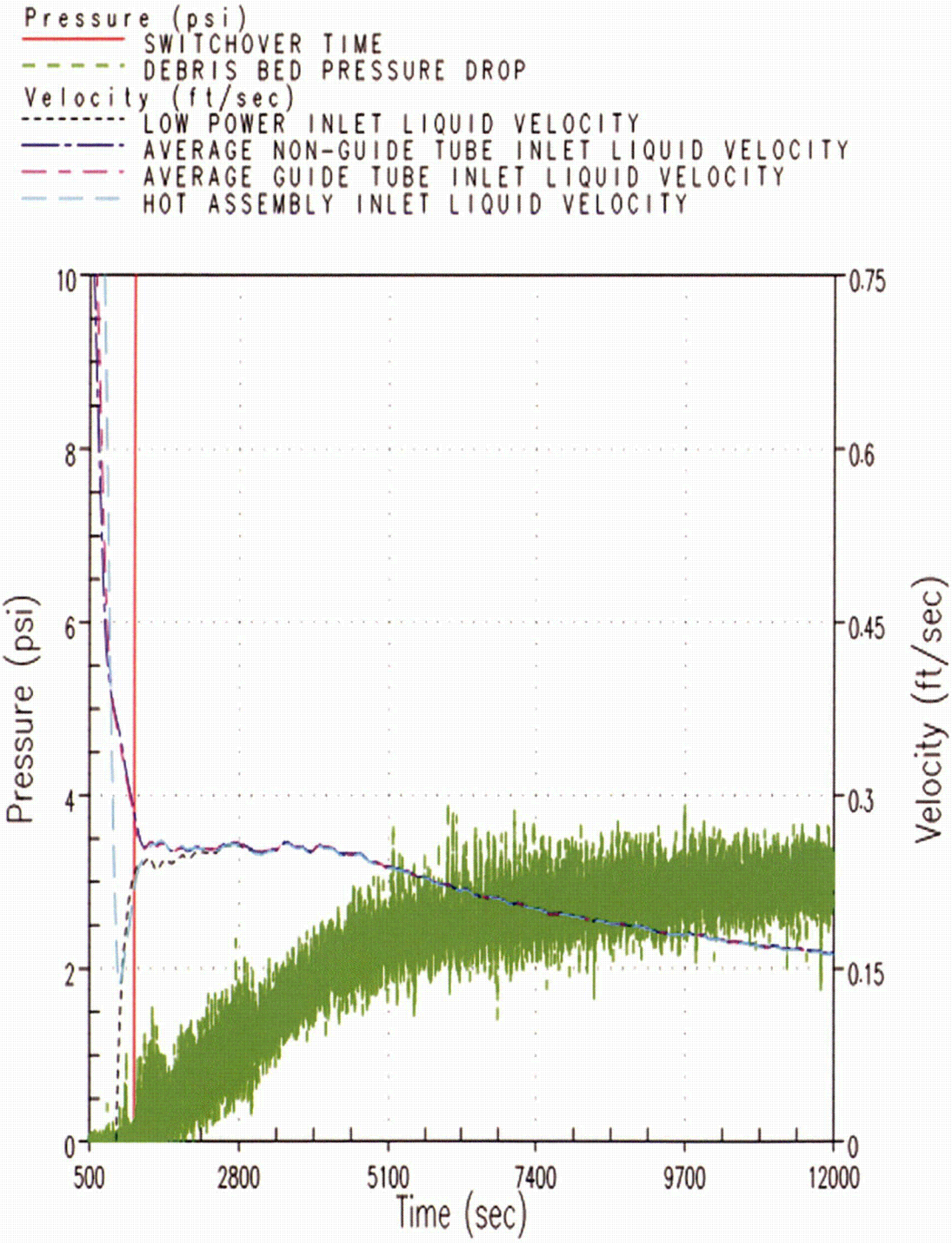

Figure 8-42 K_{split} Case 3 – Debris Bed Pressure Drop and Core Inlet Liquid Velocity

8.2.4.3 Case 5 – 8 gpm/FA

Select transient plots from Case 5 are shown in Figures 8-43 through 8-46. The RCS response to core inlet blockage was expected and is generally consistent with the transient response discussed in Section 8.2.3. Figure 8-43 shows the core inlet and BB exit flow rates compared to boil-off. The figure demonstrates that flow to the core is well above boil-off during the entire transient. The flow response to core inlet blockage is also shown by the figure. As core inlet blockage is applied, the pressure drop across the core inlet increases. Once K_{split} is reached, the BB exit flow rate becomes positive and increases as the magnitude of core inlet blockage increases. As a result, the core inlet flow rate decreases consistent with the rate that the BB flow rate increases. Comparing this flow response to the high and mid flow cases described previously, it can be seen that further reducing the ECCS flow results in a longer time period to reach K_{split}.

Figure 8-44 shows the transient downcomer and BB collapsed liquid levels. As core inlet blockage is applied, both the downcomer and BB collapsed liquid levels increase as expected. When K_{split} is reached, the BB collapsed liquid level indicates that the BB channel is completely flooded and the downcomer collapsed liquid level is several feet higher. For this case, the ECCS flow rate is not high enough to completely flood the downcomer to the cold leg elevation.

The PCT transient is shown in Figure 8-45. The figure indicates that the PCT remains well below 800°F.

Figure 8-46 shows the pressure drop across the core inlet and the core inlet liquid velocity. As expected, the core inlet velocity decreases as the pressure drop across the simulated debris bed increases.

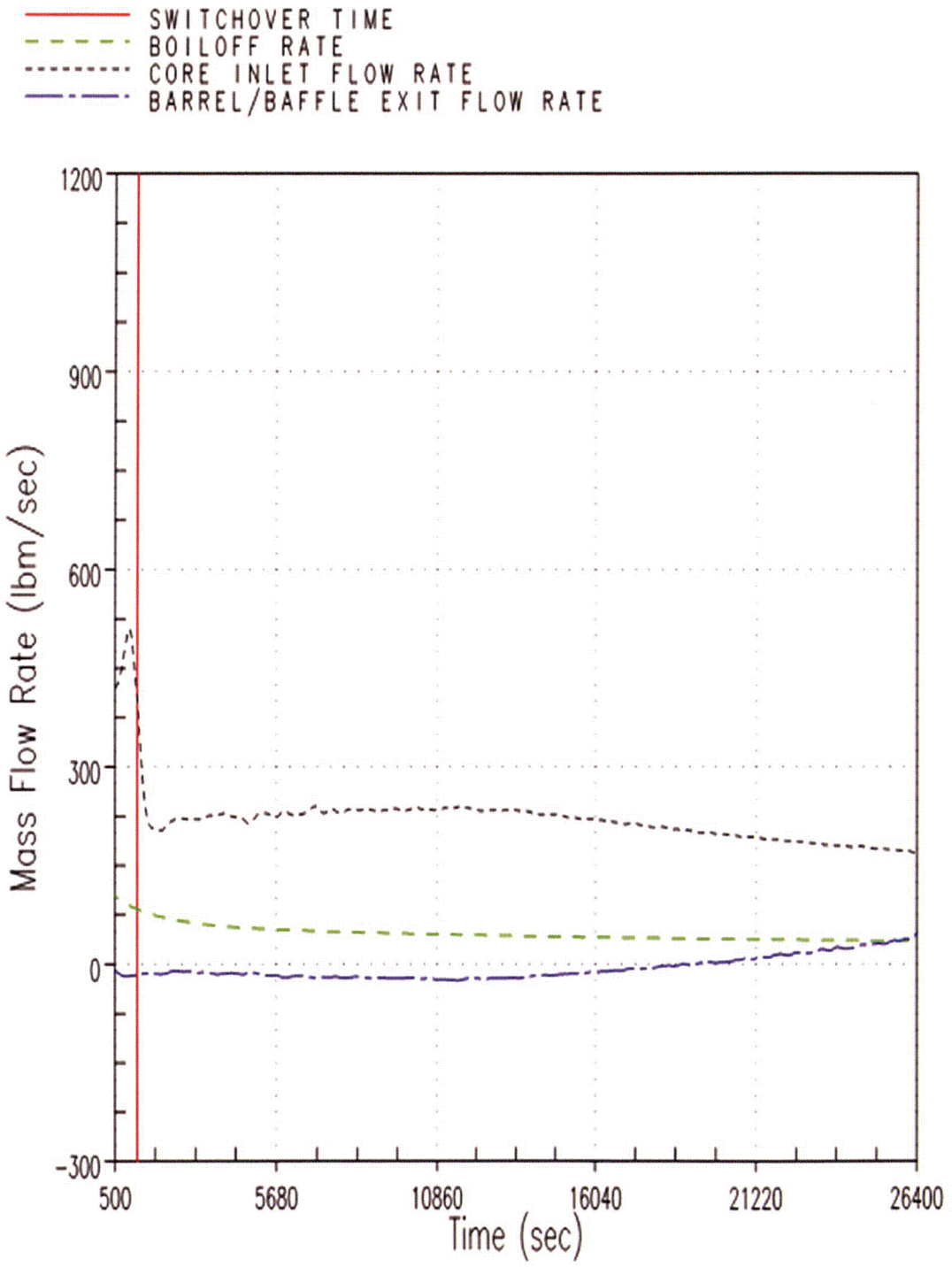

Figure 8-43 K_{split} Case 5 – Core Inlet and Barrel/Baffle Exit Flow Rates Compared to Boil-off

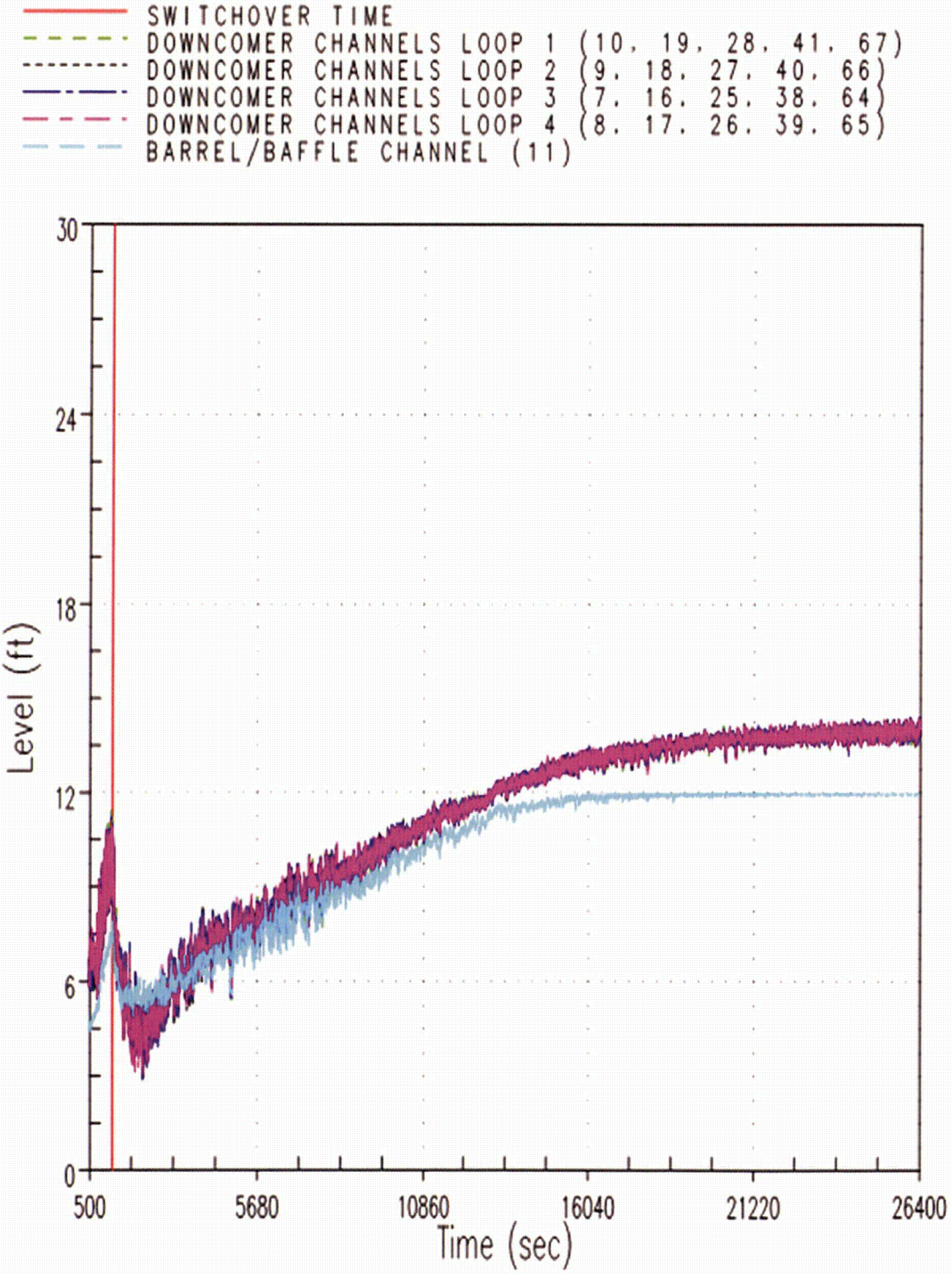

Figure 8-44 K_{split} Case 5 – Downcomer and Barrel/Baffle Collapsed Liquid Levels

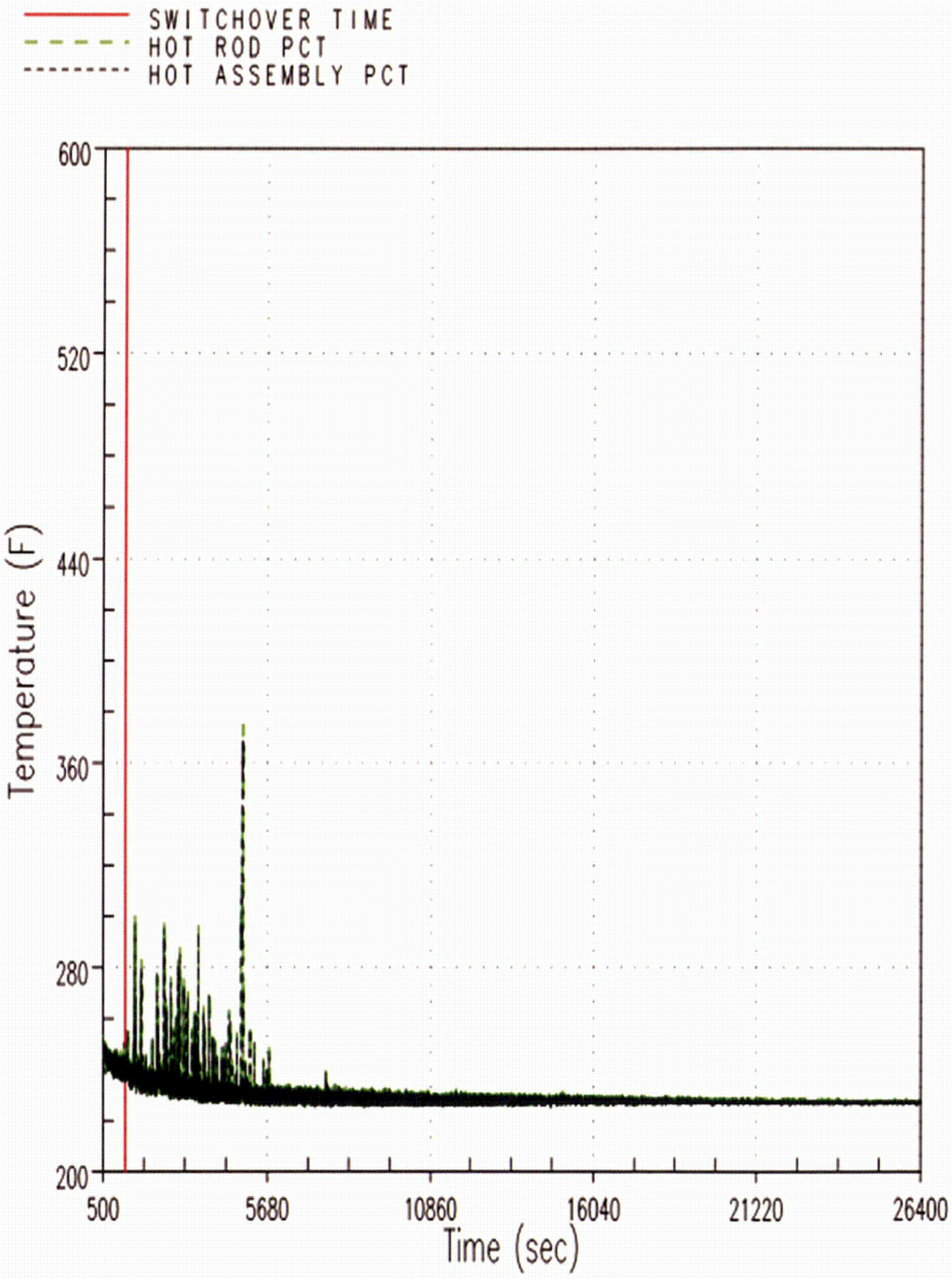

Figure 8-45 K_{split} Case 5 – Hot Rod and Hot Assembly Peak Cladding Temperatures

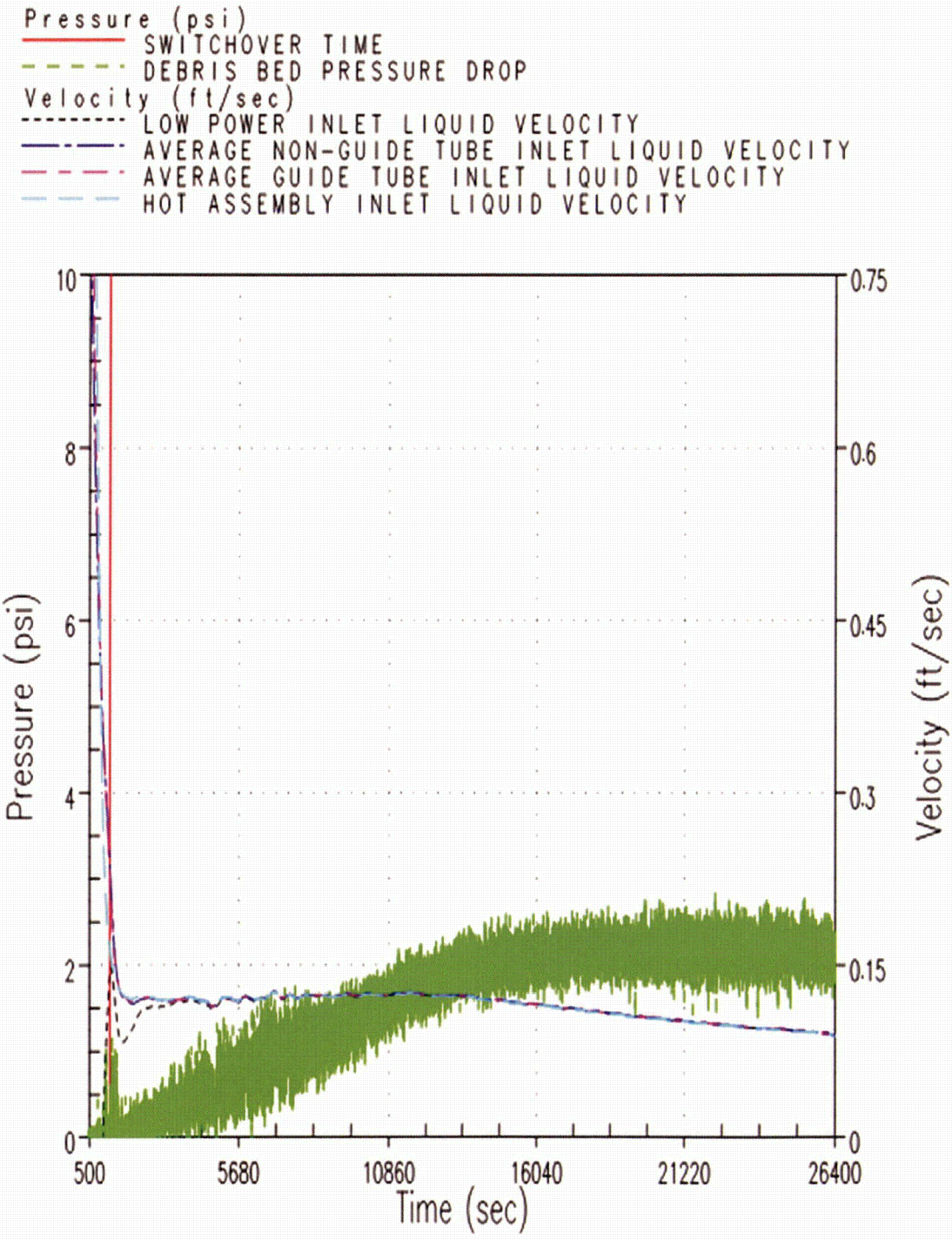

Figure 8-46 K_{split} Case 5 – Debris Bed Pressure Drop and Core Inlet Liquid Velocity

8.3 DISCUSSION OF RESULTS

During the first 20 minutes of the transient (before debris arrives), the core region has completely reflooded and the cladding temperatures are just above the saturation temperature. The core is boiling vigorously and the core average void fraction is approximately 50%. The downcomer is filling with coolant supplied to the cold legs via the ECCS. At 20 minutes, the downcomer collapsed liquid level is well below the cold leg elevation. Similarly, the BB is not liquid solid and is filling with liquid supplied from the UP region. There is a strong recirculation pattern within the core region in which the hot and average assemblies have predominately upflow while the peripheral assemblies have downflow. Vapor generated in the core flows toward the break and liquid carryover to the break is significant.

The first set of core inlet blockage simulations (Section 8.2.2) examined a scenario in which the core inlet was instantaneously completely blocked at some finite time after transfer to sump recirculation by applying a large form-loss coefficient at the core inlet. For this scenario, no partial blockage is applied prior to applying complete core inlet blockage. These simulations showed that the application of an instantaneous complete core inlet blockage resulted in a short-duration heatup within the core that was a result of core uncovery at the top of the core. When the blockage was applied, flow through the core inlet ceased and the ECCS began to fill the downcomer. Eventually, the downcomer liquid level reached a point where the driving head was sufficient to push coolant through the BB channel to the top of the core. This process resulted in recovery of the core two-phase mixture level and return of the cladding temperatures to values near the saturation temperature. It was found that the duration and magnitude of the heatup were heavily dependent on the timing of complete core inlet blockage and the ECCS flow rate. Applying the blockage earlier in the transient resulted in a longer-duration heatup with a higher PCT because the decay heat is higher and the core boiling more vigorous. Similarly, a lower ECCS flow rate resulted in a longer time to fill the downcomer and increase the driving head to a value high enough to push flow through the BB channel to the top of the core. For the range of ECCS flow rates investigated, it was determined that complete blockage of the core inlet had to be delayed until at least 143 minutes after the postulated LOCA to maintain a secondary heatup of less than 800°F.

It is recognized that the complete core inlet blockage scenario used to determine t_{block} is unrealistic relative to the prototypic system. In reality, the arrival of fibrous and particulate debris to the core inlet prior to the formation of chemical products will create a lower resistance partial blockage well before the core inlet is expected to block completely. The resulting partial blockage will aid in filling the downcomer and activating the BB channel prior to reaching complete core inlet blockage. However, neglecting this effect in the determination of t_{block} leads to a conservative value, as demonstrated by the second core inlet blockage scenario described next.

The second set of core inlet blockage simulations (Section 8.2.3) examined a scenario in which the core inlet was first partially blocked prior to applying complete core inlet blockage. For this scenario, a form-loss coefficient was applied instantaneously at the time of transfer to sump recirculation to simulate the collection of fibrous and particulate debris. The magnitude of the form-loss coefficient was such that flow through the core inlet is reduced but not stopped completely. The RCS response to the partial blockage was very similar to the response after complete core inlet blockage, other than the fact that flow through the core inlet continued. The partial blockage resistance was held constant until t_{block} was reached. At this point, a higher form-loss coefficient was applied to block the core inlet completely. Since the partial blockage applied at the time of transfer to sump recirculation was sufficient to fill the

downcomer and activate the BB channel, no significant heatups were observed when complete core inlet blockage was applied. This demonstrates the inherent conservatism in t_{block}.

The value of the form-loss coefficient applied to simulate partial blockage was iterated upon to determine the maximum value that could be tolerated and maintain the PCT below 800°F. For the range of ECCS flows investigated, it was determined that a constant form-loss coefficient of $5x10^5$ produced acceptable results.

In the prototypic system, it is unrealistic to expect all the fibrous and particulate debris to arrive at the core inlet instantaneously. It is expected that the arrival of debris will occur over some finite period of time that is on the order of hours. Since the exact timing of debris arrival is complex and will vary from plant-to-plant, the approach for determining K_{max} via application of an instantaneous ramp simplifies the approach by taking the timing of debris arrival out of the solution. Taking this approach inherently leads to a conservative K_{max} value. This is demonstrated by comparing K_{max} to the final form-losses applied to the Series 3 cases which applied a linear ramp. From Table 8-3, the final form-loss applied to the Series 3 cases was $4x10^6$, which is almost an order of magnitude higher than the K_{max} value determined from the instantaneous cases.

The third set of core inlet blockage simulations (Section 8.2.4) examined a scenario in which a gradual build-up of debris was applied at the core inlet. These are considered the most realistic cases relative to how fibrous and particulate debris is expected to arrive at the core inlet; however, these cases do not simulate complete core inlet blockage. The gradual addition of resistance at the core inlet slowly increases the downcomer level and delays the activation of the BB channel. Eventually, the downcomer driving head becomes sufficiently large to change the flow direction in the BB channel. After this point, flow from the LP is split between the core inlet and the BB and, as the core inlet resistance continues to build, the flow fraction to the BB continues to increase while the flow fraction to the core inlet decreases. From these simulations, the core inlet resistance necessary to activate the BB channel (K_{split}) was determined to be a strong function of the ECCS flow. K_{split} plotted as a function of ECCS flow rate is provided in Figure 8-4, and the corresponding flow split between the core inlet and the BB channel (m_{split}) following K_{split} is shown in Figure 8-5.

9 WESTINGHOUSE DOWNFLOW BARREL/BAFFLE DESIGNS

In this section, results from the Westinghouse downflow plant category are presented and discussed. The range of conditions and case matrix are provided in Section 9.1. Results from the analysis are presented in Section 9.2. This section is broken into several subsections and the material contained in each subsection is summarized as follows:

- In Section 9.2.1, results from a case that did not model debris build-up at the core inlet are used to describe the RCS state at the time of transfer to sump recirculation and the arrival of debris. Since all simulations are identical prior to reaching that point in time, the discussion in this section is applicable to all cases. In the simulations, transfer to sump recirculation occurs 20 minutes after the postulated LOCA.

- In Section 9.2.2, results from the case used to determine t_{block} are presented. This case did not apply partial blockage to the core inlet prior to the application of complete core inlet blockage. Complete core inlet blockage was applied instantaneously at time t_{block} and was applied uniformly across all core channels.

- In Section 9.2.3, results from the case used to determine a value for K_{max} are presented. This case applied partial blockage to the core inlet prior to the application of complete core inlet blockage. The partial blockage was applied instantaneously at the point of transfer to sump recirculation and was applied uniformly across all core channels. Complete core inlet blockage was also applied instantaneously at time t_{block} and was applied uniformly across all core channels.

- In Section 9.2.4, results from additional cases used to determine K_{split} and m_{split} are presented. For these cases, a linear ramp in resistance was applied uniformly across the core inlet and complete core inlet blockage was not simulated. Since these cases were used to assess the timing of the activation of the UHSN AFP, the build-up of core inlet resistance was applied more slowly compared to the cases used to determine K_{max}. As a result, the RCS response to core inlet blockage was much slower in that the downcomer fill rate and the activation of the UHSNs occurred over a longer period of time. It is noted that these simulations are more realistic with regard to the timing at which debris is expected to arrive at the core inlet.

Section 9.3 summarizes and discusses the key analysis results.

9.1 RANGE OF CONDITIONS AND CASE MATRIX

The simulation matrix used to determine t_{block} and K_{max} is shown in Table 9-1. For these cases, the plant model with maximum UHSN flow resistance was used. In the table, the loss coefficient column identifies the core inlet losses applied at the designated initiation times. All cases that modeled core inlet blockage applied a step change to the loss coefficient at the core inlet. Cases 0A and 0B did not model core inlet blockage and Cases 1A, 2A, and 2B applied step changes. The core inlet resistances applied for these cases are presented graphically in Figure 9-1 and Figure 9-2.

Step changes in loss coefficients are applied over a 60 second interval. For example, in Case 2A, a step change from 0 to 9.5×10^5 is applied from 1200 to 1260 seconds and an additional step change from

$9.5x10^5$ to $1x10^9$ is applied from 15,600 to 15,660 seconds. For all simulations, the sump recirculation flow rate is applied 1200 seconds after the initiation of the event.

The simulation matrix used to determine K_{split} and m_{split} is shown in Table 9-2. For these cases, the plant model with minimum UHSN flow resistance was used. In the table, the loss coefficient column identifies the core inlet losses applied starting at the designated initiation time and ending at the designated end time. For example, in Case 1, a timewise-linear ramp of the loss coefficient at a rate of 6000 /hr is applied starting at 1200 seconds and ending at 19,200 seconds. The ending value of the loss coefficient is 30,000. Complete core inlet blockage is not applied to these cases. For all simulations, the sump recirculation flow rate is applied 1200 seconds after the initiation of the event.

Table 9-1 Simulation Matrix for t_{block} and K_{max} – Westinghouse Downflow Plant Design

Case	Sump Recirculation Flow Rate (gpm/FA)	Debris Bed Model	
		Loss Coefficient	Initiation Time (sec)
0A	40	NONE	N/A
0B	18	NONE	N/A
1A	40	$1x10^9$	15,600
2A	40	$9.5x10^5/1x10^9$	1200/15,600
2B	18	$6x10^5/1x10^9$	1200/12,000

Table 9-2 Simulation Matrix for K_{split} and m_{split} – Westinghouse Downflow Plant Design

Case	Sump Recirculation Flow Rate (gpm/FA)	Debris Bed Model (Linear Ramp)		
		Loss Coefficient	Initiation Time (sec)	End Time (sec)
1	40	6000/hr	1200	19,200
2	30	6000/hr	1200	19,200
3	18	6000/hr	1200	19,200
4	12	12,000/hr	1200	26,400
5	8	12,000/hr	1200	37,200

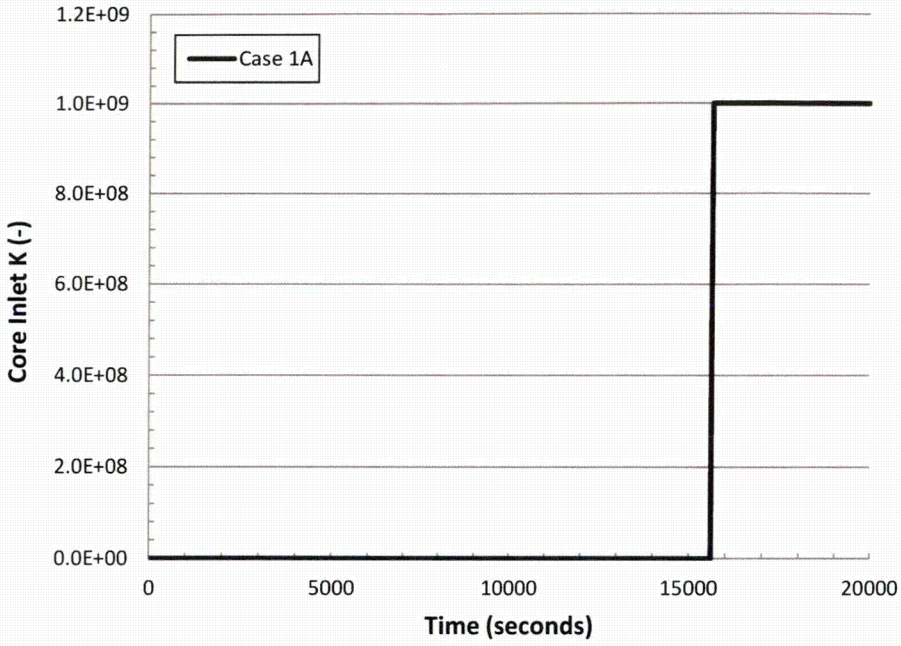

Figure 9-1 Core Inlet Resistance Transient Applied to Case 1 Simulation from Westinghouse Downflow Analysis

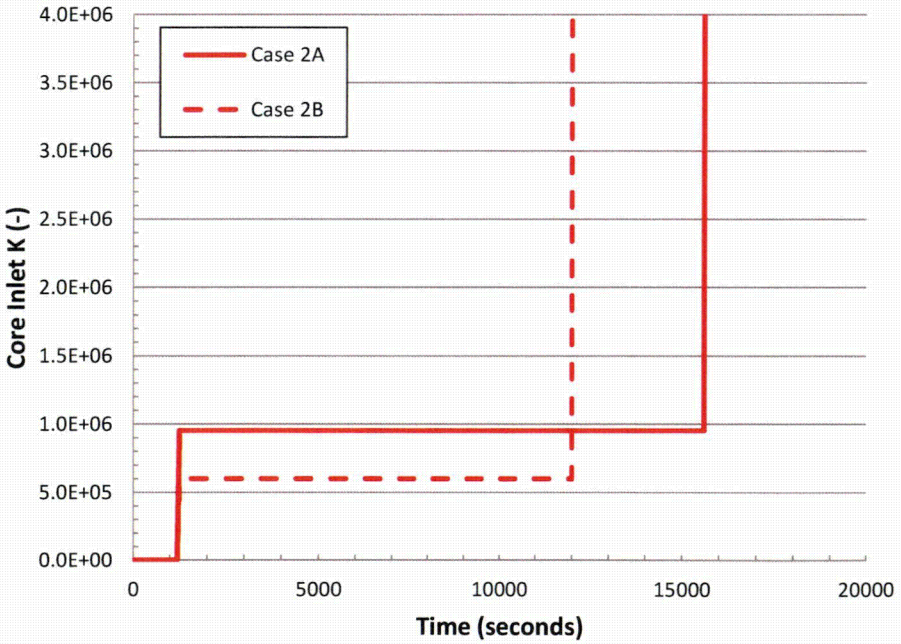

Figure 9-2 Core Inlet Resistance Transient Applied to Case 2 Simulations from Westinghouse Downflow Analysis

9.2 RESULTS OF ANALYSIS

Key results from the t_{block} and K_{max} simulations are summarized in Table 9-3. Cases 0A and 0B have no core inlet blockage applied. Case 1A applies complete core inlet blockage and determines the minimum time that complete blockage can be tolerated. Cases 2A and 2B apply resistances to the core inlet prior to reaching complete core inlet blockage and are used to determine the maximum resistance that can be tolerated prior to reaching complete blockage.

Based on the results presented in Table 9-3, it is concluded that LTCC can be maintained if complete core inlet blockage occurs 260 minutes (15,600 sec), or later, after the initiation of the LOCA event. This time is taken from the maximum ECCS recirculation flow case (Case 1A). Prior to reaching complete core inlet blockage, a maximum supportable K_{max} value of $6x10^5$, corresponding to a pressure drop of 14.8 psid across the core inlet, is determined to be the limiting value when a uniform resistance is applied instantaneously upon entering sump recirculation. These values are taken from the minimum ECCS recirculation flow case (Case 2B) and bound the range of recirculation flows investigated.

With regard to BAPC, all cases demonstrate that, after core inlet blockage, the break exit quality remains sufficiently low such that boron is flushed from the core and concentrations are expected to remain well below the solubility limit. Further, all cases demonstrate that the core mixing patterns are such that the core can be considered well-mixed and no localized regions containing higher boron concentration are expected to form.

Key results from the K_{split} and m_{split} simulations are summarized in Table 9-4. The K_{split} values shown in the table are used in conjunction with the ECCS sump recirculation flow rates to generate the curve shown in Figure 9-3. This curve will be used in subsequent downstream calculations presented in Volume 1 to track the location of fibrous debris within the RV during the LTCC phase of the transient. The time that K_{split} occurs is determined by examination of the UHSN exit flow rate. The first timestep in which the UHSN exit flow rate becomes positive is defined as the K_{split} time. If flow oscillations (positive UHSN exit flow followed by a reversal to negative flow) occur, the time of K_{split} is selected after the flow oscillations stop and the UHSN exit flow remains positive. The fraction of ECCS flow through the core inlet and UHSN shown in Table 9-4 are taken at the end of the core inlet form-loss ramp. The transient flow split between the core inlet and UHSN is shown in Figure 9-4 for the five ECCS recirculation flow rates investigated. The flow split is represented as the fraction of total ECCS recirculation flow through the UHSN and is plotted as a function of the core inlet resistance following K_{split}. These curves will be used, in conjunction with K_{split}, in downstream calculations to track the location of fibrous debris within the RV during the LTCC phase of the transient as described in Volume 1.

Table 9-3 Summary of Results for t_{block} and K_{max} – Westinghouse Downflow Plant Design

Case	Time Core Inlet Resistance Applied	Core Inlet Loss Coefficient (K)	Core Inlet Average Mass Flow Rate per FA	Core Inlet Average Velocity	Pressure Drop across Debris Bed	Break Exit Quality	PCT
---	seconds	---	lbm/sec	ft/s	psid	---	°F
0A	N/A	N/A	5.3	0.54	N/A	0.05	<250
0B	N/A	N/A	1.6	0.16	N/A	0.25	<300
1A	15,600	$1x10^9$	5.3	0.54	-	0.6	<800
2A	1200/15,600	$9.5x10^5/1x10^9$	0.58	0.058	20.6	0.6	<650
2B	1200/12,000	$6x10^5/1x10^9$	0.62	0.062	14.8	0.5	<750

Table 9-4 Summary of Results for K_{split} and m_{split} – Westinghouse Downflow Plant Design

Case	Time of K_{split}	K_{split}	Fraction of ECCS Flow through Core Inlet	Fraction of ECCS Flow through UHSNs	Final Pressure Drop across Debris Bed
---	seconds	---	---	---	psid
1	2420.5	2034	0.33	0.67	6.1
2	3702	4170	0.50	0.50	7.6
3	11,250	16,750	0.81	0.19	7.0
4	13,928	42,427	0.74	0.26	7.8
5	27,888	88,960	0.89	0.11	6.8

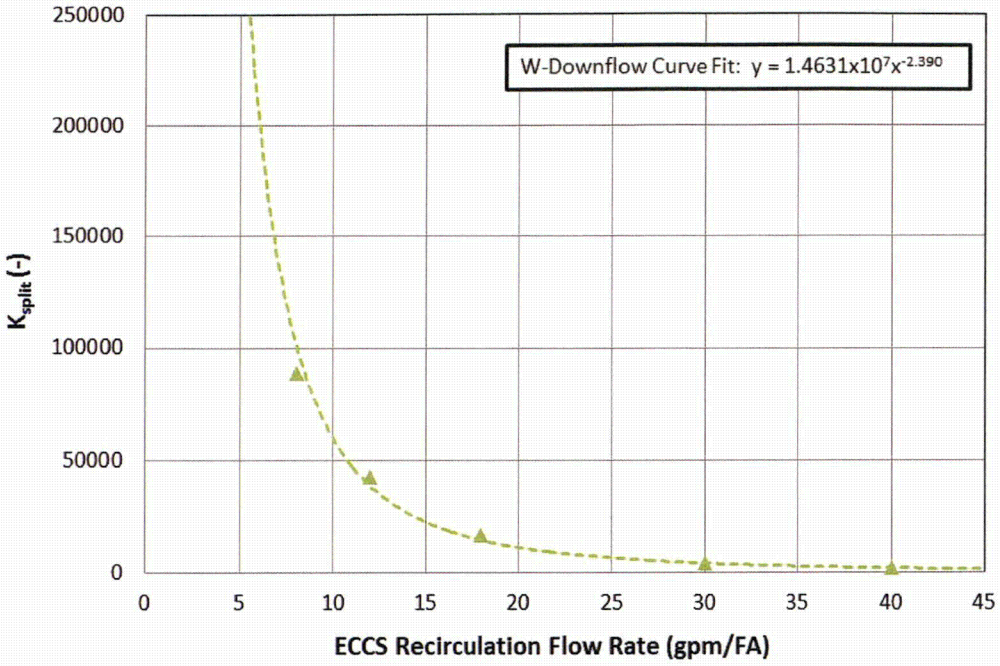

Figure 9-3 K_{split} as a Function of ECCS Recirculation Flow Rate from Westinghouse Downflow Analysis

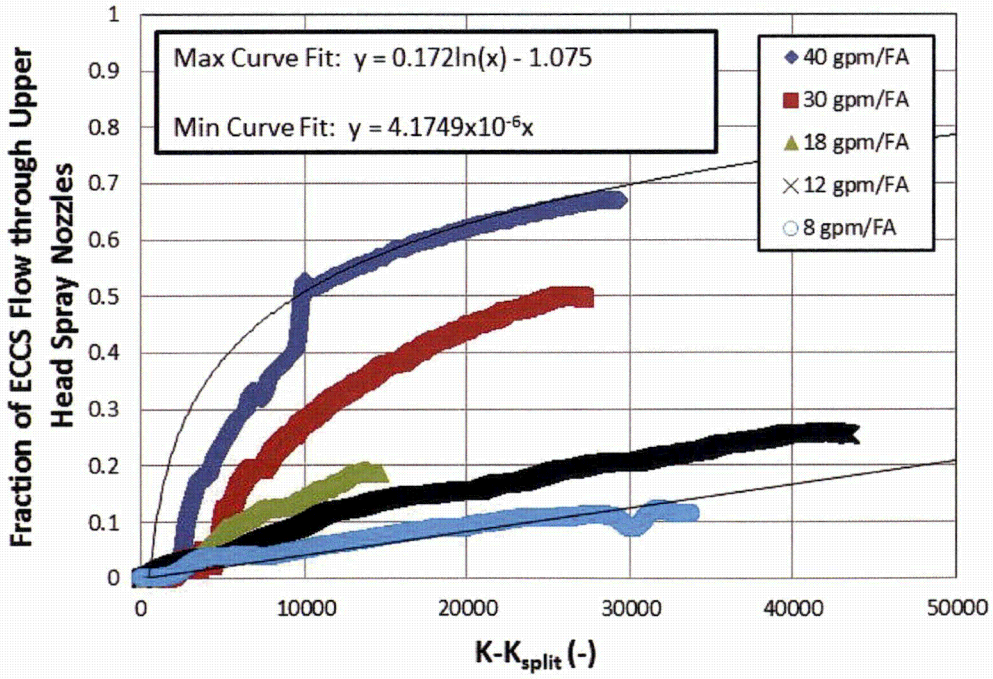

Figure 9-4 Fraction of ECCS Recirculation Flow through the BB following K_{split} from Westinghouse Downflow Analysis

9.2.1 All Cases – Before Debris Introduction

The results from Case 0A are used to describe the RCS state at the point of transfer to sump recirculation and the arrival of debris. Since all simulations are identical prior to that point in the transient, the discussion in this section is applicable to all cases. In the simulations, transfer to sump recirculation occurs 20 minutes after the postulated LOCA.

Just before transfer to sump recirculation, the RCS loop piping and SGs are mostly voided. The entire core has quenched and the cladding temperatures are just above saturation temperature as shown in Figure 9-5. The core region is covered with a two-phase mixture and the core collapsed liquid level is roughly 11feet into the active fuel region. Figure 9-6 shows the hot assembly collapsed liquid level, which indicates a sharp drop in the collapsed liquid level upon entry to sump recirculation. This is due to the removal of ECCS subcooling. During the RWST draindown phase, the ECCS coolant temperature is below 100°F. During the transfer to sump recirculation, the ECCS coolant temperature is changed to 212°F. This removal of subcooling results in increased core boiling and a reduction in the core collapsed liquid level.

Figure 9-7 shows the downcomer and upper head collapsed liquid levels. The figure indicates that the downcomer collapsed liquid level is just below the cold leg elevation at the time of transfer to sump recirculation, while the upper head has virtually no liquid in its volume.

As the pumped ECCS enters the cold legs, coolant can either travel toward the RV or go through the RCP and spill into the crossover legs of the RCS loop piping. For times prior to sump recirculation, and the arrival of debris, the ECCS flow split behavior is similar in the broken and intact loops. Figure 9-8 shows the integrated ECCS flow split on the broken loop. As shown in the figure, the slope of the integrated flow going in the direction of the RV is similar to the slope of the integrated total pumped ECCS flow, while the slope of the integrated flow going toward the RCP remains fairly flat. This behavior indicates that the majority of the total pumped ECCS flow is traveling to the RV. This behavior is expected given that the resistance to flow from the injection point to the downcomer is less than the resistance through the RCPs to the crossover legs.

Figure 9-9 and Figure 9-10 show the integrated mass flow rates at the core inlet for each of the four core channels. A positive slope indicates positive flow into the core. Just prior to sump recirculation, all of the slopes are positive, indicating flow from the LP into the four core channels (i.e., upflow). Figure 9-11 shows the integrated mass flow rate near the core outlet. The integrated outlet flow from the core is the summation of the hot assembly and two average core channels, all of which have positive flow out of the core, while the integrated outlet flow in the peripheral channel has downward flow from the UP to the peripheral channel. Figure 9-12 shows the integrated liquid mass flow through the intact SGs, UHSNs, and upper guide tubes. The figure indicates that, without core inlet blockage there is no liquid flow through the UHSNs and upper guide tubes. The figure also indicates that there is liquid flow out of the RV into the intact hot legs.

The integrated break mass flow is shown in Figure 9-13. The figure shows that all of the break flow is from the RV side, which indicates no liquid carryover through the broken loop SG to the break. The break exit quality is shown in Figure 9-14. The figure shows that the nominal break exit quality is less than 10% upon transfer to sump recirculation, which indicates a substantial amount of liquid carryover

out the break. Due to the large amount of liquid carryover prior to sump recirculation, BAP is controlled and boron concentration levels in the RV upon entry to sump recirculation are expected to be comparable to the ECCS source concentration.

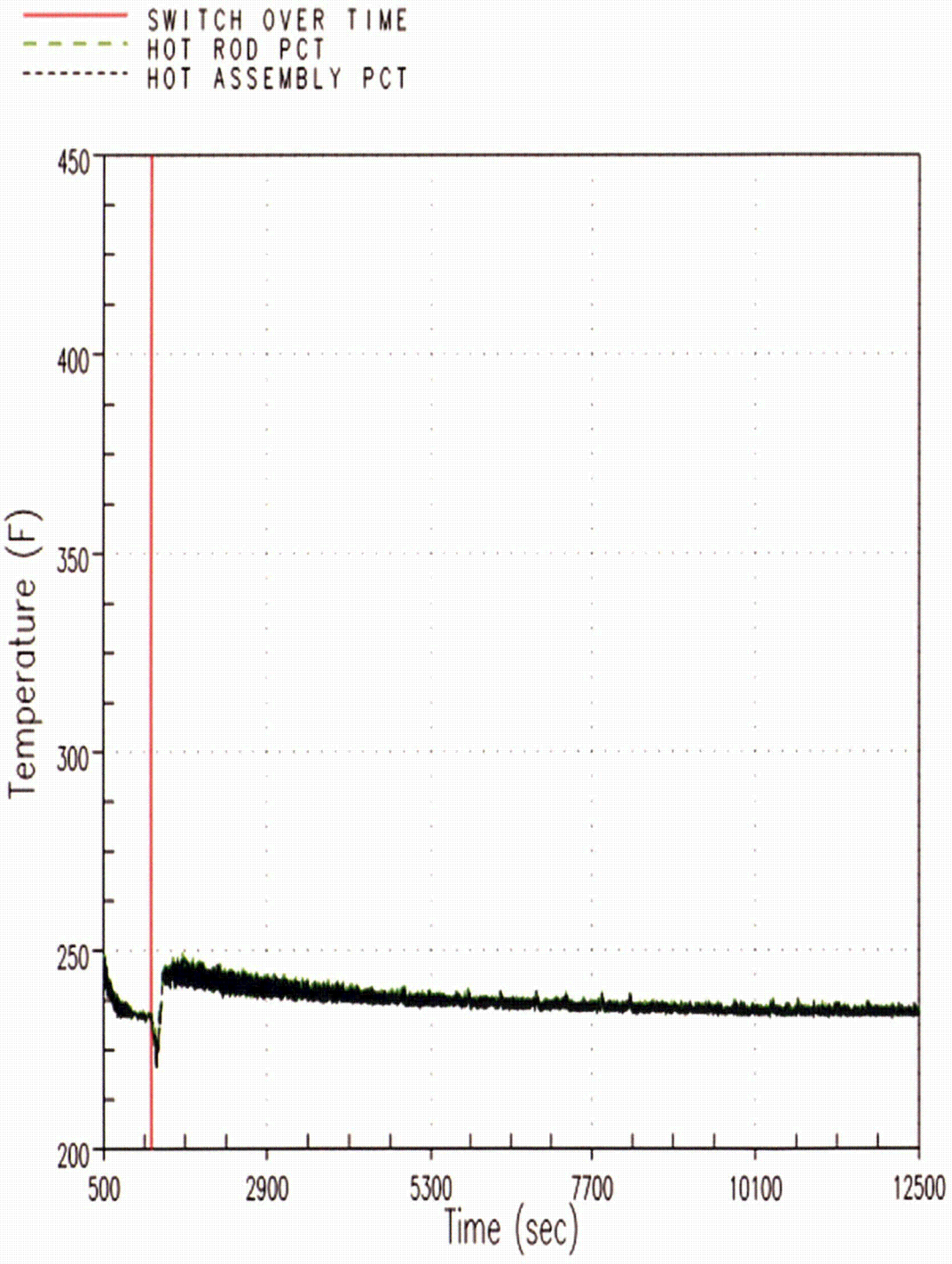

Figure 9-5 Case 0A – Hot Rod and Hot Assembly Peak Cladding Temperatures

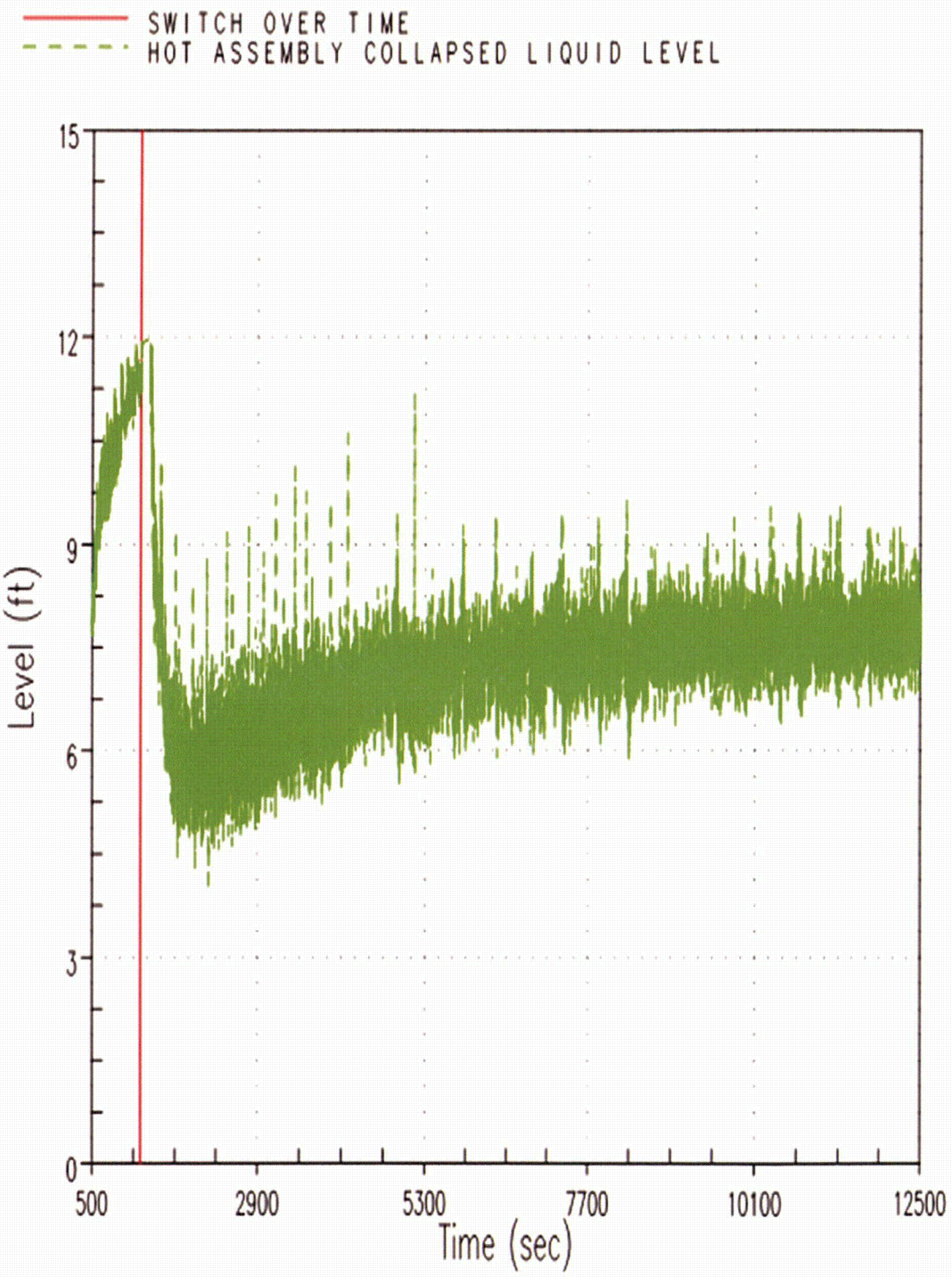

Figure 9-6 Case 0A – Hot Assembly Collapsed Liquid Level

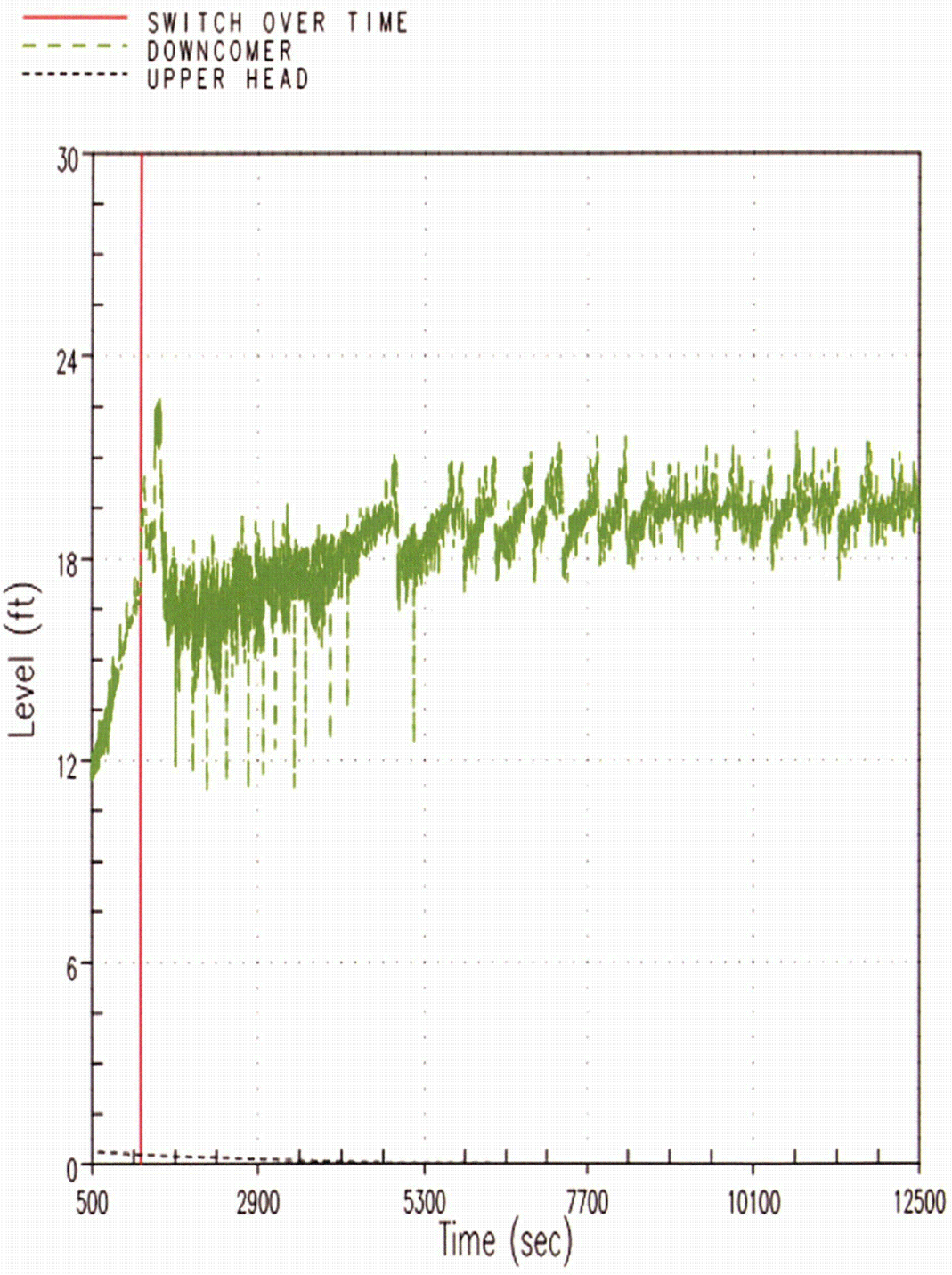

Figure 9-7 Case 0A – Downcomer and Upper Head Collapsed Liquid Levels

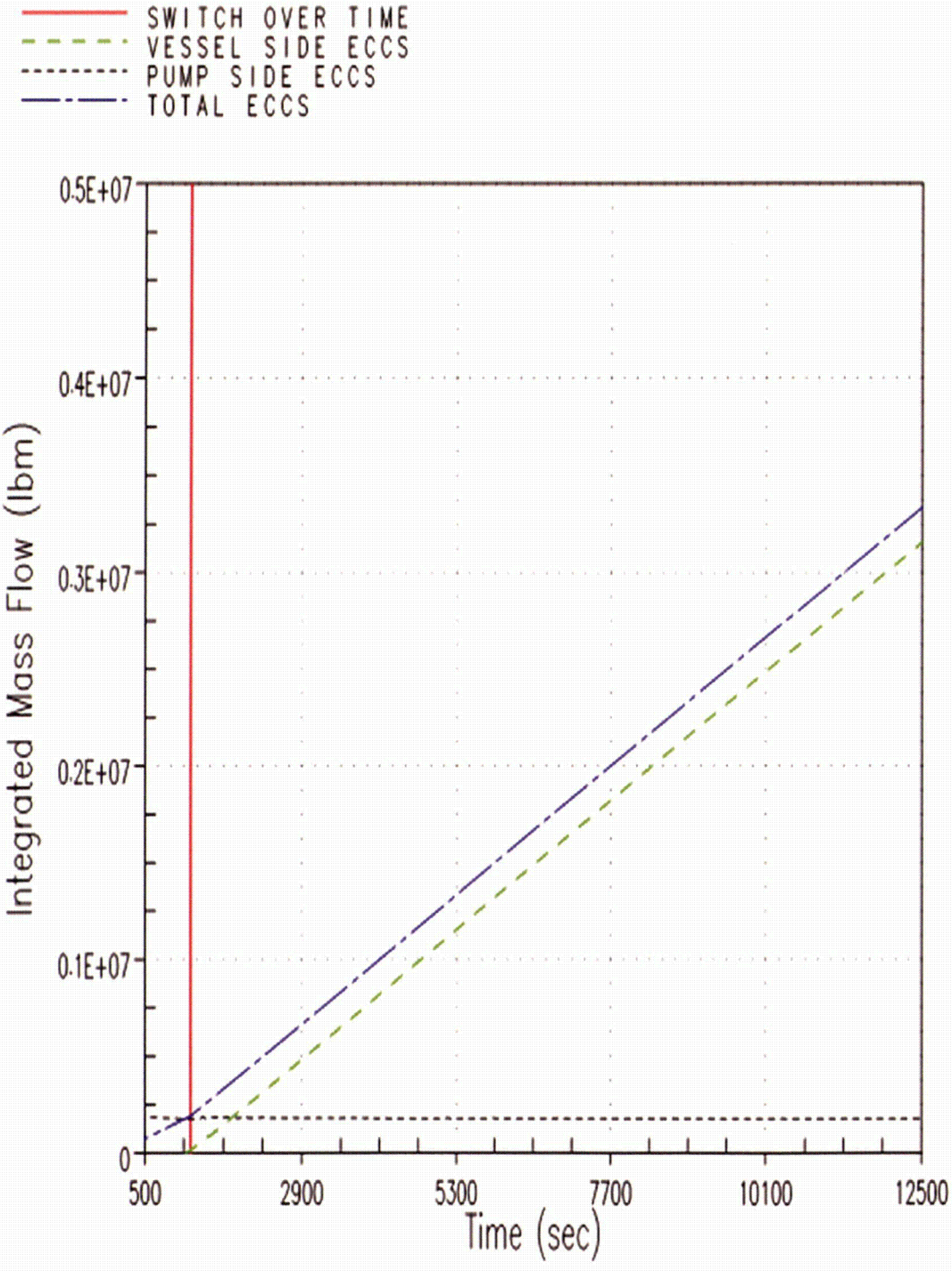

Figure 9-8 Case 0A – Integrated ECCS Flow Split in Broken Loop

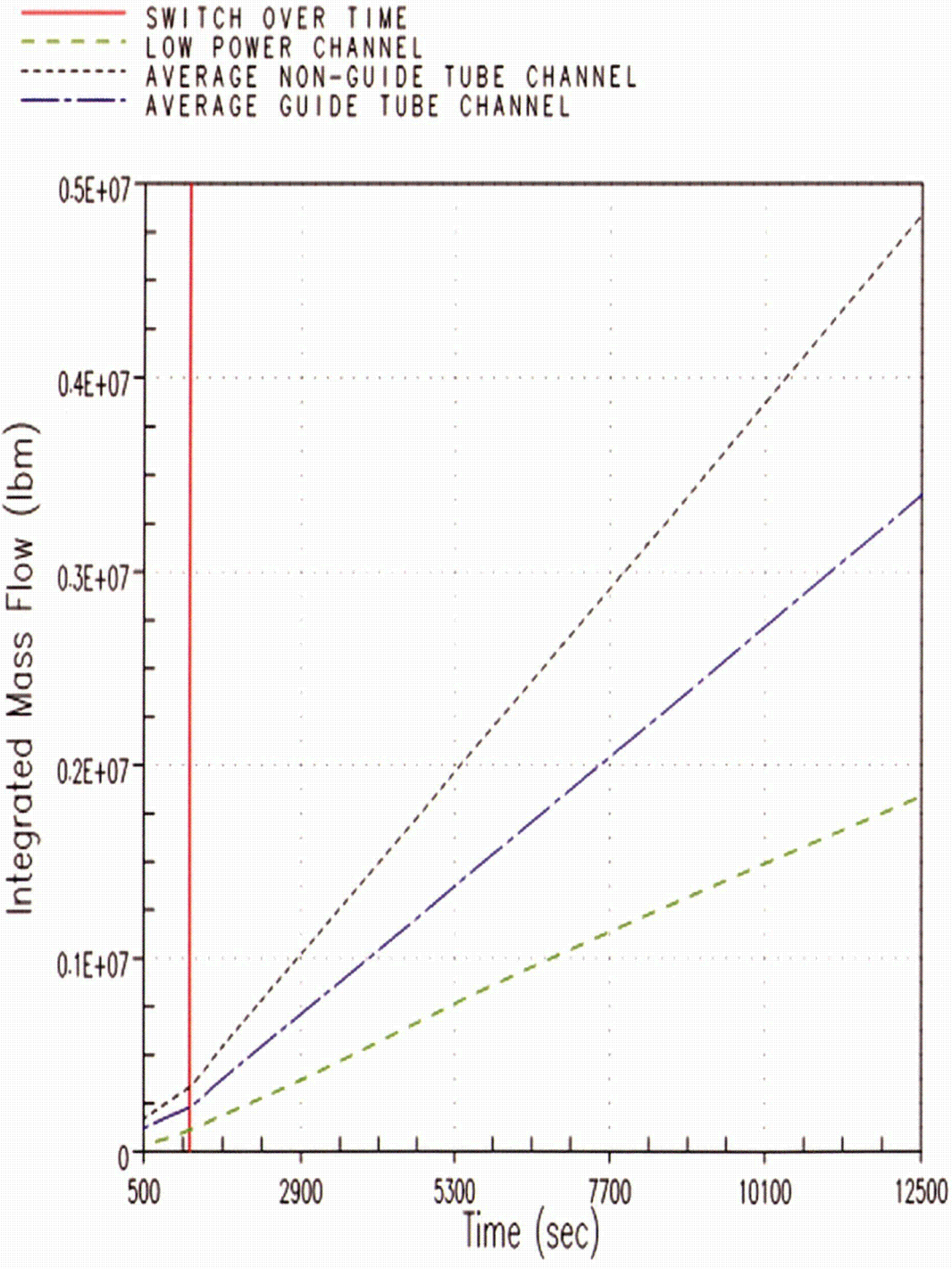

Figure 9-9 Case 0A – Integrated Core Inlet Mass Flow from Average and Peripheral Channels

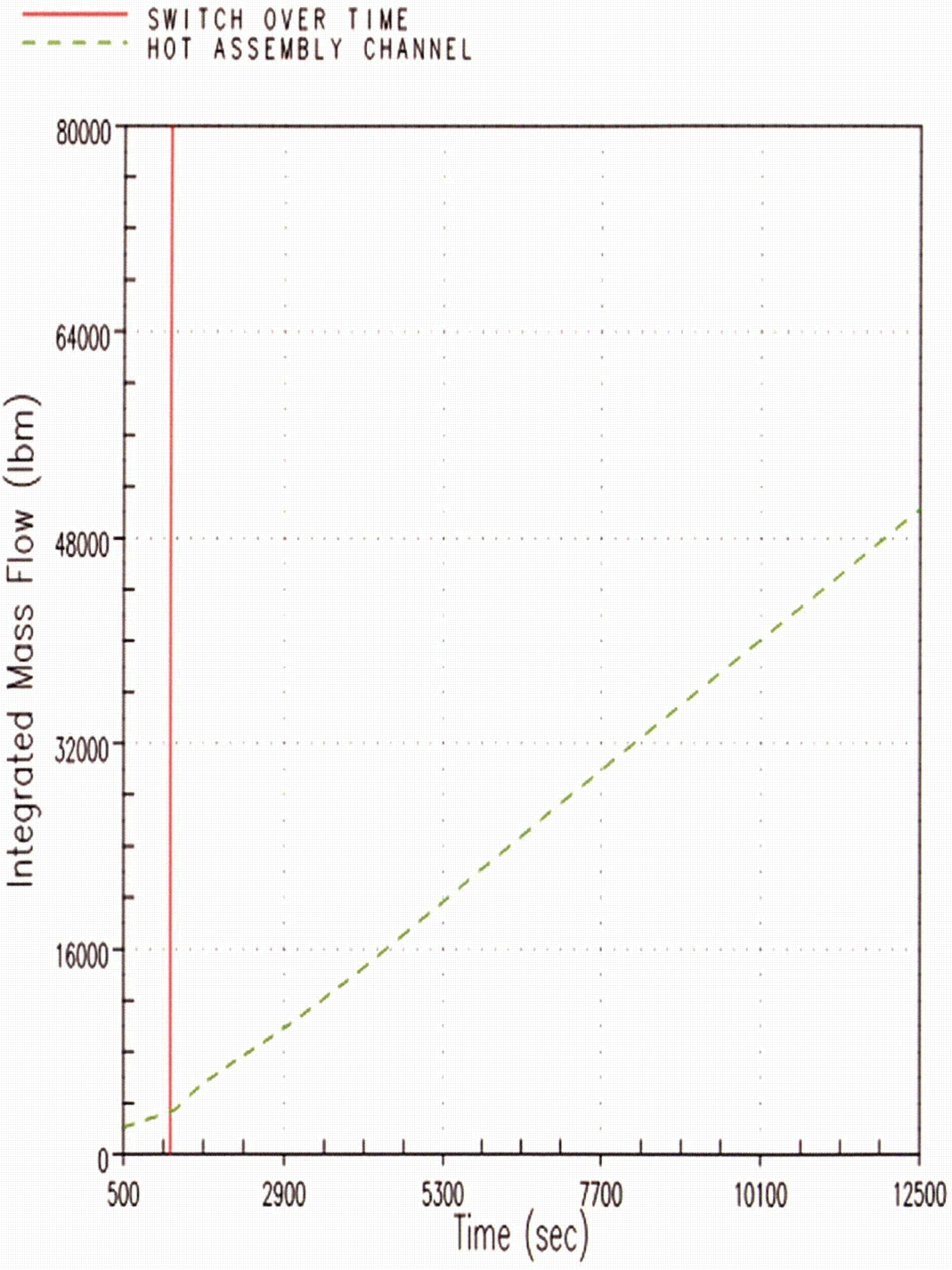

Figure 9-10 Case 0A – Integrated Core Inlet Mass Flow from Hot Assembly Channel

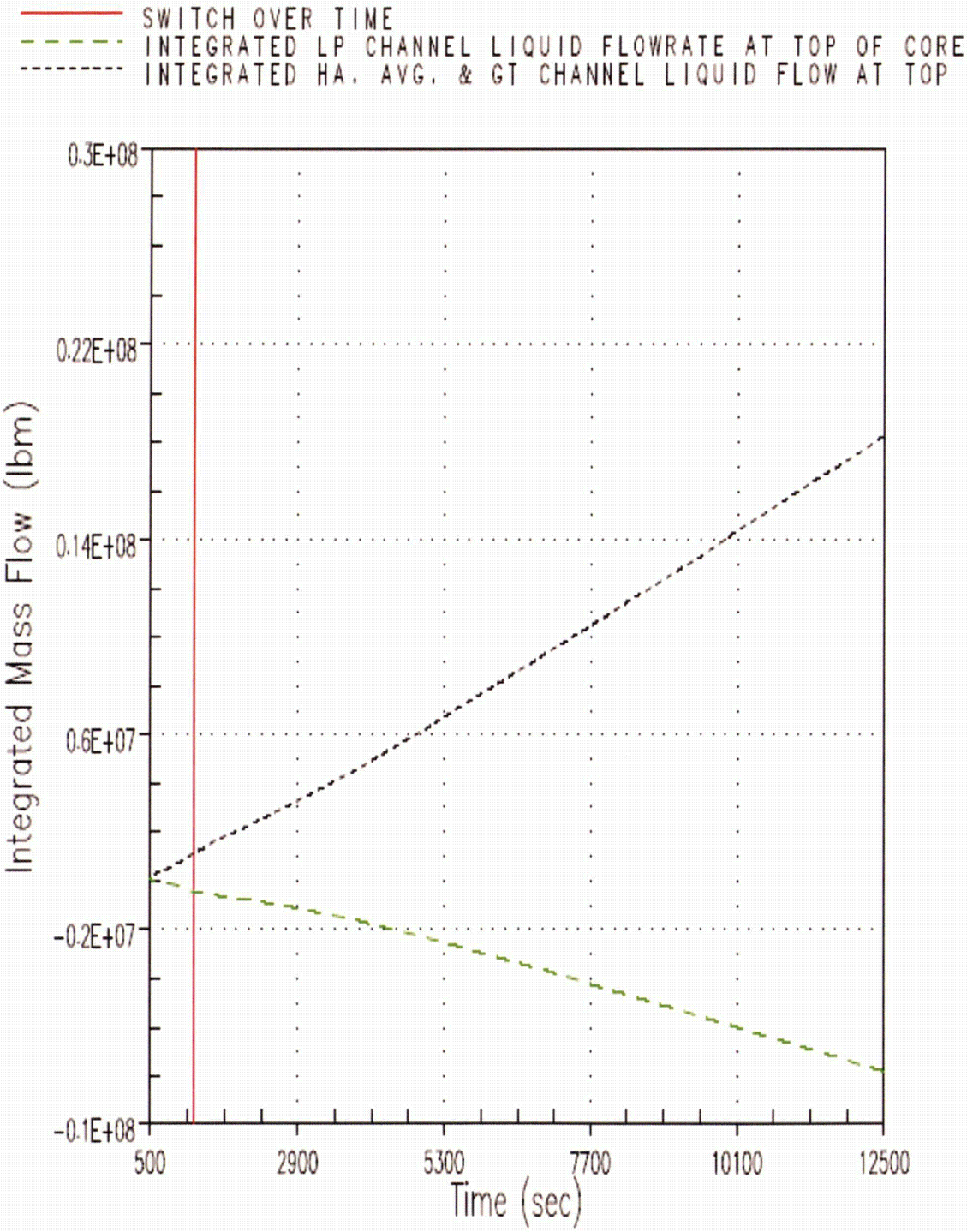

Figure 9-11 Case 0A – Integrated Core Exit Mass Flow

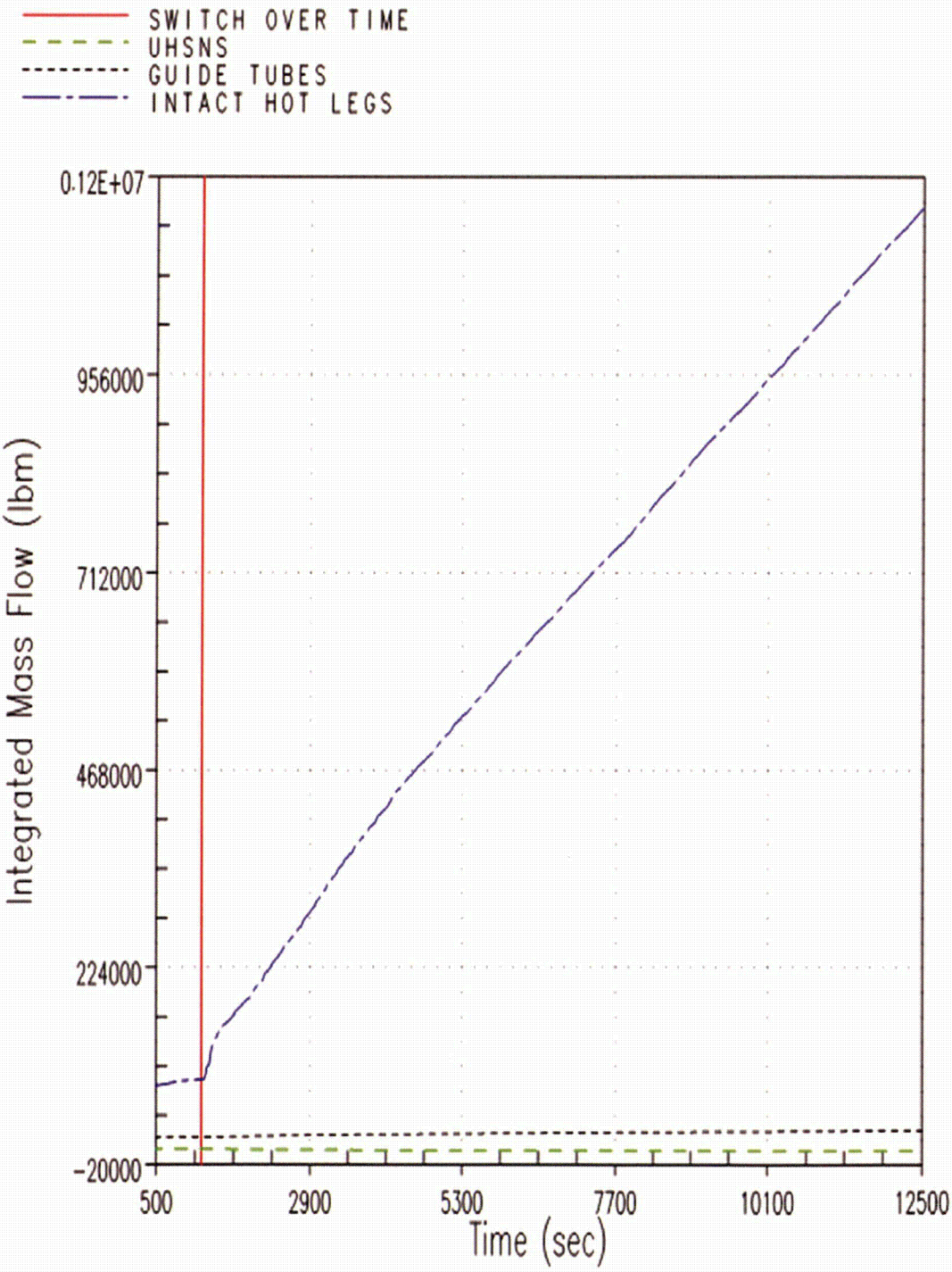

Figure 9-12 Case 0A – Integrated Liquid Flow through Intact Hot legs, Upper Head Spray Nozzles, and Upper Guide Tubes

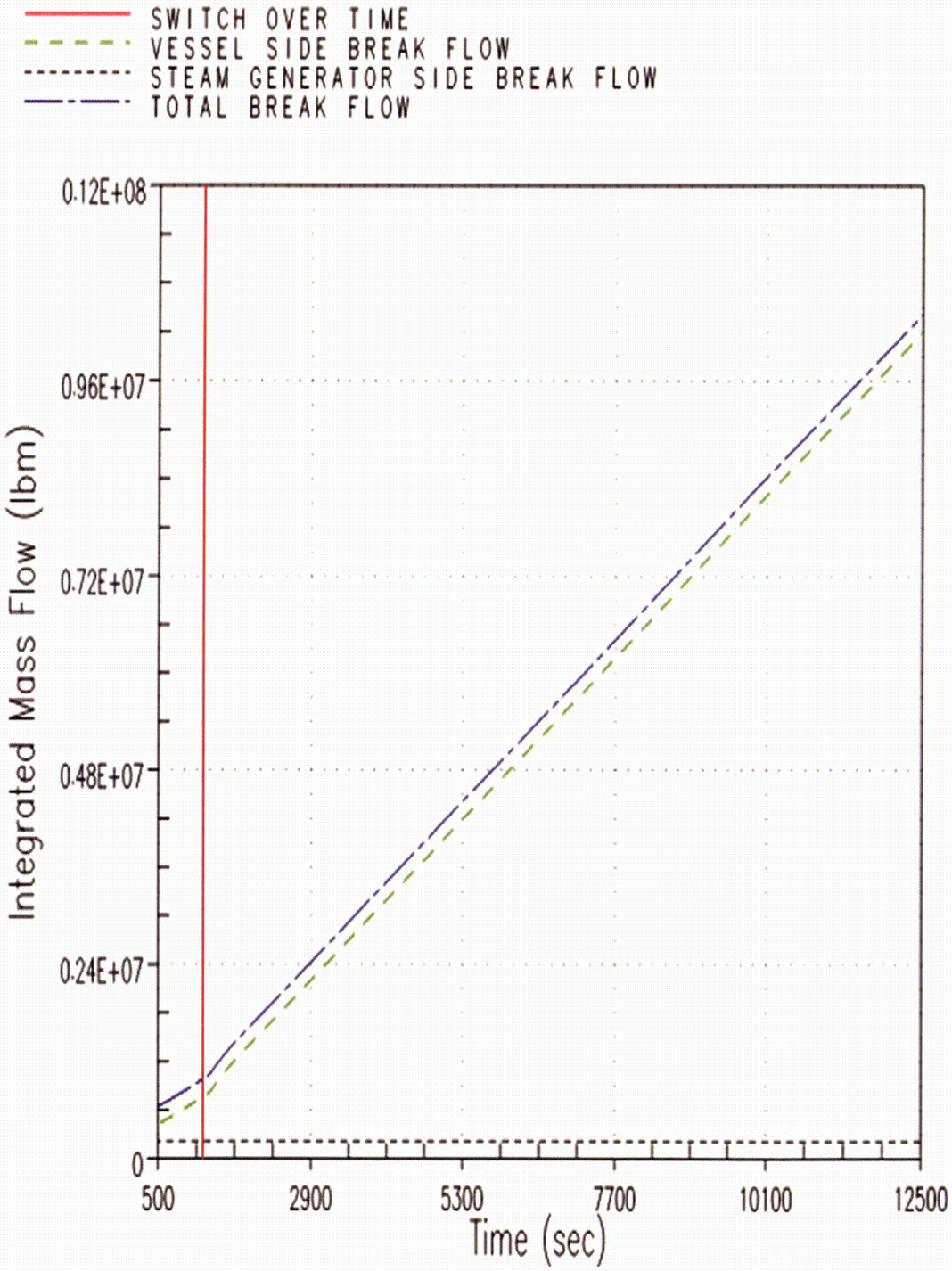

Figure 9-13 Case 0A – Integrated Mass Flow from the Break

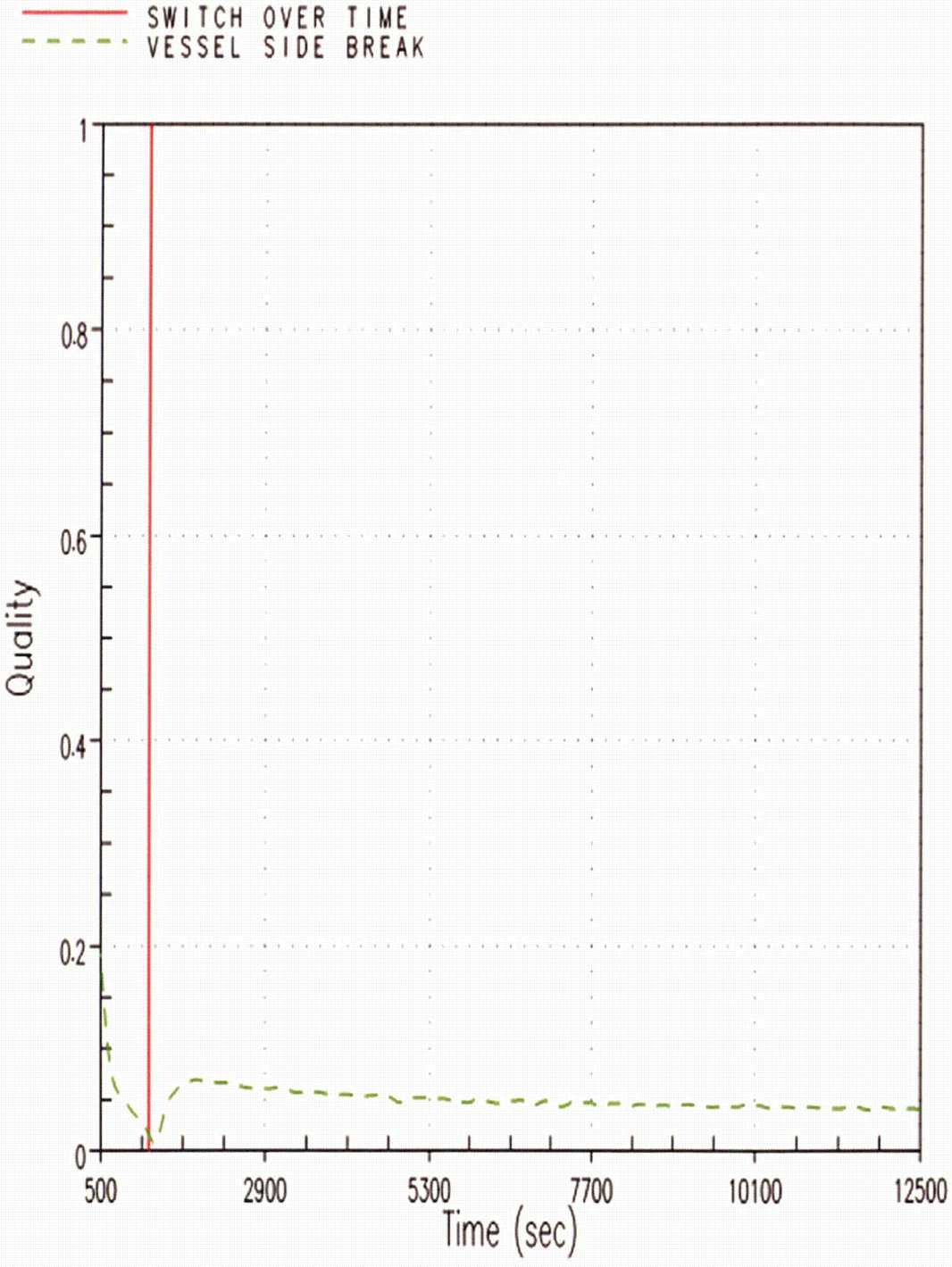

Figure 9-14 Case 0A – Break Exit Quality

9.2.2 After Debris Introduction – Calculation of t_{block}

Case 1A is used to determine t_{block}. This case does not apply any partial blockage to the core inlet prior to the application of complete core inlet blockage.

Throughout the duration of the transient, more-than-adequate core cooling flow is provided through the ECCS to the cold legs. Complete core inlet blockage is applied at 260 min (15,600 seconds). After the application of complete blockage, the ECCS flow backs up and fills the downcomer to the UHSN elevation. The ECCS continues to fill the RCS until the liquid level in the upper head reaches the upper guide tube elevation. At this point, coolant drains through the upper guide tubes into the UP where it is available to provide core cooling. Figure 9-15 shows that the core experiences a short-duration temperature excursion after the application of complete core inlet blockage; however, the PCT remains below 800°F. The temperature excursion occurs at the top of the core and is due to the delay time associated with filling the downcomer beyond the UHSN elevation. No coolant is being provided to the core while the downcomer is filling, which leads to dryout and core uncovery. Once the downcomer fills such that the UHSNs and upper guide tubes are active in providing coolant to the top of the core, the two-phase mixture level in the core is recovered as is the cladding temperature.

The RV fluid mass is shown in Figure 9-16. Prior to the application of complete core inlet blockage, the behavior is similar to that seen in the no blockage case. When complete core inlet blockage is applied, the simulation shows an initial reduction in RV fluid inventory, but the inventory quickly recovers and settles to a value that is greater than the RV fluid mass prior to complete blockage and remains fairly stable for the remainder of the transient. The increase in RV fluid volume after complete core inlet blockage can be attributed to the filling of the downcomer and resulting liquid inventory in the upper head. This trend is consistent with the behavior of the core collapsed liquid level as shown in Figure 9-17, which shows the hot assembly collapsed liquid level. The collapsed liquid levels in the other core channels show similar trends. The downcomer and upper head collapsed liquid levels are shown in Figure 9-18. When the blockage is applied, the downcomer collapsed liquid level quickly increases to the UHSN elevation due to the increased resistance at the core inlet. As a result, the upper head begins to flood with fluid from the downcomer and the total RV fluid mass increases due to the additional fluid in the upper downcomer and upper head.

The core inlet, guide tube and intact hot leg mass flow rates are compared to boil-off in Figure 9-19. The figure indicates that flow into the core is well in excess of boil-off prior to complete core inlet blockage. Flow from the RV to the intact hot legs exists prior to complete blockage and there is no liquid flow from the upper head to the UP through the guide tubes. After complete blockage, the core inlet flow is shown to decrease to zero. The intact hot leg flow is also shown to decrease, which is associated with the reduction in the core collapsed liquid level. The upper guide tube flow, which enters the top of the core, is shown to be in excess of boil-off and provides DHR.

The break exit quality is shown in Figure 9-20. The figure shows that the break exit quality remains below 60% after the application of complete core inlet blockage, which indicates a substantial amount of liquid carryover out the break. Due to the large amount of liquid carryover out the break, BAP is controlled and boron concentration levels in the RV will remain well below the solubility limit for the duration of the transient.

After complete blockage, core cooling is maintained due to flow from the upper downcomer into the upper head which drains through the upper guide tubes into the UP, where it is available to the top of the core. A review of the RV mixing patterns after complete core inlet blockage indicate that flow from the UP flows downward along the core periphery and feeds the average and hot assembly via cross flow. This trend is comparable to the core mixing patterns observed after complete core inlet blockage for the Westinghouse upflow plant category (discussed in Section 8).

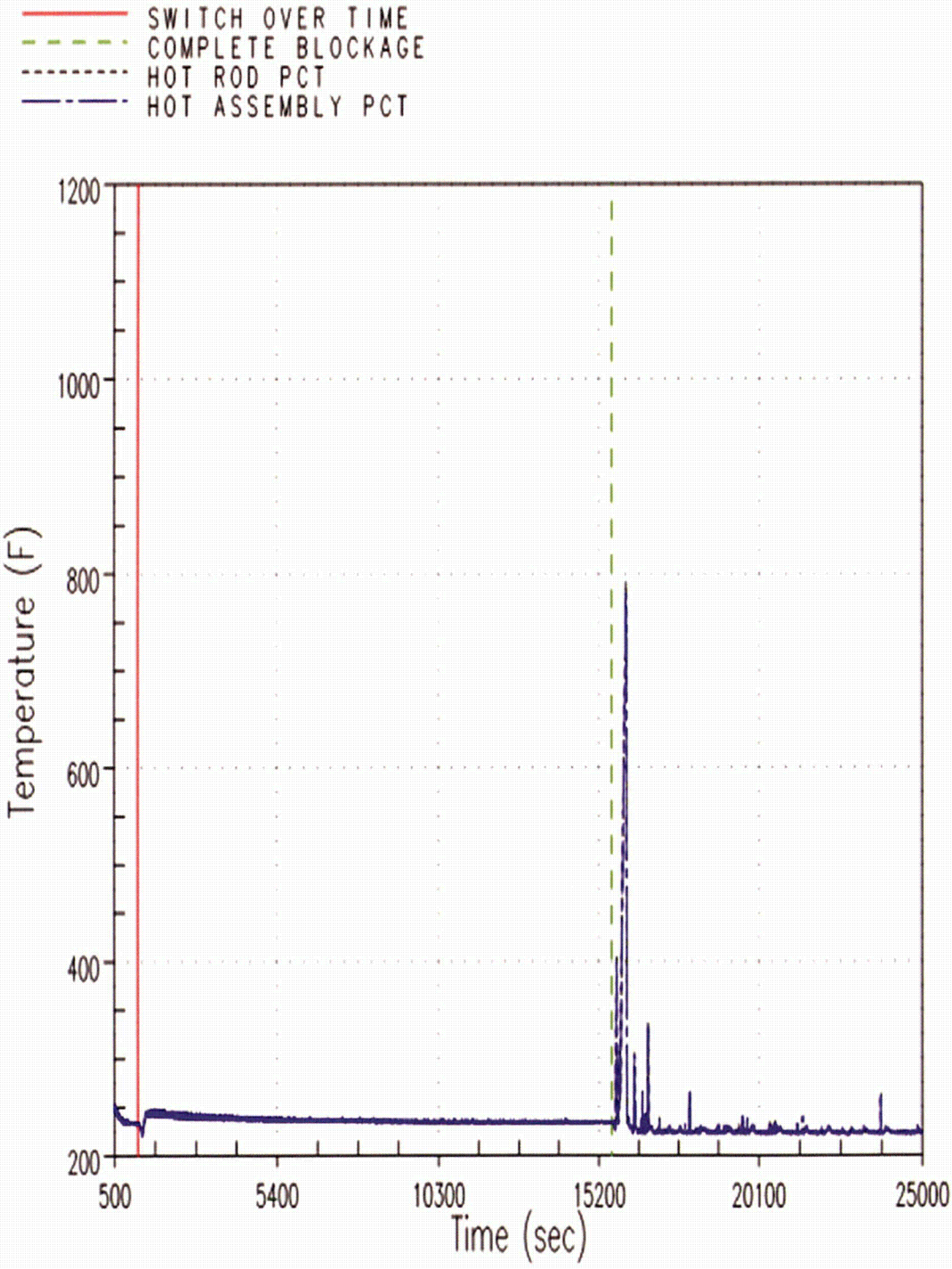

Figure 9-15 Case 1A – Hot Rod and Hot Assembly Peak Cladding Temperatures

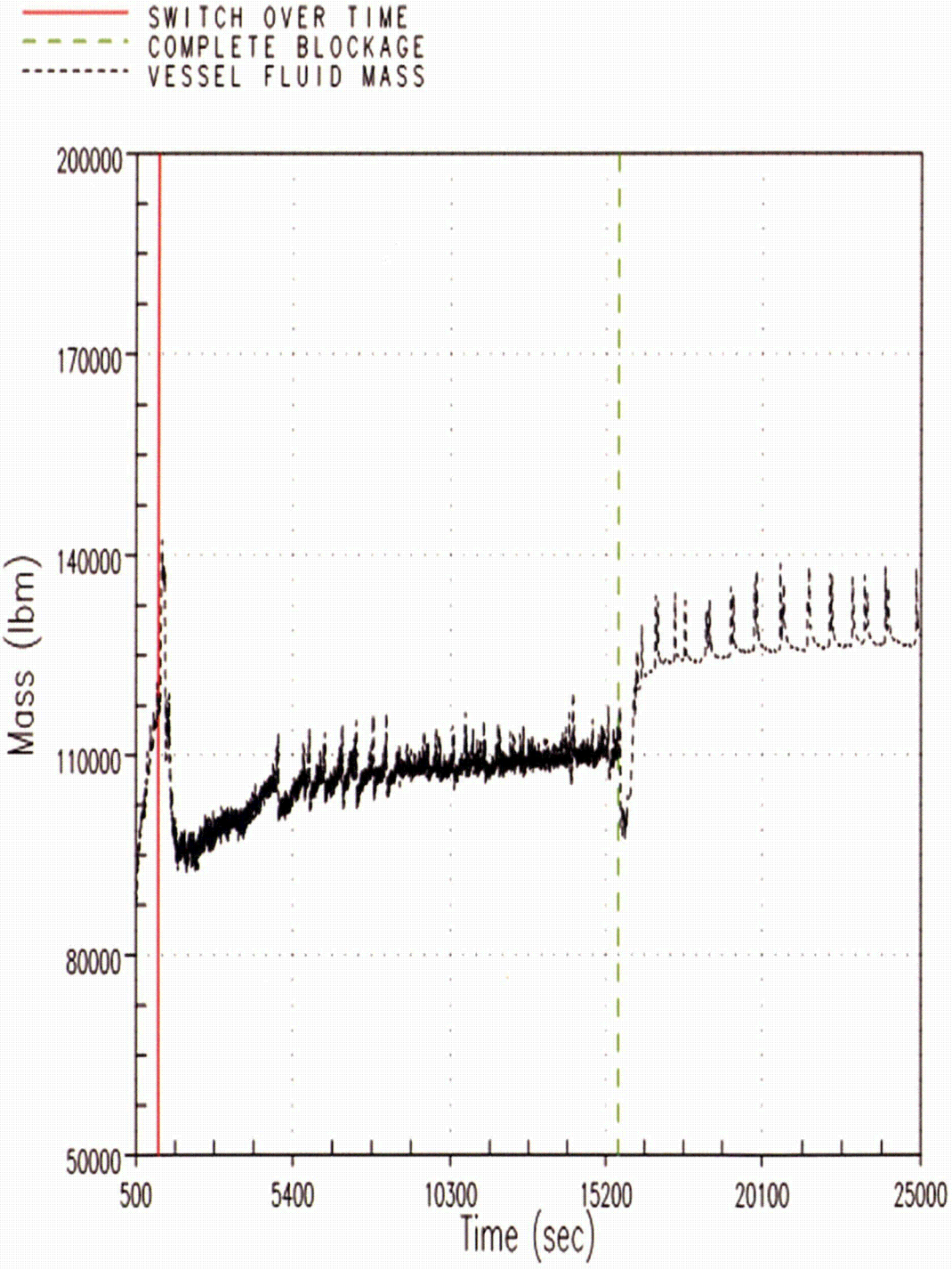

Figure 9-16 Case 1A – Reactor Vessel Fluid Mass

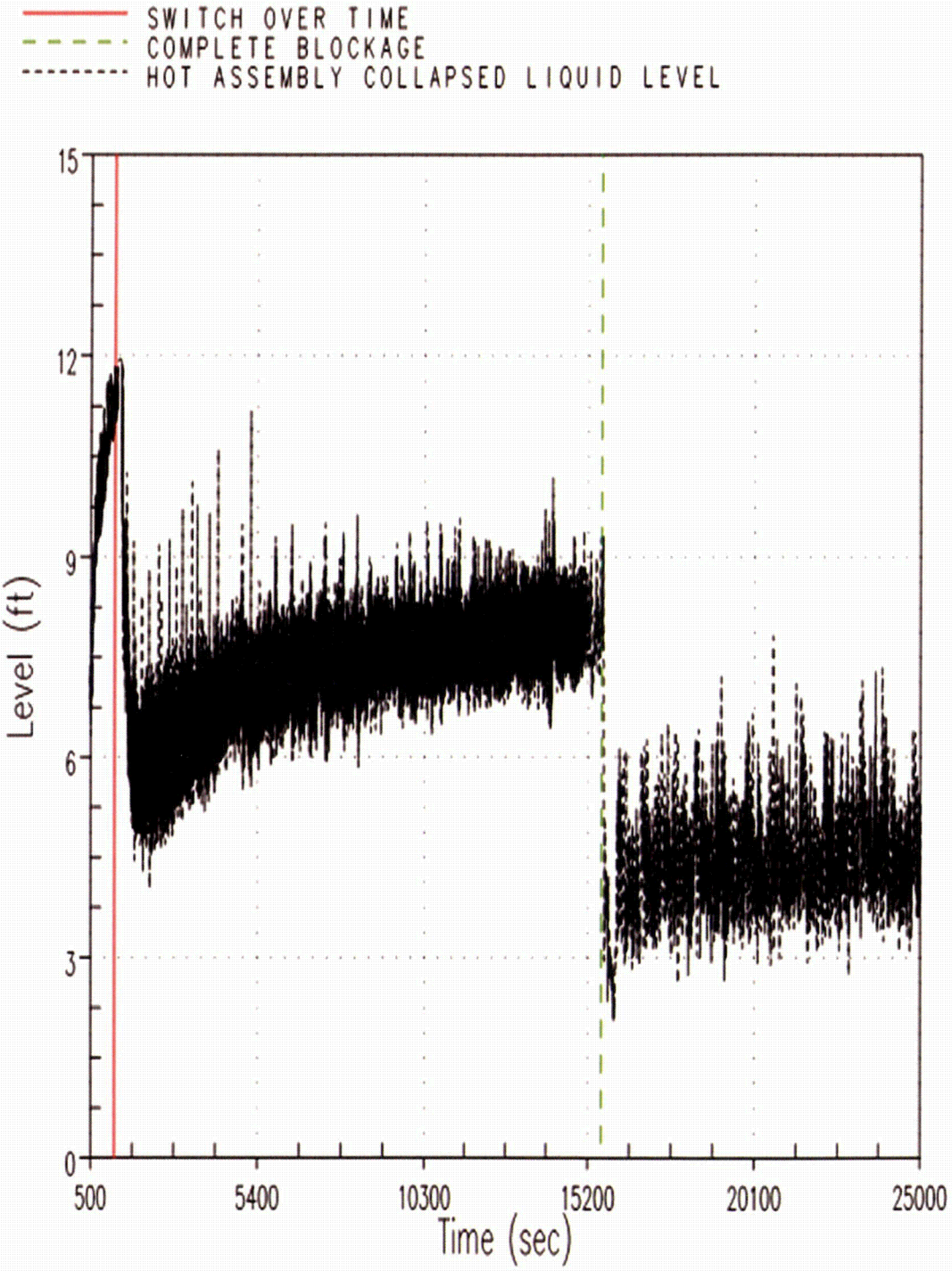

Figure 9-17 Case 1A – Hot Assembly Collapsed Liquid Level

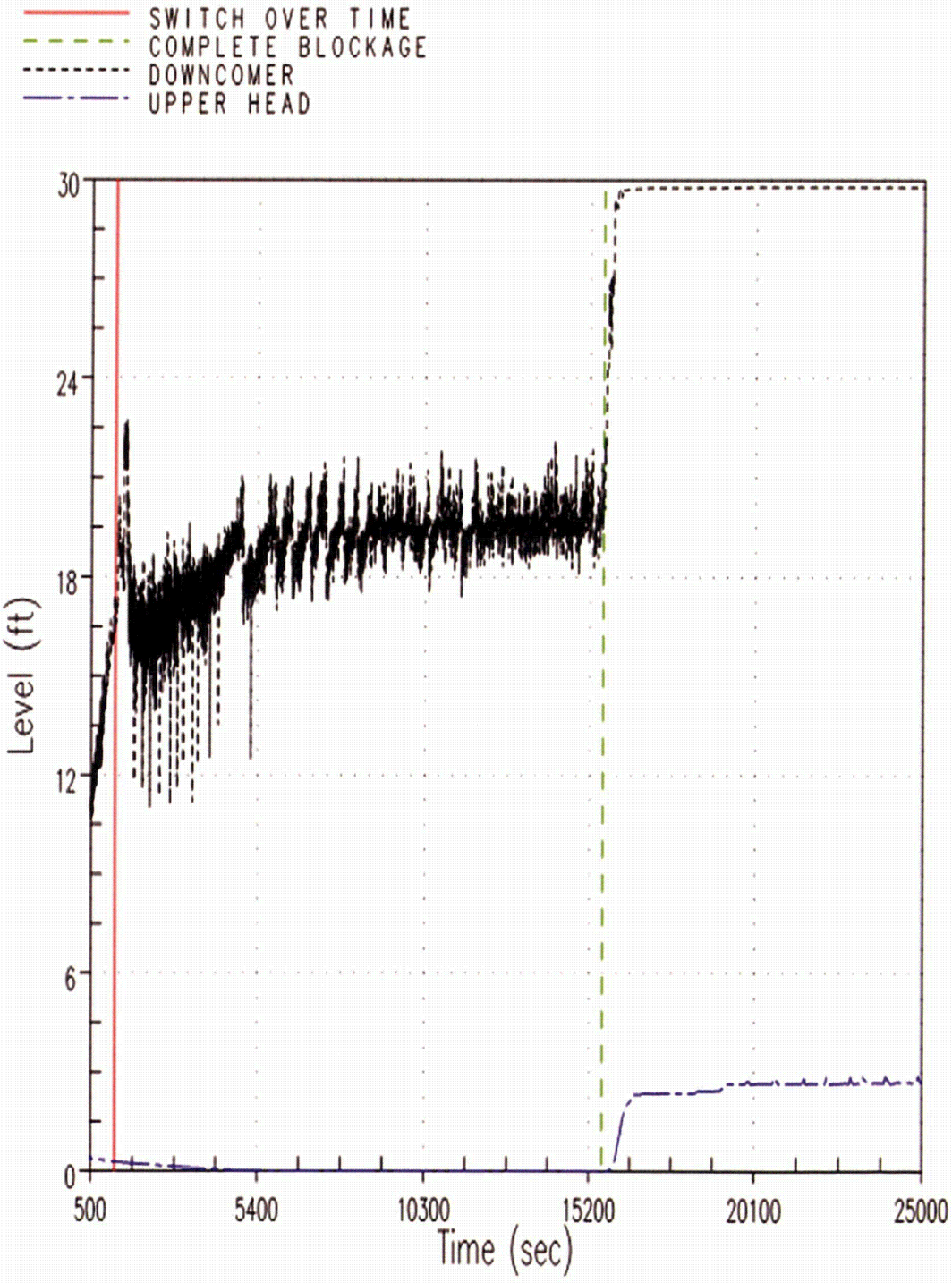

Figure 9-18 Case 1A – Downcomer and Upper Head Collapsed Liquid Levels

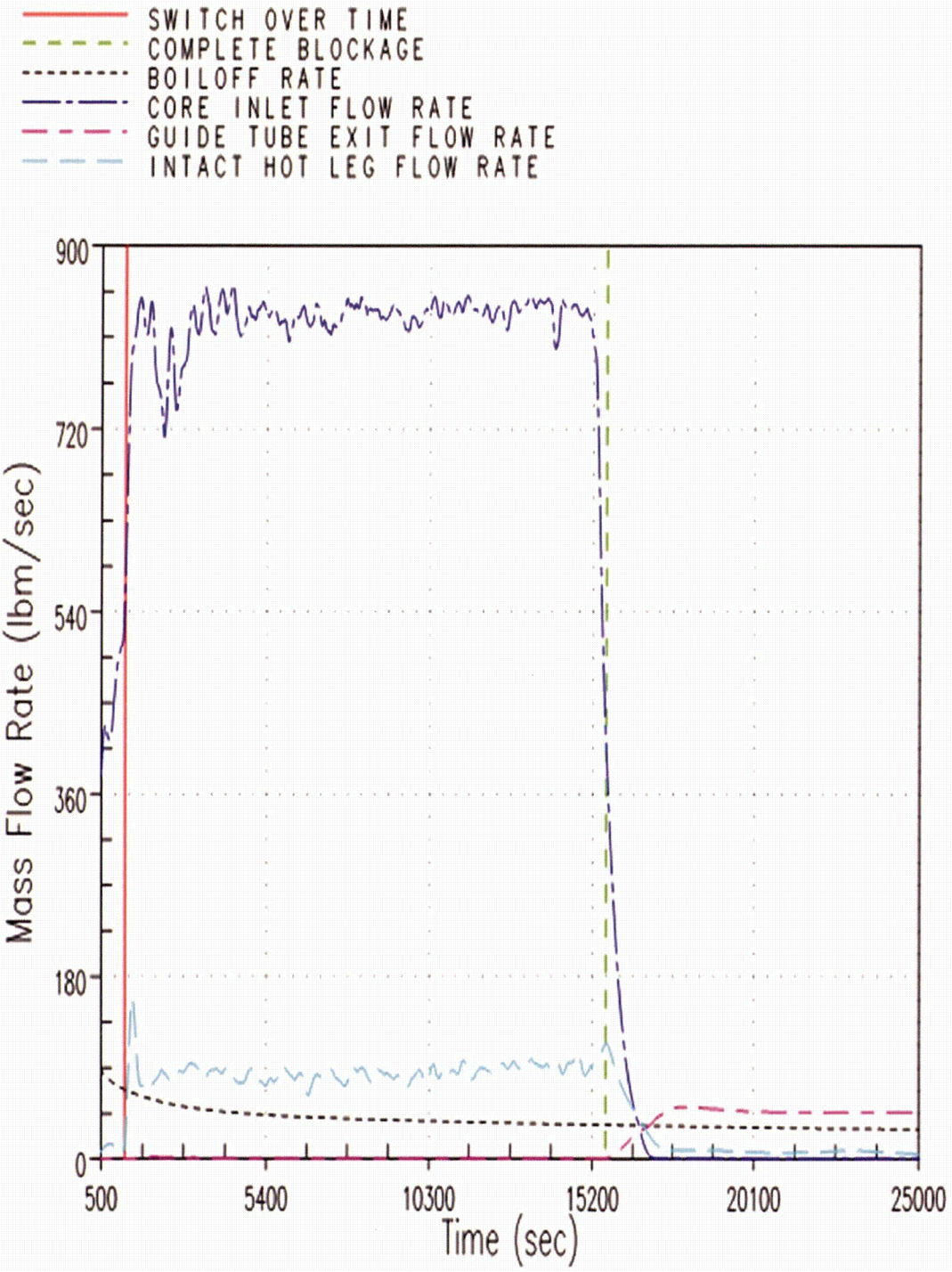

Figure 9-19 Case 1A – Core Inlet, Guide Tube Exit, and Intact Hot legs Flow Rate Compared to Boil-off

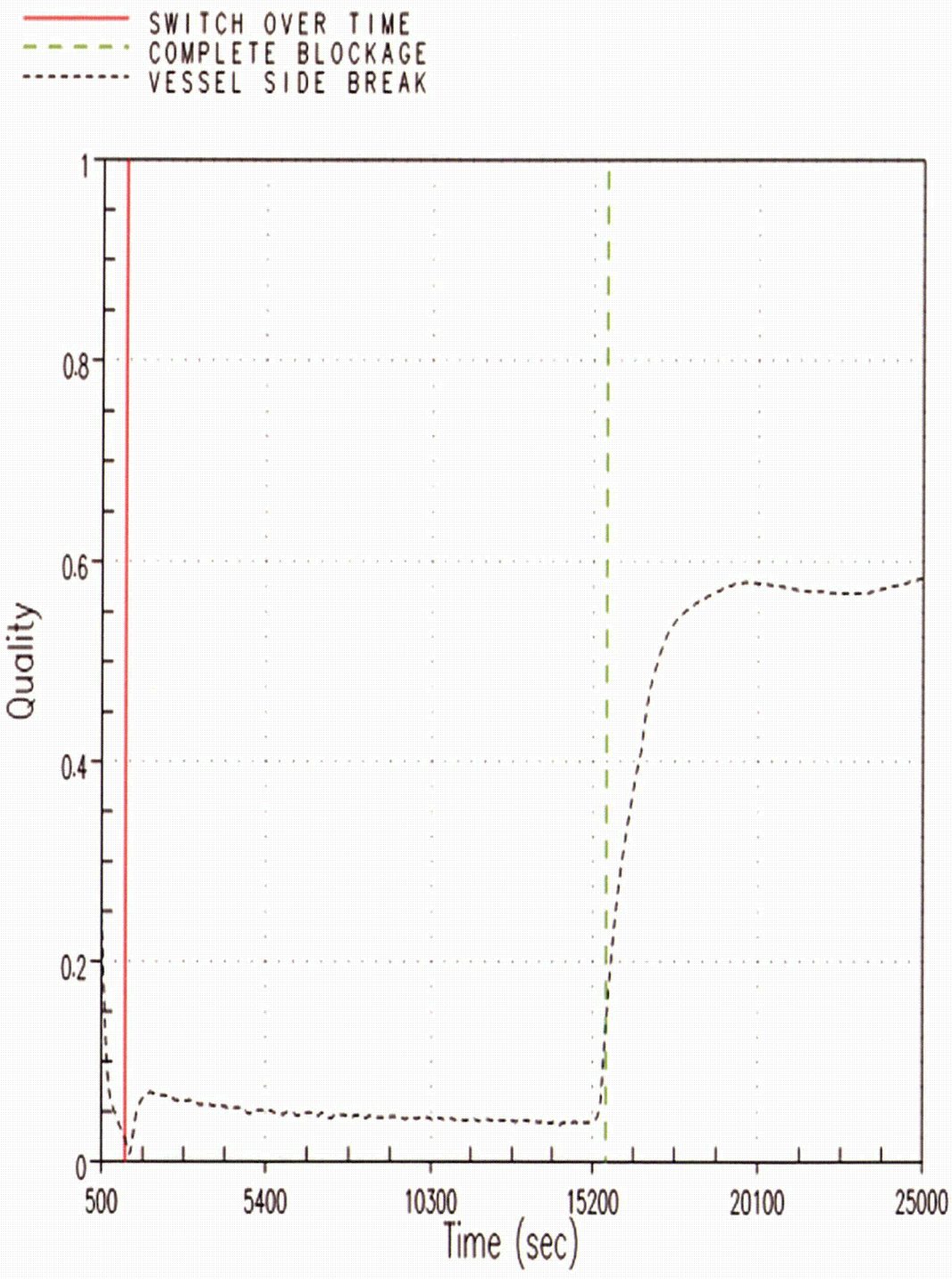

Figure 9-20 Case 1A – Break Exit Quality

9.2.3 After Debris Introduction – Calculation of K_{max}

Cases 2A and 2B are used to determine a value for K_{max}. These cases apply partial blockage to the core inlet prior to the application of complete core inlet blockage. The partial blockages are applied instantaneously at the time of transfer to sump recirculation and are applied uniformly across all core channels. Case 2B produces the lowest K_{max} value and will be discussed in this section.

Throughout the duration of the transient, more-than-adequate core cooling flow is provided through the ECCS to the cold legs. The partial blockage is applied at 20 min (1200 seconds) and complete core inlet blockage is applied at 143 min (8580 seconds). After the partial blockage is applied, the RCS response is very similar to the response seen after complete core inlet blockage, as described in Section 9.2.2, except that flow continues through the core inlet at a reduced rate. Coolant from the ECCS backs-up and fills the downcomer to the UHSN elevation. From this point forward, the total flow entering the RV is split between the core inlet and the UHSNs. Figure 9-21 shows that the core experiences a short-duration temperature excursion after the application of partial core inlet blockage; however, PCT remains below 800°F. DHR is maintained via a combination of flow through the core inlet and flow through the UHSNs to the top of the core.

The RV fluid mass is shown in Figure 9-22. When partial core inlet blockage is applied, the response in RV fluid inventory is different compared to the no blockage and complete core inlet blockage cases (Case 0A and Case 1A). The no blockage and complete blockage cases showed a sharp decrease in RV inventory upon entry to sump recirculation due to the loss of ECCS subcooling. In this case, the initial decrease is not as sharp since the application of partial blockage results in an increase in the downcomer collapsed liquid level, which offsets the reduction in RV inventory due to the loss of ECCS subcooling. The application of complete core inlet blockage later in the transient has only minimal impact on the RV fluid inventory. These trends are consistent with the behavior of the core collapsed liquid level as shown in Figure 9-23, which show the hot assembly collapsed liquid. The collapsed liquid levels in the other core channels show similar trends. The downcomer and upper head collapsed liquid levels are shown in Figure 9-24. When the blockage is applied, the downcomer collapsed liquid level quickly increases to the UHSN elevation due to the increased resistance at the core inlet. As a result, the upper head begins to flood with fluid from the downcomer and the total RV fluid mass increases due to the additional fluid in the upper downcomer and upper head.

The core inlet mass flow rate and guide tube exit flow rate are compared to boil-off in Figure 9-25. The figure indicates that flow in excess of boil-off is maintained through the core inlet even after the application of the partial blockage. It is not until complete core inlet blockage is applied that the core inlet flow decreases to zero. In terms of guide tube flow, it is seen that after partial blockage, there is a delay associated with filling the downcomer and upper head to the upper guide tube elevation, after which liquid flow through the guide tubes begins. After complete core inlet blockage is applied, the amount of flow through the guide tubes is equivalent to boil-off.

Figure 9-26 shows the pressure drop across the debris bed and the core inlet liquid velocities. The figure confirms that flow through the core inlet continues after the application of partial blockage and ceases after the application of complete core inlet blockage.

The break exit quality is shown in Figure 9-27. This figure shows that the quality prior to the application of partial core inlet blockage remains below 10%. After the application of partial blockage, the case shows a spike in the break quality (consistent with the core uncovery), which recovers and stabilizes at approximately 40% prior to the application of complete core inlet blockage. When complete core inlet blockage is applied, the break exit quality increases sharply and then recovers to a value of roughly 50%. Due to the large amount of liquid carryover out the break during the transient, BAP is controlled and boron concentrations in the RV will remain well below the solubility limit.

A review of the RV mixing patterns after complete core inlet blockage indicates that flow from the UP flows downward along the core periphery and feeds the average and hot assembly via cross flow. This trend is comparable to the core mixing patterns observed after complete core inlet blockage for the Westinghouse upflow plant category (discussed in Section 8).

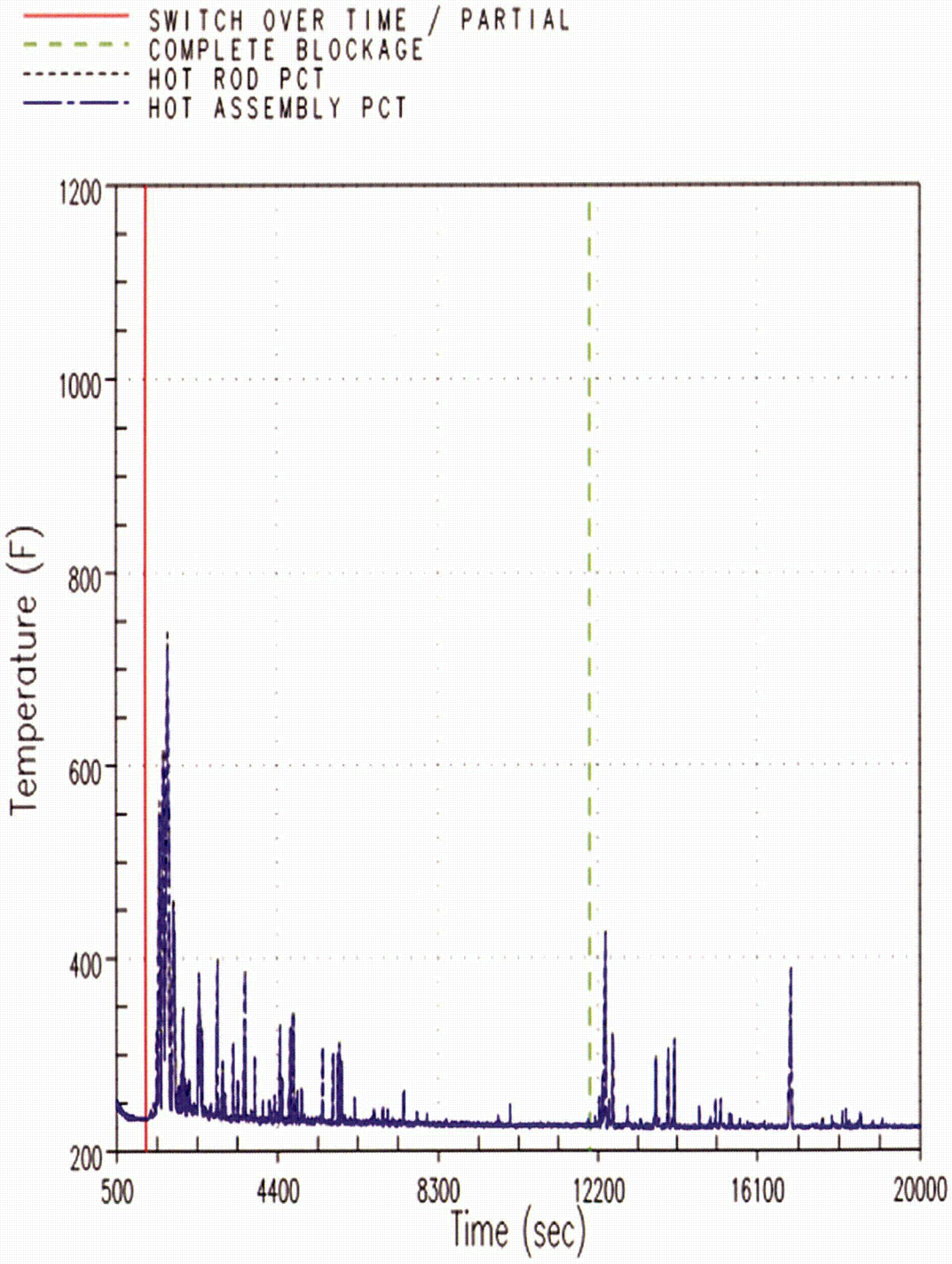

Figure 9-21 Case 2B – Hot Rod and Hot Assembly Peak Cladding Temperatures

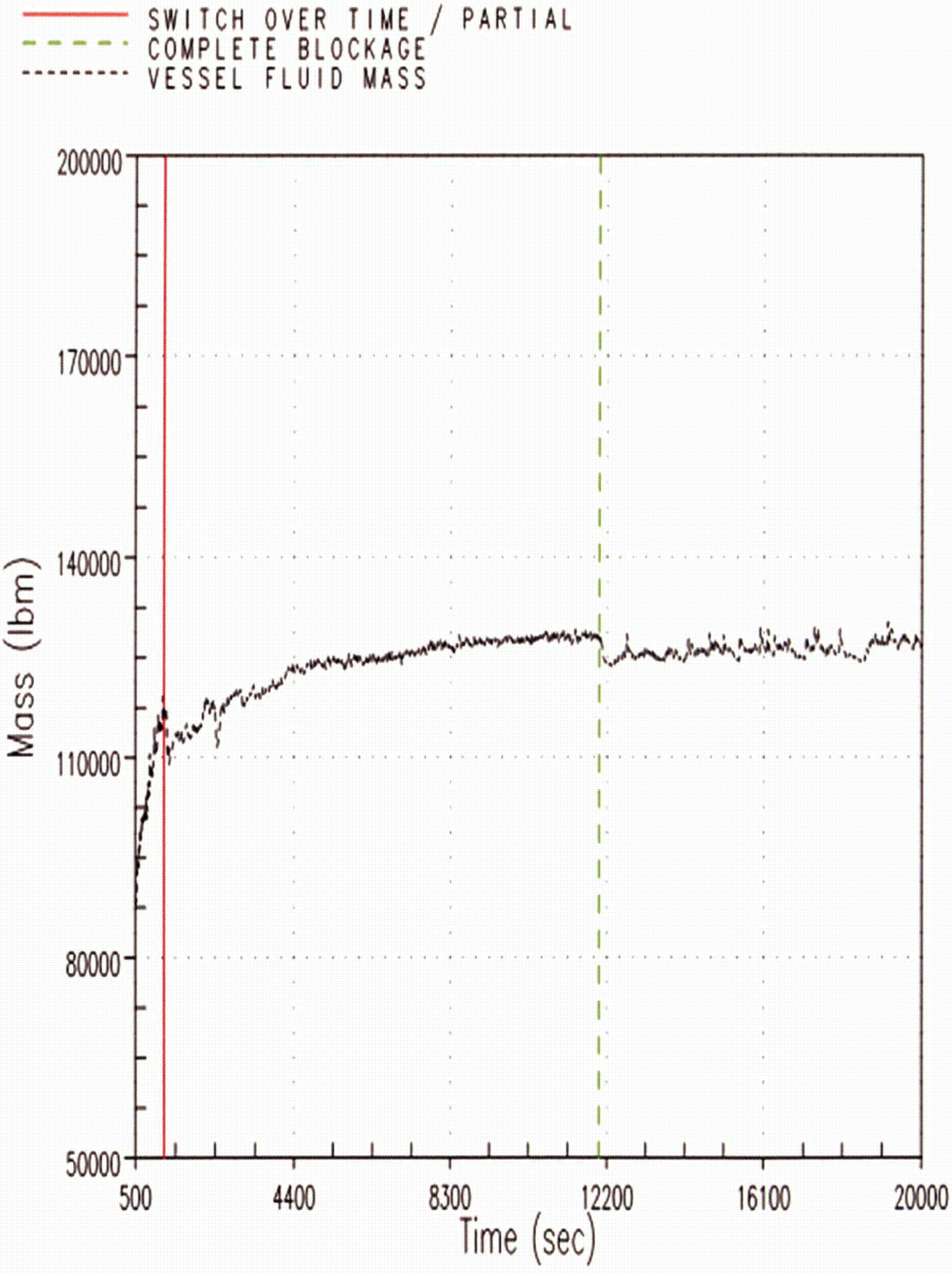

Figure 9-22 Case 2B – Reactor Vessel Fluid Mass

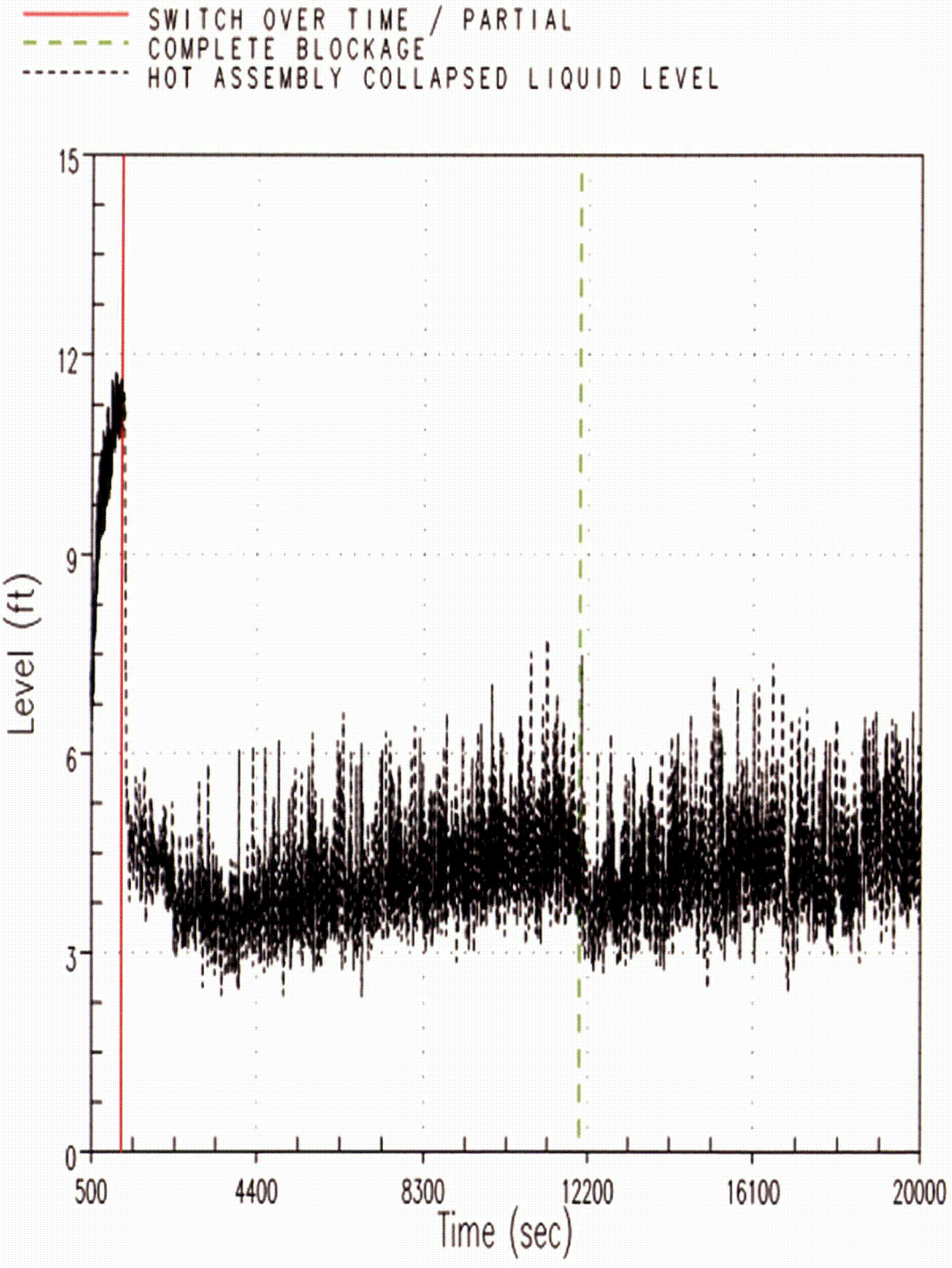

Figure 9-23 Case 2B – Hot Assembly Collapsed Liquid Level

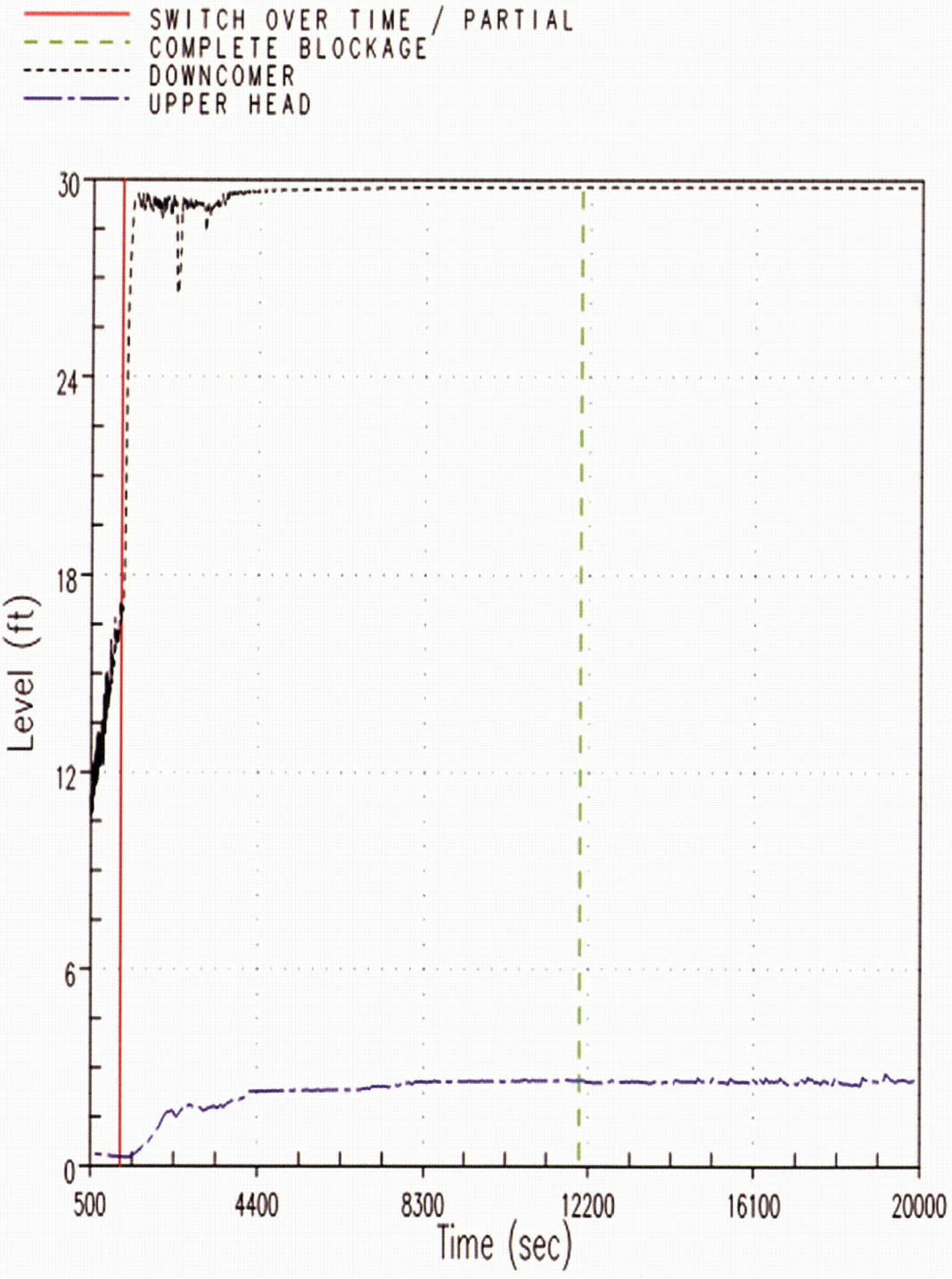

Figure 9-24 Case 2B – Downcomer and Upper Head Collapsed Liquid Levels

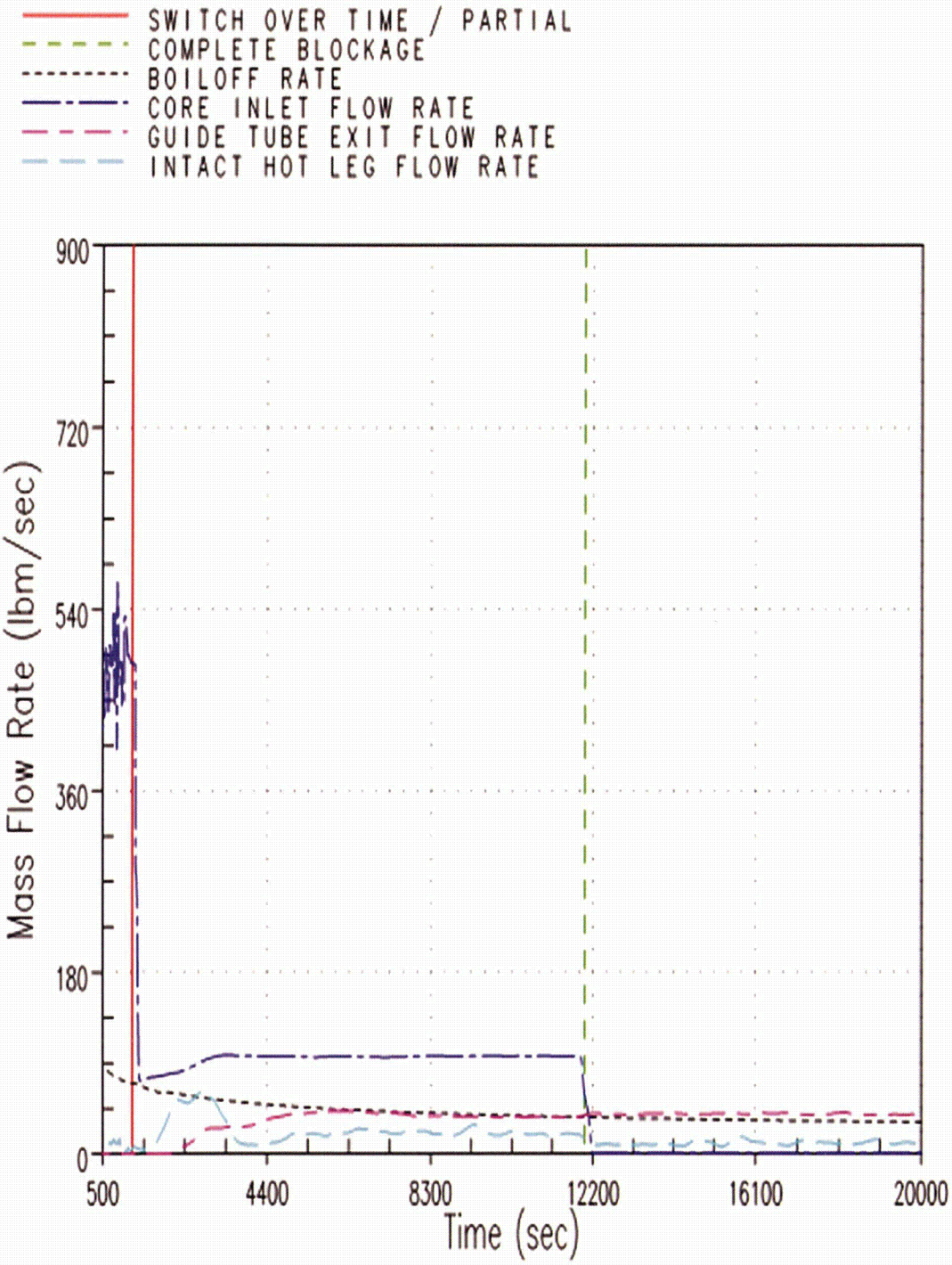

Figure 9-25 Case 2B – Core Inlet, Guide Tube Exit, and Intact Hot legs Flow Rate Compared to Boil-off

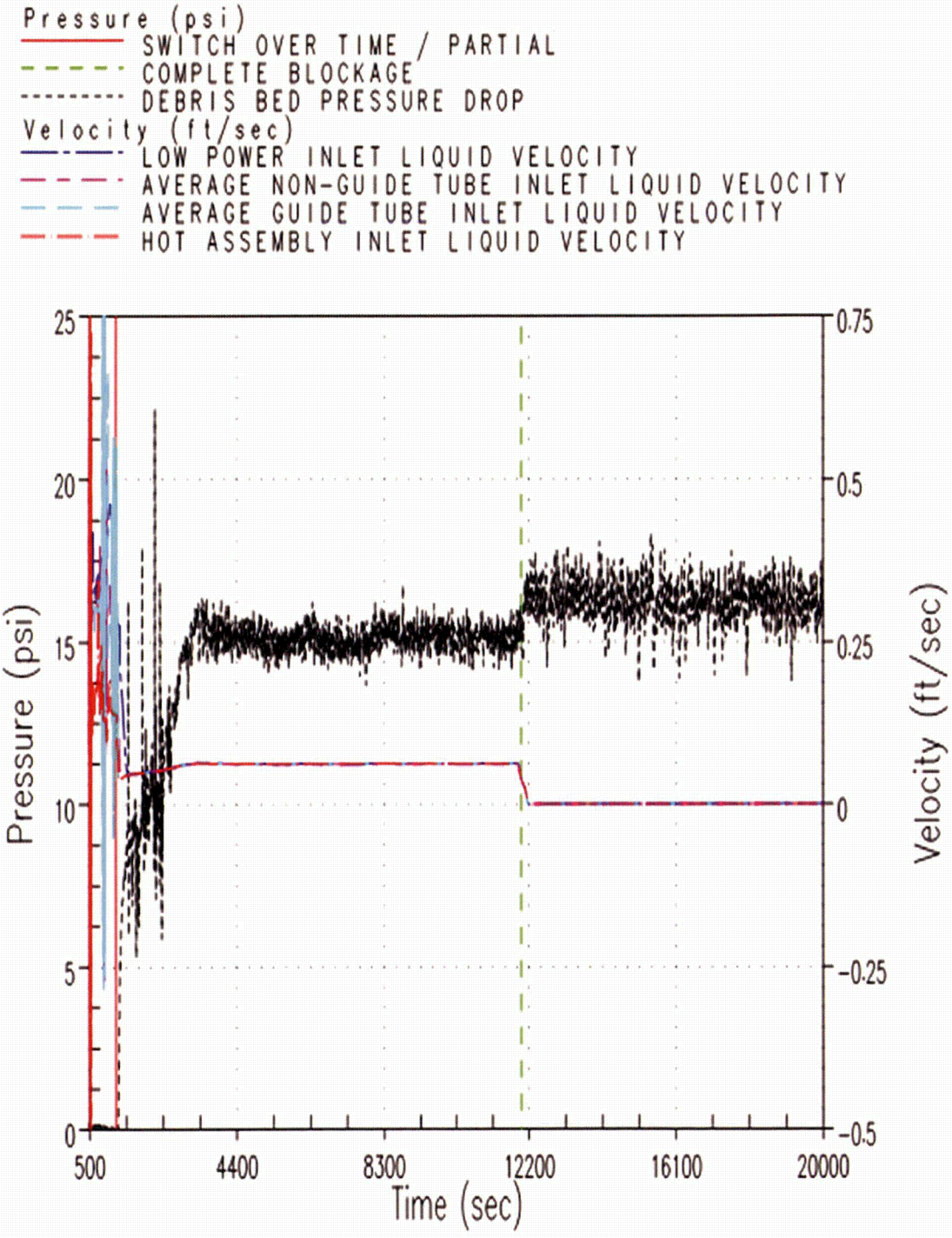

Figure 9-26 Case 2B – Pressure Drop across Debris Bed and Core Inlet Liquid Velocities

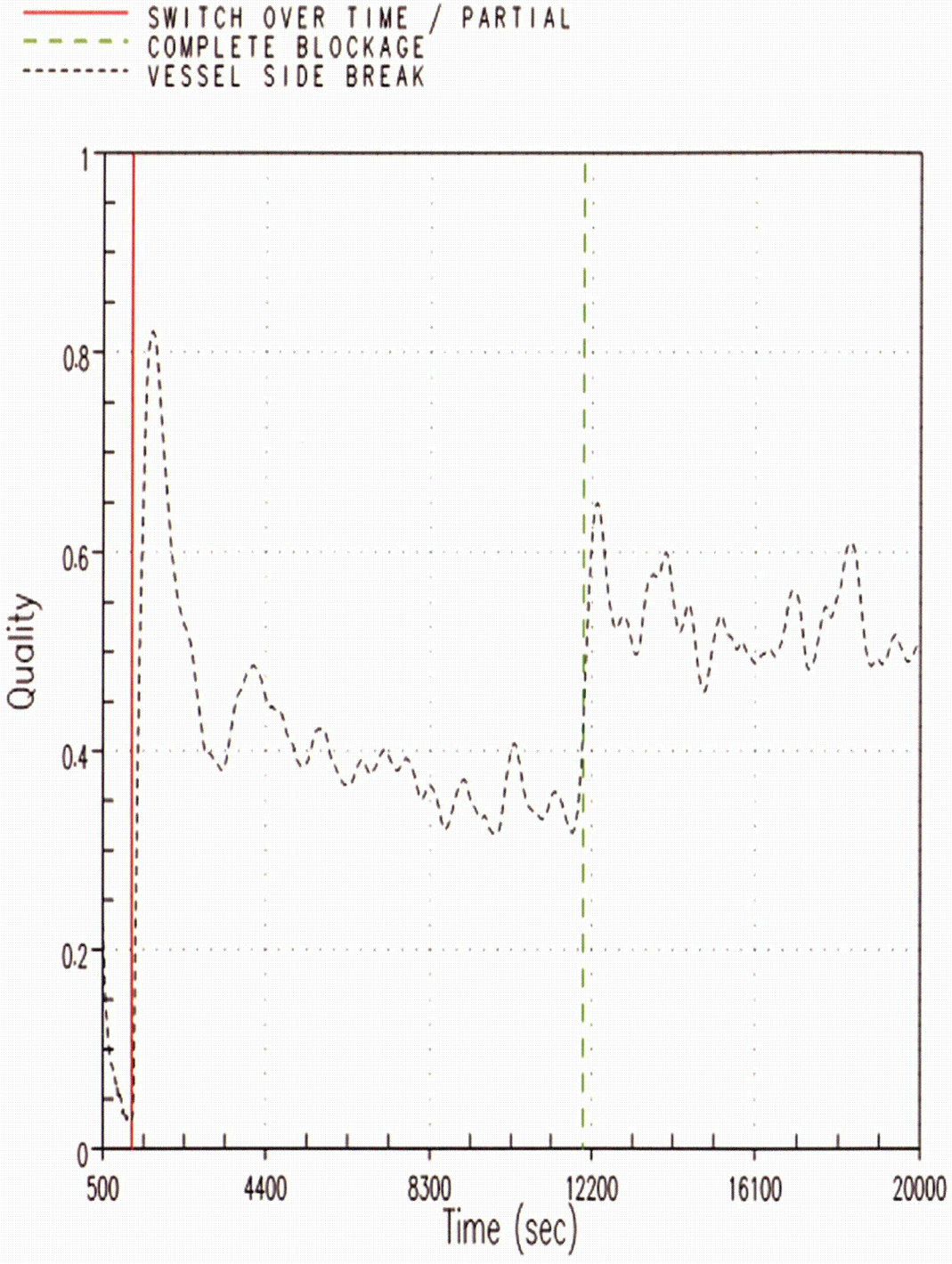

Figure 9-27 Case 2B – Break Exit Quality